MODULATION OF HOST CELL TRANSLATION AND METABOLISM BY KAPOSI'S SARCOMA-ASSOCIATED HERPESVIRUS

Aadra Prashant Bhatt

A dissertation submitted to the faculty of the University of North Carolina at Chapel Hill in partial fulfillment for the degree of Doctor of Philosophy in the Department of Microbiology and Immunology.

Chapel Hill
2013

Approved by:

Blossom Damania, PhD

Nancy Raab-Traub, PhD

Kristina Abel, PhD

Dirk Dittmer, PhD

Mohanish Deshmukh, PhD

© 2013
Aadra Prashant Bhatt
ALL RIGHTS RESERVED

ABSTRACT

AADRA PRASHANT BHATT: Modulation of Host Cell Translation and Metabolism by Kaposi's Sarcoma-associated Herpesvirus
(Under the direction of Blossom Damania, PhD)

Kaposi sarcoma-associated herpesvirus (KSHV) causes Kaposi sarcoma, multicentric Castleman's disease and primary effusion lymphoma (PEL), an aggressive subtype of B cell non-Hodgkin lymphoma (B-NHL). The lack of a vaccine, and poorly tolerated standard treatments are the onus for devising efficacious therapeutics for KSHV-associated malignancies. Several KSHV proteins deregulate cell signaling, creating a favorable environment for viral persistence, with cancer being a casualty for the host cell. Thus, understanding how KSHV, an obligate intracellular parasite, manipulates host cell processes may reveal avenues for therapeutic intervention for these cancers.

The interplay between KSHV and the host PI3K/AKT/mTOR signaling pathway forms the common theme of this dissertation. This signaling pathway regulates diverse cellular processes; among them are apoptosis, proliferation and metabolism. KSHV encodes several proteins that manipulate this pathway, which is highly active in latently infected cells, thus underscoring the importance of PI3K/AKT/mTOR signaling for the virus. Therefore, we first examined the relative contribution of each arm of this pathway in latently infected PEL cells. We found that compared to single inhibitors, dual inhibitors of PI3K/AKT/mTOR

kinases were significantly more effective at inhibiting PEL proliferation in both in vitro and preclinical in vivo models. Dual inhibitors also potently diminished autocrine and paracrine proliferative loops, further demonstrating their broad efficacy.

PI3K/AKT/mTOR kinases are essential regulators of cellular anabolic and catabolic processes. However, the metabolic sequelae of hyperactive signaling in B-NHL were largely unknown. Using metabolomics, we found that two metabolic pathways, glycolysis and fatty acid synthesis, were upregulated in latently infected PEL cells. Enhanced glycolysis was found to be essential for generating intermediates for fatty acid synthesis. The lipid biosynthetic enzyme fatty acid synthase is aberrantly expressed in PEL. FASN inhibition induces apoptosis in PEL, and further, sensitizes PEL to PI3K/AKT/mTOR inhibitors, highlighting the utility of developing FASN as a therapeutic target.

We discovered that the KSHV viral protein kinase (vPK) activates PI3K/AKT/mTOR signaling by phosphorylating the downstream effector ribosomal S6 protein, a critical player in protein translation. Furthermore, vPK expression imparts resistance to PI3K/AKT/mTOR pathway inhibitors, and determining the extent and mechanism of resistance is a future goal of this study.

To My Family:

Daksha and Prashant and Shachi

Marc

Ba and Dada

With love, respect, admiration and gratitude.

ACKNOWLEDGEMENTS

I am indebted to my preceptor, Blossom Damania. Her direction, guidance and mentorship over the years have shaped my development as a scientist and a thinker. Her dedication to science continues to be inspirational. I look forward to many more opportunities for us to work together, over the years.

A big thank you to every one of the “Damaniacs”, both past and present, for making each day in the lab enjoyable and for tolerating my (awful) sense of humor. Special thanks to: Dr. Prasanna Bhende, for being a great rotation mentor and a good friend; Dr. Kwun Wah Wen who made discussing science an absolute joy; Dr. John West, with whom I have shared so many talks and pop music; Dr. Patrick Dillon for always making a bad joke better; Dr. Sarah Jacobs who provided welcome instruction (metabolic assays!) and distraction (cooking); Louise Giffin, for being the world’s best sport and a nice person; Dr. Zhigang Zhang for providing warm wishes and warmer dumplings.

I am grateful to my dissertation committee, Drs. Nancy Raab-Traub, Dirk Dittmer, Mohanish Deshmukh and Kristina Abel for their insight, encouragement, and excitement at our committee meetings. Their collective support, input and feedback have contributed to the successful completion of my doctoral work. Thanks to Lorrie Cramer for an enriching TA-ship experience, and friendship, and Dixie Flannery for always knowing the answer to every question.

I am thankful for the many constellations of friends who have supplied support and sanity, and a lot of laughs. In particular, much love and thanks to Sirin Yaemsiri, Ginny Lewis, Shane Rea and Milena Girotti, the Norman-Aybar-Stefan family, Lisa Heimbach and Shauna Swanson. My family-in-law provide me so much love and encouragement, for which I count myself incredibly lucky and am so thankful for. My mother Daksha, taught me cell culture when I was in high school; it was a treat to teach her how to do a plaque assay 14 years later. My father Prashant encourages me to be a better scientist and think outside the box, and have a lot of laughs along the way. My sister Shachi provides unconditional love, and her resolve continues to inspire me. Meow to Curie and Tesla for providing therapeutic cuddle time and shenanigans. And to my husband, Marc Weinberg, for being my world…thank you.

TABLE OF CONTENTS

LIST OF TABLES

CHAPTER 3

LIST OF FIGURES

CHAPTER 1

CHAPTER 2

CHAPTER 3

CHAPTER 4

CHAPTER 5

LIST OF ABBREVIATIONS

2DG	2-Deoxyglucose
4EBP1	Eukaryotic initiation factor 4E binding protein 1
AGC	Protein A, C and C family of kinases; includes AKT, mTOR, S6K
AIDS	Acquired Immunodeficiency syndrome
AKT	Protein kinase B
ALT	Alternative lengthening of telomeres pathway
AMPK	Adenosine monophosphate-activated protein kinase
AP-1	Activator protein 1 transcription factor
ATP	Adenosine triphosphate
B-NHL	B cell non-Hodgkin lymphoma
BCR	B cell receptor
Bfgf	Basic Fibroblast Growth Factor
BL	Burkitt lymphoma
C75	Tetrahydro-4-methylene-2R-octyl-5-oxo-3S-furancarboxylic acid
Camk	Calcium/calmodulin kinase
CCR5	C-C chemokine receptor 5

CDK1	Cyclin dependent kinase 1
CGH	Comparative genome hybridization
CHPK	Conserved herpesvirus protein kinase
CK1	Casein kinase 1
CMGC	CDK, MAPK, GSK, CK family of kinases
COX-2	Cyclooxygenase 2
CREB	Cyclic AMP response element-binding protein
CXC	C-X-C motif chemokine
CXCL12	Stromal cell-derived factor-1; C-X-C motif ligand 12
DC-SIGN	Dendritic cell-specific Intercellular adhesion molecule-3-grabbing non-Integrin
DLBCL	Diffuse large B cell lymphoma
DMSO	Dimethyl sulfoxide
EBV	Epstein-Barr virus
EF1α	Elongation factor 1α
EIF4a	Eukaryotic initiation factor 4A
EIF4b	Eukaryotic initiation factor 4B
EIF4e	Eukaryotic initiation factor 4E

EMT	Epithelial-mesenchymal transition
Endmt	Endothelial-mesenchymal transition
Enos	Endothelial nitric oxide synthase
ERK1/2	Extracellular signal related kinase 1/2
FAK	Focal adhesion kinase
FAO	Fatty acid oxidation
FAS	Fatty acid synthesis
FASN	Fatty acid synthase
FDA	Food and Drug Administration
FL	Follicular lymphoma
FOXO1	Forkhead box protein O1
Glc	Glucose
GLUT1	Glucose transporter 1
GRO	C-X-C motif chemokine; CXCL1, CXCL2 (MIP2α), CXCL3 (MIP2β)
GRO-α	C-X-C motif chemokine 1
GSK3β	Glycogen synthase kinase 3β
Gtpase	Guanosine triphosphatase

HCC	Hepatocellular carcinoma
HCMV	Human cytomegalovirus
HD	Hodgkin disease
Hem	Hematologic malignancy
HGF	Hepatic growth factor
HHV6	Human herpesvirus 6
HHV7	Human herpesvirus 7
HIF-1α	Hypoxia-inducible factor 1α
HIV	Human Immunodeficiency virus
HNC	Head and neck cancer
Hsp40	Heat shock protein 40
HSV1	Herpes simplex virus 1
HSV2	Herpes simplex virus 2
Htert	Telomerase reverse transcriptase, human
HUVEC	Human umbilical vein endothelial cell
IC50	Half maximal inhibitory concentration; measure of efficacy of a compound
Ig	Immunoglobulin

Ikbα	Inhibitor of NF-κb
IKK	Ikbα kinase kinase
IL-6	Interleukin 6
IL-10	Interleukin 10
IP-10	Interferon γ-induced protein 10; CXCL10
IRF-7	Interferon response factor 7
ITAM	Immunoreceptor tyrosine activating motif
JNK	Janus N-terminal kinase
K1	KSHV unique ORF K1
K3	KSHV unique ORF K3
K5	KSHV unique ORF K5
KSHV	Kaposi sarcoma associated herpesvirus
LANA	Latency associated nuclear antigen
LCL	Lymphoblastoid cell lines
LPS	Lipopolysaccharide
MAPK	Mitogen-activated protein kinase
MCD	Multicentric Castleman's disease

MEK	Mitogen-activated protein kinase kinase
MHC	Major histocompatibility complex
MIG	Monokine induced by γ interferon; CXCL9
MKK4	Dual specificity mitogen-activated protein kinase 4; MAP2K4
MKK7	Dual specificity mitogen-activated protein kinase 7; MAP2K7
MT1-MMP	Membrane type 1 matrix metalloprotease
MTOR	Mammalian target of rapamycin
MTORc1	Mammalian target of rapamycin complex 1
MTORc2	Mammalian target of Rapamycin complex 2
MTS	[3-(4,5-dimethylthiazol-2-yl)-5-(3-carboxymethoxyphenyl)-2-(4-sulfophenyl)-2H-tetrazolium, inner salt
NF-AT	Nuclear factor of activated T-cells
NF-κb	Nuclear factor κ-light chain-enhancer of activated B cells
NHL	Non-Hodgkin lymphoma
NO	Nitric oxide
NOD-SCID	Non-obese diabetic, severely compromised immune deficiency
Oct-2	Octamer transcription factor

ORF36	Open reading frame 36
ORF45	Open reading frame 45
ORF64	Open reading frame 64
OXPHOS	Oxidative phosphorylation
P38 MAPK	P38 mitogen activated protein kinase
PBS	Phosphate-buffered saline
PDK1	Phosphoinositide-dependent kinase-1
PEL	Primary effusion lymphoma
PH	Pleckstrin homology domain
PI3K	3'-Phosphatidylinositol kinase
PIK3CA	3'-Phosphatidylinositol kinase catalytic subunit; p100.
PIP2	Phosphatidylinositol-(4,5)-bisphosphate
PIP3	Phosphatidylinositol-(3,4,5)-triphosphate
PK	Protein kinase
PKC	Protein kinase C
PLC	Phospholipase C; cleaves $PI(4,5)P_2$ to IP_3 and diacylglycerol
Pparγ	Peroxisome proliferator-activated receptor γ

PTEN	Phosphatase and tensin homolog
Pyk2	Protein tyrosine kinase 2
RSK1	Ribosomal S6 kinase 1
RSK2	Ribosomal S6 kinase 2
RTA	Replication and transcription activator
S6	Ribosomal protein S6
S6K	Ribosomal protein S6 kinase
SD	Standard deviation
SDF-1	Stromal cell-derived factor-1
SEM	Standard error of the mean
Ser	Serine
STE	Homolog of Sterile group of kinases
STP	Saimiri transforming protein
THP1	Human acute monocytic leukemia cell line
Thr	Threonine
TIP60	Histone acetyltransferase Tip60
TK	Thymidine kinase

TKL	Tyrosine kinase-like group of kinases
TSC1	Tuberous sclerosis complex1; Tuberin
TSC2	Tuberous sclerosis complex1; Hamartin
Tyr	Tyrosine
Vccl	Viral CC-chemokine 2
VEGF	Vascular endothelial growth factor
Vflip	Viral FADD-like interferon converting enzyme (FLICE) inhibitory protein
VGPCR	Viral G-protein coupled receptor
VIL-6	Viral interleukin 6
Vmip	Viral macrophage inflammatory protein
Vox2	Viral CD200
VPK	Viral protein kinase
VZV	Varicella zoster virus
XBP-1	X-box binding protein 1
Xct	Cystine/glutamate transporter

Y	Tyrosine

CHAPTER 1: AKTIVATION OF PI3K/AKT/mTOR SIGNALING PATHWAY BY KSHV[12]

INTRODUCTION

Kaposi sarcoma-associated herpesvirus (KSHV; also known as human herpesvirus 8) is a human ɣ-herpesvirus that was discovered in Kaposi's sarcoma (KS) biopsies in 1994 (1). Following this seminal discovery, KSHV has been found in all forms of KS, including KS associated with AIDS patients, as well as HIV-negative and transplant-associated KS. In addition to KS, which is a vascular endotheliosarcoma, KSHV is also tightly associated with two lymphoproliferative disorders: primary effusion lymphoma (2) and the plasmablastic variant of multicentric Castleman's disease (3), both arising from infection of B cells. Owing to the association with these three cancers, KSHV has been extensively studied, and the results of these studies have revealed fascinating mechanisms by which this oncogenic herpesvirus alters the infected cell in order to promote transformation and tumorigenesis.

---

[1] Aadra P Bhatt and Blossom Damania

[2] This work was originally published as a review in Frontiers in Immunology, doi: 10/3389/fimmu.2012.00401. 7 January 2013. Copyright © Bhatt and Damania

B LYMPHOCYTE DEVELOPMENT

B and T cells descend from a common lymphoid progenitor cell, itself derived from a hematopoietic stem cell precursor. In humans, B cell development occurs in the bone marrow, where the earliest progenitor (or pre-pro) B cell expresses germline heavy and light chain immunoglobulin genes (4). As the B cell matures, movement along the bone marrow and interaction with stromal cells leads to maturation. D-J gene rearrangement occurs in early pro-B cells, and continues to V-DJ rearrangement in the late pro-B cell. These gene rearrangements create a unique variable domain in the immunoglobulin. Allelic exclusion is enforced by the pre-B cell receptor, whereby only one allele encoding the rearranged heavy chain is expressed, thereby ensuring that each B cell has specificity for a single antigen (4). Many rounds of cell division occur during the transition of pro-B cells to the pre-B cell stage, leading to the formation of numerous small pre-B cells with a specific rearranged μ heavy-chain gene. Pre-B cells undergo light chain gene rearrangement, which is also accompanied by allelic exclusion. Since these pre-B cells now produce both heavy- and light-chain proteins, they are classified as immature B cells, and bear intact IgM molecules on their cell surface (4). For a review describing normal B cell development, please see (5).

In addition to allelic exclusion, isotype exclusion also occurs in immature B cells, wherein the immature B cell expresses only one light chain (either λ or κ) (4). In humans, because the κ gene rearranges prior to the λ gene, many more

mature B cells express the κ light chain rather than λ. The average distribution of κ to λ-bearing B cells in humans is approximately 65%:35%, and aberration from this ratio is indicative of lymphoproliferative disorders, reflecting dominance of one clone (4).

PATHOPHYSIOLOGY OF KSHV-ASSOCIATED B CELL MALIGNANCIES

Primary effusion lymphoma: Primary effusion lymphoma mainly afflicts HIV-infected patients, and occurs in body cavities such as the peritoneal, pleural and pericardial cavities (6, 7). Some KSHV-positive lymphomas can also present as extranodal solid masses, which may subsequently develop into an effusion. Cells have an immunoblastic appearance with a high mitotic index. KSHV-positive solid lymphomas represent an extra-cavitary variant of primary effusion lymphoma (8). In PEL, every tumor cell expresses between 50-150 copies of the KSHV genome. The genome is found as an episome tethered to the host cell chromosome by the virus-encoded Latency Associated Nuclear Antigen (LANA) protein (9-12). Some PEL are co-infected with Epstein-Barr virus (EBV), another lymphotropic γ-herpesvirus (7, 13).

Patients with PEL present with lymphomatous effusions within body cavities, in the absence of a solid tumor mass (7, 14). Cells contained within the effusions are large, with abundant cytoplasm, and display morphological aspects common to both large-cell immunoblastic and anaplastic large cell lymphoma (7). Analysis of *Ig* rearrangements suggests that PEL arises from clonal expansion of

an infected B cell (6). PEL express syndecan 1/CD138, which is a plasma cell surface marker, in addition to CD45 (15).

Although most PEL cell lines do not have translocations and mutations as associated with *c-myc* and *p53*, many PEL possess numerous genetic aberrations (16). Sophisticated comparative genome hybridizations (CGH) studies reveal extensive copy number aberrations comprising predominantly of gains and amplifications. Two genes, *SELPLG* and *CORO1C* were found to be the targets of amplification at chromosome 12q24.11. *SELPLG* encodes a membrane-bound glycoprotein that binds to P, E and L-selectins, and is important for leukocyte recruitment to sites of inflammation (17). *CORO1C* is a member of the coronin gene family that regulate actin-dependent processes such as motility and vesicle trafficking, and whose expression is associated with enhanced invasion and metastatic capability (18). Deletions of the two fragile site tumor suppressors, *WWOX* and *FHIT*, were also recently reported in PEL (19).

Multicentric Castleman's disease*:* Prior to the discovery of KSHV, Castleman's disease, an atypical lymphoproliferative disorder, was divided into the hyaline vascular type, and the plasmablastic type. KSHV is associated with the plasma cell variant of multicentric Castleman's disease (MCD), which is multicentric in that several lymph nodes and the spleen are involved in disease. In the context of HIV infection, MCD is systemic, aggressive, and is associated with high fatality. KSHV genomes are detected in almost all HIV+ MCD cases, and ~50% of non-HIV+ cases of MCD (20, 21). AIDS patients diagnosed with MCD suffer sustained

fevers, weight loss, lymphadenopathy and hepatosplenomegaly (22). MCD frequently progresses to lymphoma or Kaposi sarcoma.

MCD is localized to the marginal zone of lymph nodes and the spleen. The germinal centers resemble follicular hyperplasia, and the mantle zone is generally intact and surrounded by mature KSHV-infected plasmablasts (23-25). MCD cells resemble plasmablast or pre-plasma cells (26). All KSHV-infected plasmablasts within the lesion exclusively express the λ light chain of IgM (22), and the presence of λ light chains and absence of CD138 on MCD cells further suggest they originate from the infection of a less differentiated B cell (27). Lymph nodes involved in MCD are characterized by germinal center expansion and vascular endothelial proliferation. MCD is characterized by elevated serum IL-6 levels in the patient (28). These elevated IL-6 levels, partially augmented by virally encoded IL-6 (vIL-6), create an inflammatory microenvironment that significantly contributes to the pathophysiology of MCD.

KSHV ALTERS NORMAL B CELL PROLIFERATION AND DIFFERENTIATION, LEADING TO LYMPHOPROLIFERATIVE DISORDERS

Both MCD and PEL are associated with infection of a pre-terminally differentiated plasma cell. Gene expression arrays indicate that PEL have a plasma cell expression profile, and enhanced expression of genes involved in inflammation, adhesion and invasion (26), likely contributing to their malignant phenotype. MCD is characterized by the polyclonal expansion of KSHV-infected plasmablasts that exclusively express the λ light chain. No functional significance

exists in whether a plasmablast bears either λ or κ, as the isotype exclusion is purely a function of order of light chain gene rearrangement.

It was unknown whether KSHV preferentially infected λ light-chain bearing B cells due to an inherent, yet unknown survival advantage to the virus/infected cell, or whether KSHV infection of a more undifferentiated cell (prior to light chain rearrangement) drove the expansion of λ-expressing B cells.

Hassman *et al* attempted to address this question in a recent study in which they infected *ex vivo* suspensions of human tonsillar cells with purified KSHV (27). Despite the presence of various cell types, KSHV infection was shown to preferentially occur in B cells, as evidenced by LANA+ staining. The tonsillar cultures contained both κ- and λ-expressing B cells, however, all LANA+ staining was observed within the λ subset. Furthermore, infection with KSHV enhanced the proliferation of this IgMλ subset, which was further augmented by treatment with IL-6. KSHV-positive cells mirrored phenotypic characteristics of MCD cells, such as blasting morphology and increased expression of IgMλ, CD27, Ki67 and IL-6R.

This study also suggested that rather than naïve B cells, KSHV preferentially infects IgM memory B cells, resident within sub-epithelial regions of the tonsil and spleen. During plasmablast differentiation, IgM memory B cells acquire phenotypic markers such as Ki67+, IgM+ and CD27+, similar to MCD. This model is concordant with molecular and seroepidemiological data suggesting that the primary mode of KSHV transmission is via saliva (29).

Plasmablast differentiation, including that of IgM memory B cells, can result from NF-κB activation, a signaling event that occurs during KSHV infection, and also during latency. The viral FADD-like IL-1β-converting enzyme (FLICE/caspase-8) inhibitory protein (vFLIP) activates NF-κB signaling in latently-infected cells by associating with the IκB kinase (IKK) complex, and driving degradation of IκBα, and thus, NF-κB release into the nucleus. A consequence of NF-κB signaling is the promotion of cell survival and proliferation pathways. Ballon *et al* constructed an inducible CD19- or Cɣ1-driven conditional vFLIP knock-in mouse, which targeted vFLIP expression to various stages of B cell development (30). vFLIP expression in B cells was found to prevent germinal center development, Ig class switching, and affinity maturation; vFLIP expression resulted in splenomegaly in the mice. Although transgenic mice did not recapitulate phenotypes of PEL, B cells mimicked an MCD phenotype, with expansion of IgM λ plasmablasts, concordant with the findings of Hassman *et al*., indicating that vFLIP leads to expansion of the IgMλ subset upon KSHV infection. Moreover, impaired GC formation and class switch recombination resulting from vFLIP expression suggests that inhibition of the adaptive response is a means of escaping immune surveillance.

Interestingly, 20-month old vFLIP-expressing mice developed B cell-derived histiocytic/DC sarcoma. This finding is important as it underscores the ability of vFLIP to either reprogram or transdifferentiate the infected lymphocytes or the bystander cells in a paracrine manner, into other cell types. These findings

also reveal insights into the biology of B lymphocytes, and demonstrates their inherent plasticity (31).

The collective body of research suggests that KSHV viral oncogenesis is mediated by expression of both latent and lytic viral gene products. Viral latent proteins are expressed in every tumor cell, whereas lytic proteins are expressed in a small percentage of tumor cells undergoing reactivation, and are thought to promote cell proliferation in an autocrine or paracrine manner. KSHV can infect a wide range of cell types *in vitro* and *in vivo* including THP-1 monocytes, plasmacytoid dendritic cells, fibroblasts, keratinocytes, B-lymphocytes, endothelial and epithelial cells. (27, 32-45). To guarantee successful replication within these distinct cell types, KSHV encodes an arsenal of viral proteins that are capable of modifying the host cell environment, either directly or indirectly, with the outcome being beneficial for the virus. Modulation of host cell pathways includes evasion of both immunity as well as apoptosis, induction of cell proliferation, and the promotion of cellular metabolism, macromolecular synthesis, and protein translation. One way KSHV accomplishes these alterations is by targeting the phosphatidylinositol 3'-kinase (PI3K)/AKT/mammalian target of rapamycin (PI3K/AKT/mTOR) pathway. Similar to KSHV, many DNA viruses encode one or more viral proteins that either activate or inactivate various nodes of this pathway (46).

KSHV LIFE CYCLE

KSHV establishes lifelong latency within the host, punctuated with sporadic bouts of reactivation and lytic replication. During latency, the KSHV genome exists as a circular, extra-chromosomal viral genome (episome), with minimal expression of a subset of latent viral proteins: K12/Kaposin, K13/vflip, ORF72/vcyclin, ORF73/LANA, vIL-6 and K1 (47). In contrast, during the lytic replication phase, most of the viral genome is expressed and viral assembly, egress and dissemination follow viral replication. The lytic switch protein Replication and Transcription Activator (RTA) governs KSHV reactivation (48, 49). Chemicals such as phorbol esters, sodium butyrate, and histone deacetylase inhibitors reactivate the virus by activating the RTA promoter (50), and thus are useful for studying the viral life cycle. Hormones (norepinephrine and epinephrine), cytokines such as interferon-ɣ, oncostatin M and hepatocyte growth factor reactivate KSHV, as does the hypoxic microenvironment typical of solid tumors and serous cavities, thus stimulating the expression of viral proteins that are beneficial to the host cell (51, 52). Terminal differentiation of B cells, resulting from expression of X-box binding protein 1 (XBP-1) can also activate the RTA promoter, inextricably linking virion production to the host cell life cycle (53, 54). Furthermore, stimulation of toll-like receptors (TLRs) 7 and 8 by microbes can also reactivate KSHV from latently-infected cells (55); stimulation of these pattern recognition receptors generates an anti-viral state, and

expressed lytic proteins have many functions which antagonize the host immune system.

KSHV reactivation from latency significantly alters the physiology of the infected cell. Viral replication can reveal viral nuclei acid or peptide motifs that can activate host immune surveillance pathways. Viral replication also increases the demand for macromolecules such as nucleotides and amino acids to synthesize progeny virions. Cellular energy pools are substantially depleted in order to fuel the increased biosynthetic rates associated with viral replication. The combined effect of enhanced biosynthetic rates and unfulfilled energy demands is the activation of cellular stress responses, resulting in cell cycle arrest or apoptosis, in an attempt to resolve these deficits. To circumvent activation of stress responses, lytic proteins efficiently block cell death pathways, and maintain the host cell in a constant state of proliferation. Moreover, many lytic and latent proteins co-opt cellular signaling pathways, which sustain proliferation, block cell death, and enhance cellular metabolism, in order to maintain latent virus or facilitate lytic replication and dissemination of KSHV. One such pathway is the pleiotropic PI3K/AKT/mTOR pathway, which governs many cellular processes.

THE PI3K/AKT/mTOR SIGNALING PATHWAY

The following brief introduction describes the various effectors of PI3K/AKT/mTOR signaling, and relates their activation to distinct physiological outcomes for the cell. While no means exhaustive, this description provides a primer for subsequent sections, which describe KSHV's interaction with this

pathway. For recent reviews describing up-to-date targets of PI3K/AKT/mTOR signaling, their regulation and relevance to malignancies please refer to (56-59).

The phosphatidylinositol 3-kinases (PI3K) are lipid kinases that phosphorylate the 3'-hydroxyl of the inositol ring of phosphoinositide, a component of the interior side of eukaryotic cell membranes (60). Phosphoinositides help form membrane cell signaling complexes and are essential for intracellular trafficking. PI3K are divided into four classes, IA, IB, II and III, all of which have differing substrate specificities and modes of regulation. Class IA and IB PI3K catalyze the phosphorylation of phosphatidylinositol-4,5-bisphosphate (PIP_2) at the 3' carbon on the inositol ring into phosphatidylinositol-3,4,5-triphosphate (PIP_3). $PI(3,4,5)P_3$ production by PI3K allows for pleckstrin homology (PH)-domain containing proteins to localize to the plasma membrane (60). PIP_3 also functions as a cellular second messenger capable of controlling cell shape, survival, proliferation, growth, and motility. Class I PI3Ks are heterodimeric proteins comprising a regulatory subunit and a catalytic subunit. The regulatory subunits are p85α, p85β, p55α, p55ɣ and p50α (60). The catalytic subunits are comprised of one of four isoforms: p110α, p110β, p110δ and p110ɣ. Most mammalian tissues widely express p110α, β and ɣ catalytic subunits, whereas p110δ is restricted to lymphocytes (61). Phosphatase and tensin homology (PTEN) is a phosphatase that catalyzes dephosphorylation of the 3' carbon on the inositol of $PI(3,4,5)P_3$ back to PIP_2 (62). PTEN is one of the most frequently lost tumor suppressors in various cancers. Mutations or deletions in *PTEN* cause hyperactivation of PI3K signaling, leading to increased cell

proliferation as well as evasion of apoptosis. AKT is a PH-domain containing protein that plays a central role in varied cellular processes such as glucose metabolism, evasion of apoptosis, and promotion of cell proliferation, transcription and cell migration (63). AKT can also stimulate protein synthesis via activation of mTOR (discussed below) (56). Once AKT is localized to the cell membrane through its PH-domain, it is phosphorylated on Threonine^{308} by phosphoinositide dependent kinase 1 (PDK1), and Serine^{473} through the mTORc2 complex (64), both of which are activating modifications. AKT has several different effectors, which control distinct biological processes, thus, AKT activation has pleiotropic effects upon the cell. AKT inhibits cell death by phosphorylation-mediated inactivation of pro-apoptotic factors Bad, Caspase-9, and the FOXO group of transcription factors (65-68). Phosphorylation of the FOXO transcription factors sequesters them within the cytoplasm, thus preventing them from transcriptionally activating target pro-apoptotic genes such as Fas ligand and Bim.

AKT regulates the cell cycle by phosphorylating and inactivating key regulators of cell cycle progression. For instance, AKT promotes the transcriptional activation of *c-Myc* and *cyclin D1* genes (69), and interacts with two regulators of the cell cycle, p27 and p21 (70, 71). Maintaining a quiescent state requires high intracellular p27 levels, and PI3K activation was shown to reduce the cellular reserves of p27 (72). AKT phosphorylates the p53-induced protein p21, a negative regulator of cell cycle progression (70). The net result of

these inhibitory phosphorylation events is the maintenance of cell cycle progression and the de-regulation of cellular checkpoint signaling.

AKT also activates the non-canonical branch of the NF-κb family of transcription factors. NF-κB regulates many aspects of innate and adaptive immunity and cell survival. NF-κB is normally sequestered in the cytoplasm by inhibitory proteins such as inhibitor of κB (IκBα), which is degraded following phosphorylation by the upstream IκB kinase complex (IKK complex), comprised of IKKα and IKKβ. IκBα is a direct target of IKKβ, that when degraded, releases NF-κB p65 thus activating genes involved in innate immune responses, IKKα activates non-canonical NF-κB, leading to formation of p52 which activates genes involved in adaptive immunity (73-75), AKT regulates non-canonical NF-κB p52 processing by increasing the activity of IKKα (76). Studies using constitutively active AKT demonstrated elevated p52 transcriptional activity. Non-canonical NF-κB activity was severely inhibited by using PI3K inhibitors, kinase-dead AKT or cells lacking AKT isoforms 1 or 2 (76, 77). Thus, AKT modulates both cell survival and regulation of adaptive immune responses. De Oliveira and colleagues (78) provide an excellent review of the role of NF-κB signaling with regard to KSHV infection.

The serine/threonine kinase mammalian (or mechanistic) target of Rapamycin (mTOR) is a downstream target of PI3K/AKT signaling. In addition to being activated by essential signaling pathways such as PI3K and MAPK, mTOR is activated by a wide range of cellular stimuli such as growth factors, stress signals, and nutrient, energy, and amino acid abundance. mTOR activity is

negatively regulated by the tuberous sclerosis complex (TSC), comprised of TSC1 and TSC2. TSC2 is an AKT target, and when phosphorylated, inhibits Rheb, also a negative regulator of mTOR (63). MTOR exists in two distinct multiprotein signaling complexes, mTORc1 and mTORc2, which have differing sensitivities to the macrolide rapamycin; mTORc1 is sensitive, whereas mTORc2 is insensitive. MTORc1 regulates protein translation, cell size regulation, intracellular transport, metabolism and lipid biogenesis. mTORc1 phosphorylates S6K1 and 4EBP1, which are two proteins critical for translation of eukaryotic capped mRNAs. S6K1 phosphorylates the S6 ribosome, thus stimulating protein synthesis. Unphosphorylated 4EBP1 tightly binds and represses the eukaryotic initiation factor 4E (eIF4e); hyperphosphorylated 4EBP1 releases eIF4e, thereby enabling cap-dependent translation (79). MTOR has a wide plethora of other targets for e.g. ULK1 which regulates autophagy (57). Because protein translation is central to both cancer growth and viral persistence, mTOR is a very important signaling protein. The rapamycin-insensitive mTORc2 complex regulates cell survival and cytoskeleton dynamics. MTORc2 activates AKT, thereby paradoxically activating AKT/mTOR signaling even upon rapamycin treatment, demonstrating a feedback activation loop (80).

Solid tumors are characterized by hypoxic microenvironments, therefore, *de novo* angiogenesis as well as remodeling existing blood vessels is essential to provide the rapidly growing cells with nutrients and oxygen. The viscosity and shear forces of blood against the walls of blood vessels govern the enzymatic activity of endothelial cell-expressed NOS (eNOS), and consequently, the

continual synthesis and release of nitric oxide (NO). In endothelial cells, AKT is activated in a PI3K-dependent manner, both by shear forces and VEGF, which collectively activate eNOS (81). NO has pleiotropic functions ranging from angiogenesis, remodeling of the vasculature, and the control of blood vessel tone (82).

The AKT/mTOR axis is a critical regulator of cellular metabolism. Activated AKT stimulates glucose uptake by relocalizing the GLUT1 glucose transporter, thus bringing glucose into the cell for fueling various cellular processes (83). Activation of the mTORc1 complex promotes glycolytic flux, upregulates the pentose phosphate pathway, and stimulates *de novo* lipogenesis, all of which contribute to metabolic reprogramming essential for rapidly dividing cancer cells (84).

As mentioned above, hyperactivation of PI3K/AKT/mTOR signaling is a characteristic of many malignancies. Deregulated signaling may result from inactivation of negative regulator phosphatases e.g. TSC2 or PTEN, or from mutations in catalytic domains of kinases e.g. PIK3CA. Although KSHV-infected PEL cells are not known to have activating mutations in any of these three kinases, PI3K/AKT/mTOR signaling is highly upregulated in these cells (85, 86). As we will discuss further, a variety of viral proteins can activate this signaling pathway.

Proper PI3K/AKT/mTOR signaling is essential for the differentiation and developmental program of normal T and B lymphocytes, as well as other immune

cells. PI3K is downstream of numerous cytokine receptors- CD40, Toll-like receptors and the BCR itself. The current body of research suggests that PI3K signaling regulates the development of bone marrow B cell precursors, as well as the differentiation and development of B cell subsets (87-89). Moreover, PI3K signaling also governs many aspects of activation and proliferation of mature B cells. For an excellent review describing the PI3K pathway with regard to B cell development, please see (61).

KSHV ACTIVATES PI3K SIGNALING DURING DE NOVO INFECTION

KSHV activates the PI3K signaling pathway during viral infection. The widely-expressed proteoglycan heparan sulfate, α3β1 integrins, DC-SIGN and xCT are the primary receptors for KSHV, and their differential distribution in various cell types contributes to the wide tropism of KSHV (reviewed in (90)). KSHV enters target cells by endocytosis. Viral entry activates many cellular signaling pathways, which does not require active viral replication, as demonstrated by studies using UV-inactivated KSHV (90). Viral ligation of cell-surface integrins triggers the phosphorylation and activation of focal adhesion kinase (FAK) in fibroblasts (91). FAK further activates downstream signaling molecules including Src, Rho GTPases, Diaphanous 2, and PI3K (92-96). In turn, these molecules further activate their own downstream effectors such as Ezrin, protein kinase C (PKC), MEK, NF-κB, ERK 1/2 and p38 MAPKs, and AKT.

Integrin-mediated tyrosine phosphorylation of FAK occurs minutes after KSHV infection of fibroblasts (90). Reduced viral genomes and gene expression are observed in cells lacking either FAK or Pyk2, a FAK family member,

illustrating their essential role in viral infection of target cells. (91, 96). FAK and Pyk2 signaling converge onto the Src kinase family, whose downstream effectors are PI3K and Rho GTPases. FAK, Src and PI3K are also phosphorylated following infection of THP-1 monocytes, as are NF-κB and ERK-1 and 2 (97). PI3K activation is crucial for *de novo* infection due to its activation of various GTPases involved in actin cytoskeleton remodeling, endosome formation and vesicle trafficking. These intracellular processes allow for viral entry and delivery into the nuclear compartment. PI3K and Rho GTPase activation collectively induces other Rho GTPase family members, which precipitate the formation of subcellular structures such as lamellipodia (through Rac), stress fibers (through RhoA) and filopodia (through Cdc42) (91). Further, activation of the PI3K target, AKT, leads to the inhibition of pro-apoptotic factors, thus protecting KSHV-infected cells from cell death.

Activation of cellular signaling is imperative for successful viral infection. The signaling nodes described above activate the processes of vesicle formation, intracellular motility, and evasion of cell death. Furthermore, transcription factors activated by these signaling pathways also play a role in activation of the viral transcription program, as well as induction of cellular proteins that facilitate viral replication. Thus, the collective activation of these intracellular signaling pathways creates an environment benefitting the KSHV life cycle.

KSHV VIRAL PROTEINS THAT ACTIVATE PI3K/AKT/mTOR SIGNALING

Currently, four of the approximately hundred genes and microRNAs encoded by KSHV are known to impinge upon the PI3K/AKT/mTOR signaling pathway. They are K1, vGPCR, vIL-6 and ORF45. We will discuss the mechanisms, extent, context and physiological relevance of each of these proteins below.

K1

K1 is the first ORF encoded by KSHV, and is located at the extreme left end of the viral genome. K1 is a transmembrane glycoprotein whose expression in rodent fibroblasts induces morphological changes and the ability to grow in foci, indicating K1's transformation capacity (98). Further, infection of T lymphocytes with a recombinant herpesvirus Saimiri expressing K1 instead of the oncoprotein Saimiri transforming protein (STP) conferred IL-2 independent growth, suggesting that K1 is also an oncoprotein (98). All KSHV-associated tumors express low levels of K1 transcript, and K1 expression is highly upregulated early during lytic replication (99-103). K1 transgenic mice leads display constitutively active NF-κB and Oct-2 transcription factors, increase in expression of basic fibroblast growth factor (bFGF), as well as upregulated expression and activity of the Lyn tyrosine kinase (104). A physiological consequence of K1-mediated alteration of the cellular transcription program is the development of tumors similar to spindle-cell sarcomatoid tumor and malignant plasmablastic lymphoma (104). This observation highlights the ability of K1 to exploit the inherent plasticity of cell types to induce transdifferentiation.

Various studies describe the extent to which K1 also deregulates normal cellular signaling (Figure 1). The regulatory p85 subunit modulates PI3K activity, and tyrosine-phosphorylation of p85 results in activation of PI3K (105). K1 expression leads to increased tyrosine phosphorylation of p85, in addition to phosphorylation of Vav and Syk, thus activating signaling networks downstream of these kinases, which have pleiotropic effects on the cell (101, 106, 107). Further, activation of transcription factors downstream of these kinases, for example, NFAT, downstream of Syk signaling, further augments deregulation of cellular signaling and promotes cell survival.

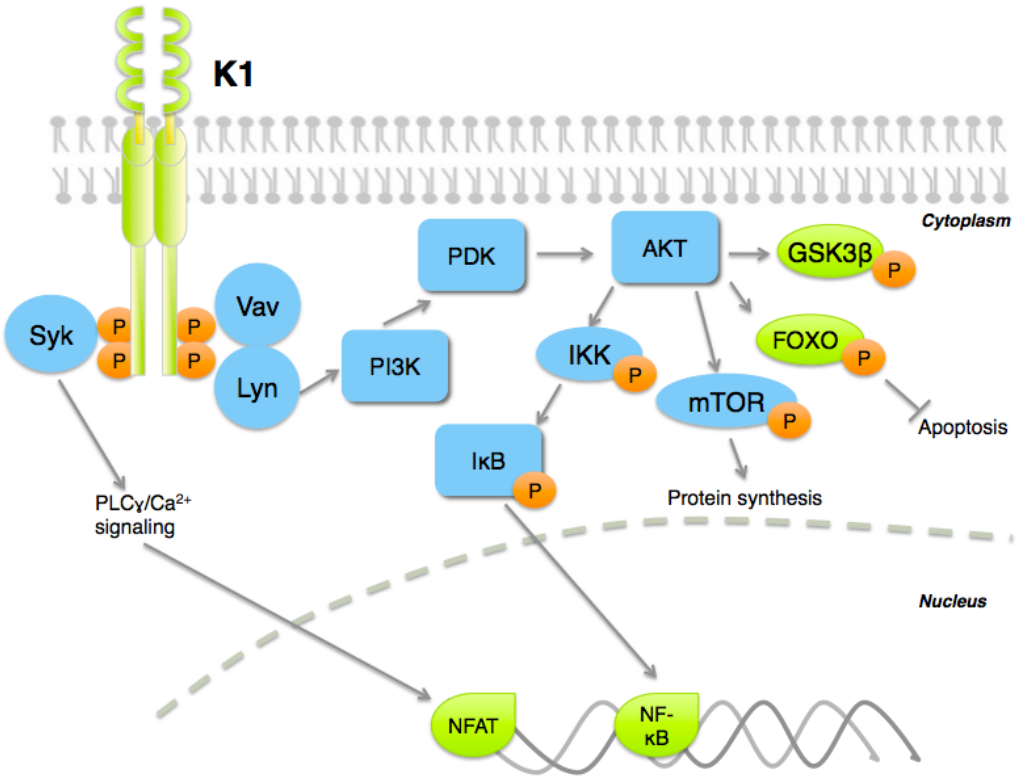

Figure 1: K1 activates PI3K/AKT/mTOR signaling.

In B lymphocytes, ectopic K1 expression was found to activate AKT signaling in two simultaneous ways: K1 expression induced AKT phosphorylation on Thr^{308} and Ser^{473}, and also inactivation of the negative regulator PTEN (106). K1-mediated AKT activation also induced the cytoplasmic sequestration of the FOXO family of transcription factors, and subsequent reduction of Fas ligand expression, thus conferring a cell survival advantage to K1-expressing cells (106). K1 also stabilizes AKT through interaction with the cellular chaperones heat shock protein 90 β (Hsp90β) and the endoplasmic reticulum-associated Hsp40 (Erdj3/Dnajb11) (108), both of which are important for enhancing the signaling function of AKT (109, 110). Chaperone-mediated stabilization of AKT by K1 is essential for sustained signaling, as their inhibition induced caspase-3 dependent apoptosis in FasL-treated, K1-expressing cells (108).

K1's cytoplasmic tail contains an immunoreceptor tyrosine-based activation motif (ITAM) (100, 101). ITAMs are essential for signal transduction in immune cells, therefore are found on immunoreceptors, for e.g., CD79 α and β, subunits of the B cell receptor complex. Upon ligand binding, the tyrosine residues on ITAMs are phosphorylated, which allow for docking of SH2-domain containing molecules (Figure 1). Downstream transduction of the extracellular signal induces calcium mobilization from the endoplasmic reticulum, and activates the lymphocyte. K1 does not require ligand binding to induce signaling, thus functions as a constitutively active ITAM (111). The K1 ITAM is closely conserved across KSHV strains, indicating the importance of this motif for K1 function (112, 113). The constitutive activity of the K1 ITAM activates a variety of

downstream signaling pathways that not only protect the infected cell, but also neighboring cells in a paracrine fashion. Notably, K1 also activates PI3K/AKT/mTOR signaling in endothelial cells (102, 114). Components of the K1 signalosome have been identified, and indicate that the K1 ITAM interacts with a diverse set of cellular signaling proteins (115). Overall, K1's interactions with cellular proteins augment global cellular signal transduction, activation of transcription facts such as NF-κB and AP-1, and induction of inflammatory cytokines (115).

Interactions of the K1 N-terminal domain with the BCR complex induce BCR sequestration within the endoplasmic reticulum (116). Because normal BCR signaling can potentially induce apoptosis, BCR sequestration preempts this possibility, thus conferring a long-term survival advantage to the infected cell.

K1 expression is upregulated during viral reactivation from latency. Lytic replication may induce pro-apoptotic signals resulting from immune detection of replicating KSHV. Viral replication places increased demands for energy and nutrients on the cell (117) which may be unmet, and possibly activating apoptosis resulting from stress signaling. These collective pro-apoptotic signals can be subverted by K1 expression (106, 108), thereby supporting productive lytic replication and further dissemination of KSHV. Moreover, activating signaling downstream of PI3K can also re-start protein translation and metabolic programs, halted as a result of apoptosis induction, ensuring that raw materials for production of progeny virions are plentiful.

KSHV vGPCR

KSHV ORF74 encodes a viral G-protein coupled receptor (vGPCR), a seven-pass transmembrane protein homologous to the cellular IL-8 chemokine receptor (13). vGPCR is a ligand-independent receptor expressed during the lytic cycle. Genes expressed during lytic replication are potently transformative, as they exert strong survival signals to prolong the life of the host cell, which ultimately dies as a result of viral replication and associated cellular stress. vGPCR has potent transforming properties; it promotes focus formation in mouse NIH3T3 cells, and vGPCR-expressing cells form tumors in nude mice (118). Human umbilical vein endothelial cells (HUVECs) are immortalized by vGPCR expression, and also protected from apoptosis induced by serum-starvation (119). In various mouse models, vGPCR expression leads to formation of vascular tumors and KS-like angioproliferative lesions, with cell surface markers and circulating cytokine profiles resembling KS (120-122).

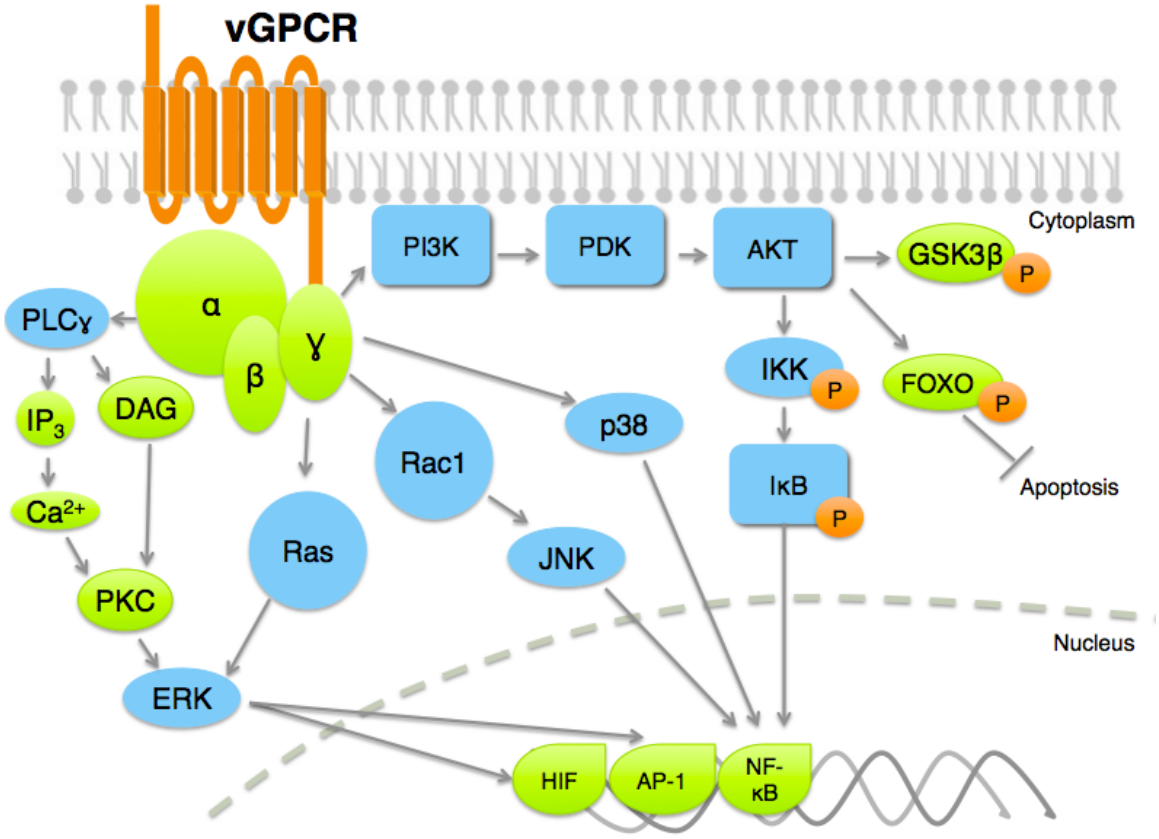

Figure 2: vGPCR broadly activates PI3K and MAPK pathways. This leads to increased production of cytokines and growth factors, with a concurrent increase in cell proliferation, and inhibition of apoptotic pathways. Orange circles denote phosphorylation.

Being a constitutively active receptor protein, vGPCR can function without the need of ligand binding (123). However, vGPCR is capable of binding members of both CXC and CC chemokine families (124). Some CXC chemokines, such as GRO-α and IL-8, enhance vGPCR signaling (125), whereas Interferon ɣ-inducible 10-kDa protein (IP-10/CXCL10) and stromal cell-derived factor 1 α (SDF-1α) inhibit vGPCR signaling (126). IL-8 is a major mediator of inflammation, and recruits neutrophils, basophils and T cells. IL-8 released during immune response to lytic KSHV replication may enhance the function of vGPCR in lytically infected cells, thereby providing anti-apoptotic signaling to delay the death of the infected cell. More puzzling is why SDF-1/CXCL12, a stimulator of B-cell progenitor proliferation, inhibits vGPCR activity (126). However, since vGPCR is primarily expressed during the lytic cycle, this might not have a consequence for latently infected B cells.

KSHV vGPCR activates a plethora of cellular signaling molecules as well as transcription factors, by means of which it promotes transformation in endothelial, epithelial and fibroblast cells (Figure 2). VGPCR activates pathways such as PLC/PKC, Pyk2/Lyn, ERK, p38, and JNK, downstream of which are transcription factors that control many growth- and angiogenesis-promoting genes. For e.g., HIF-1α activation resulting from vGPCR-dependent p38 and MAPK signaling activates the vascular endothelial growth factor (VEGF) promoter (127). vGPCR also activates AP-1, NF-AT and NF-κB transcription factors, which in turn promote expression of a panoply of pro-inflammatory cytokines, growth factors and adhesion molecules (119, 128-130). The vGPCR-

mediated secretion of such a wide array of factors may enhance proliferation and survival in neighboring, uninfected cells in a paracrine manner (Figure 3). Indeed, a recent report demonstrates that cytokines secreted by a small number of vGPCR+ tumor cells activates signaling pathways in neighboring cells, converging on mTOR-dependent VEGF upregulation (131). Inhibiting paracrine mTOR activity in non-expressing cells abrogated the tumor promoting activities of GPCR-expressing cells *in vivo*. On the other hand, its expression may directly induce transformation of the vGPCR-expressing cell, due to upregulated signaling resulting from the same secreted factors. These two methods of transformation may act in concert, rather than in isolation, leading to transformation of both the infected and bystander cells.

PI3K/AKT/mTOR signaling is a common pathway downstream of many growth factor and cytokine receptors. In particular, the tissue-restricted γ isoform of PI3K is crucial for relaying vGPCR signaling downstream to AKT/mTOR, in endothelial cells (132). Paracrine secretions resulting from vGPCR expression activate PI3K/AKT/mTOR signaling (for e.g. VEGF), and moreover, vGPCR directly activates AKT in a PI3K-dependent manner (119).

vGPCR expression in the B cell neoplasms PEL and MCD exhibits a distinct gene expression profile compared to endothelial cells (133), and is also characterized by elevated PI3K/AKT and ERK/p38 MAPK signaling. Ectopic vGPCR expression in B cells activates several transcription factors: AP-1, CREB, NFAT and NF-κB, thereby promoting cell survival, although the mechanisms of activation of these transcription factors differ (134).

As mentioned above, although capable of constitutive activity, vGPCR can also signal by coupling with cellular $G\alpha_q$ and $G\alpha_i$ subunits (135), further amplifying PI3K/AKT signaling, as both $G\alpha_q$ and $G\alpha_i$ subunits signal through this pathway (136). Additionally, vGPCR-mediated activation of AP-1 and CREB, (but not NF-κB and NFAT) in B cells was found to be dependent on PI3K/AKT (135). VGPCR also activates endogenous Lyn tyrosine kinase in a $G\alpha_i$- and PI3K-dependent manner. Pharmacologic and genetic ablation of Src family kinases abolished AP-1 and CREB transcriptional activity, confirming that these transcription factors are activated by vGPCR through a $G\alpha_i$-PI3K/AKT-Src signaling axis. Further, this study showed that Src inhibitors decreased AKT phosphorylation in PEL, indicating that in B cells, Src may be upstream rather than downstream of PI3K/AKT signaling, suggestive of a positive feedback loop. Importantly, this study revealed that NF-κB and NFAT are not activated in a PI3K/AKT dependent manner in B cells (135). Subsequent studies indicated that the Ras-related small G protein Rac1 may be required for NF-κB activation *via* vGPCR (137). For an excellent review describing the role of NF-κB signaling in the KSHV life cycle please see (78).

The previous paragraphs describe the extent to which vGPCR activates cellular signaling. The lytically-replicating, vGPCR-expressing cell activates transcription factors and signaling entities within the infected cell; induction of secreted factors further amplifies signaling in neighboring cells, with the collective outcome of enhanced proliferation and sustained survival.

VIRAL INTERLEUKIN-6 (vIL-6)

Viral interleukin-6 (vIL-6), encoded by ORF-K2, is a homologue of the human IL-6 (hIL-6) cytokine, with 24.8% amino acid sequence similarity and 49.7% sequence identity (138). Functionally, vIL-6 is a faithful mimic of hIL-6, as vIL-6 secreted by KSHV-infected B lymphocytes supports proliferation of B-lymphocytes and also hIL-6 dependent mouse myeloma cell lines, demonstrating its functional similarity (138-140). All latently infected cells express vIL-6, with upregulated expression during lytic replication (25, 103, 141, 142). Similar to its cellular counterpart, vIL-6 signaling activates the JAK/STAT, MAPK and H7-sensitive pathways (143). Although v- and hIL-6 have similar sequence and function, their receptor usage is substantially different. Cellular IL-6 requires two IL-6 receptor subunits: IL-6Rα and gp130. However, vIL-6 is capable of signaling via only the gp130 subunit (144). Thus KSHV vIL-6 circumvents the requirement for a second receptor, thereby subverting cellular checks against uncontrolled, exuberant signaling.

vIL-6 is implicated as a linchpin in the pathology of all KSHV-associated malignancies, due to its angiogenic properties, as well as potent proliferative and survival effects. VIL-6 is detected, in increasing order, in KS, PEL and MCD patients (145, 146). However, only a subset of cells express vIL-6 in KS tissue (Cannon 1999, Parravicini 2000, Staskus 1999), suggesting that like vGPCR, vIL-6 effects are primarily paracrine, activating proliferative signaling pathways in bystander cells. Similarly, in MCD, vIL-6 is expressed in lymphoid cells in mantle

zones, and hIL-6 was detected in germinal centers (Cannon 1999, Parravicini 2000, Staskus 1999).

Injection of vIL-6-expressing NIH3T3 cells into athymic mice led to tumor formation, hematopoiesis, and plasmacytosis, all of which were absent in control mice. Tumors derived from vIL-6-expressing cells were highly vascularized, and correlated with elevated secreted VEGF (147). A recent report of transgenic mice constitutively expressing vIL-6 describes elevated serum vIL-6, increased levels of phospho-STAT3 levels in the spleen and lymph nodes, and a manifestation of human MCD-like symptoms (148). Importantly, when vIL-6 was constitutively expressed in a mouse lacking endogenous hIL-6, no MCD-like symptoms were observed. These studies indicate that vIL-6 and hIL-6 cooperate in the pathogenesis of MCD.

Lymphatic reprogramming resulting from KSHV infection of endothelial cells also occurs via engagement of the gp130 receptor (149). Specifically, gp130 receptor activation leads to the activation of JAK2/STAT3 and PI3K/AKT pathways. Activated AKT promotes the expression of Prox1, a lymphatic transcription factor necessary for VEGFR-3 induction, and Prox1 itself is known to potentiate the lymphatic reprogramming of endothelial cells upon *de novo* KSHV infection (150). Furthermore, STAT3 amplifies signaling cascades by activating gp130 receptor expression. Podoplanin, another marker of lymphatic reprogramming, is also expressed following KSHV activation of gp130. While not found to be necessary, vIL-6 is sufficient to induce lymphatic reprogramming in endothelial cells infected with KSHV (151). Thus, through gp130, vIL-6 can

enhance lymphangiogenesis and lymphatic reprogramming in both paracrine and autocrine manner.

ORF45

ORF45 is an immediate early gene product that plays a crucial role in lytic replication. ORF45 expression is induced upon entry into the lytic cycle and subsequently increases as the life cycle advances, with expression restricted to the cytoplasm. ORF45 is incorporated into the KSHV virion (152), suggesting that it may immediately influence the environment of the *de novo* infected host cell, exemplified by the observation that ORF45 acutely inhibits type 1 IFN induction upon infection. ORF45 mediates the inhibition of innate immune responses by sequestering the cellular transcription factor, interferon regulatory factor-7 (IRF-7), to the cytoplasm (153).

In addition to the modulation of cellular anti-viral responses, ORF45 also exerts an effect upon the cellular signaling *milieu*. Cellular MAPKs are activated during KSHV infection (94, 154), and ORF45 interacts with two important MAPK substrates RSK1 and RSK2, which are both p90 ribosomal S6 kinase (RSK) family members. RSK1 and 2 not only phosphorylate ORF45, but their association further augments the kinase activities of these two proteins (155, 156).

Another consequence of formation of the RSK/ERK/ORF45 complexes is phosphorylation of ribosomal protein S6, and eIF4b, an important member of the complex that recruits ribosomes to 5’ capped mRNAs. Phosphorylated eIF4b

complexes with eIF4a, eIF4g, 4E-BP1, and 5' capped mRNAs to recruit the 40S ribosome, thereby initiating protein translation. Normally, S6 and eIF4B are activated by p70 S6 kinase, itself regulated by upstream mTOR signaling; eIF4B is also a target of the p90 S6 kinase, regulated by MAPK signaling. However, ORF45 allows for eIF4B phosphorylation in an mTOR- and MAPK-independent manner. These observations indicate that protein translation may occur upon KSHV infection in an mTOR-independent manner. They also demonstrate the existence of unique viral strategies to directly enhance protein translation despite a situation within the host cell that may potentially be inhibitory to protein translation.

KSHV-MEDIATED TRANSFORMATION AND THE HALLMARKS OF CANCER

The hallmarks of cancer are a conceptual framework to understand the multistep progression of cancer (157, 158). The hallmarks of cancer take into account that neoplasms, rather than being a singular, isolated entity, are a collection of distinct cell types, comprised of tumor cells, tumor-associated stroma as well as normal, non-cancerous cells. These diverse cell types cooperate to collectively confer hallmark capabilities, which further enhance the development of a tumor microenvironment. Acquisition of one hallmark by a normal cell facilitates the development of others, thus increasing the likelihood of cellular transformation. The classical hallmarks of cancer are sustained proliferation signaling, evasion of growth suppression, replicative immortality, induction of angiogenesis, evasion of cell death, and invasion and metastasis. Three additional hallmarks have also been recently proposed: deregulation of

cellular energetics, tumor-promoting inflammation, and avoidance of immune recognition.

The endpoint of the productive KSHV life cycle is the production of new virions that can subsequently infect new cells, and begin another round of the viral life cycle. To successfully replicate and generate progeny virions, KSHV must evade immune recognition during latency, and also counter antiviral and death-inducing signaling during lytic replication. A plethora of viral proteins successfully grant invisibility from immune recognition, and prolong the life of the infected cell by altering cellular signaling, as described above.

Sustained proliferative signaling: Proliferation is a carefully controlled process in normal cells. Uncontrolled growth would lead to nutrient scarcity as well as overgrowth in the physical niche. Like other cancer cells, KSHV encodes genes that activate cellular proliferative pathways both in a paracrine and autocrine fashion (Figure 3) (101, 106, 107). This hallmark is particularly evident in KS, as not all cells within the lesion are KSHV-positive; expression of viral and cellular factors bestows neighboring cells with enhanced proliferative capabilities. Sustained proliferation results from growth factor binding to their cognate cell surface receptors, and subsequent signaling that further promotes expression of the same growth factors and receptors, in a positive feedback loop.

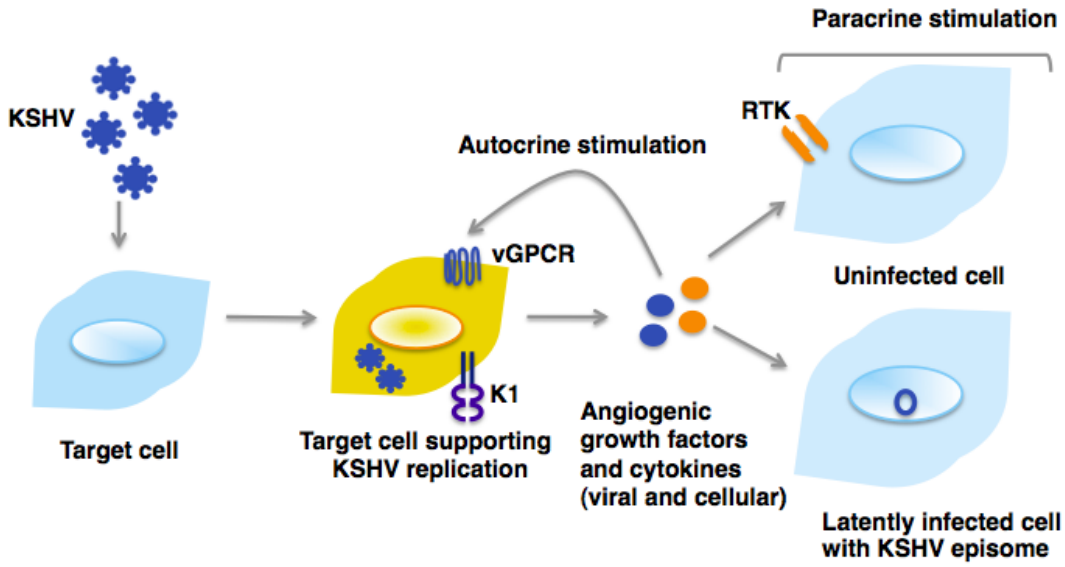

Figure 3: Viral proteins enhance cell proliferation by autocrine and paracrine mechanisms. Viral and cellular cytokines and growth factors can activate signaling pathways within the cell they are secreted from (autocrine), or on distant cells that may either be uninfected or latently-infected with KSHV (paracrine). RTK= receptor tyrosine kinase.

Evasion of growth suppression and cell death: Powerful growth inhibitory programs are intrinsic to the host cell to prevent uncontrolled proliferation. Hyperproliferation can trigger cell senescence via activation of checkpoint signaling. Alternatively, apoptosis may also result from aberrant oncogene activation. Immune cells that detect virally infected cells may also transduce apoptotic signals to facilitate viral clearance.

KSHV encodes several proteins to protect the infected cell from these growth-suppressive and cell death-inducing signals, during latency and the lytic cycle. For example, vCyclin, a homolog of cellular Cyclin D forces quiescent rodent cells to enter the S-phase to overcome RB-mediated growth arrest

induced by CDK inhibitors (159). In the same vein, cells supporting lytic replication do not die prematurely despite increased cellular stress, due to the presence of viral proteins that inhibit apoptotic signaling. For example, K1-dependent, AKT-mediated sequestration of FOXO transcription factors and inactivation of Bad can protect B cells from apoptosis (106). Similarly, vFLIP expression also protects cells from apoptosis by upregulating NF-κB transcription and pro-survival factors (160-162). In the context of the whole virus, KSHV-infected primary HUVEC cells are more resistant to apoptotic stimuli such as etoposide, staurosporine and serum-starvation, compared to uninfected cells (163). Thus, evasion of both cell death and growth suppression by viral proteins expressed during latency and the lytic cycle, contribute to the development of KSHV-associated cancer.

Replicative immortality: Somatic cells within the body divide a finite number of times, i.e., they have limited replicative potential. Upon reaching their limit, normal cells senesce and cannot proliferate any further. The number of cell divisions is governed in part by telomeres, which are stretches of repetitive DNA at the ends of chromosomes that shorten after every cell division. However, cancer cells can replicate indefinitely owing to activation of one of two pathways: activation of human telomerase (hTERT), or the activation of an alternative (ALT) pathway, both of which lead to lengthening of telomeres. KSHV LANA has been shown to increase the expression of the catalytic subunit of telomerase, hTERT by upregulating its promoter, thereby contributing to replicative immortality (164).

Additionally, K1 expression in primary HUVECs endows replicative immortality, mediated by activation of the ALT pathway (102).

Induction of angiogenesis: All cells, whether normal or otherwise, require a reliable blood supply to provide nutrients and oxygen, and to eliminate carbon dioxide and metabolic waste products. Tumor cells promote formation of vasculature by activating angiogenesis, as well as remodeling of existing vasculature and sprouting new vessel growth. Often, tumor-associated vessels are erratically branched, aberrantly sized, excessively convoluted and structurally unsound, all resulting from hyperactivated induction of angiogenic factors (165, 166). Vascular endothelial growth factor (VEGF) is a key mediator of angiogenesis, and its expression is governed by upstream signaling pathways such as PI3K/AKT (167). Other inflammatory cytokines can also drive angiogenesis. KSHV vGPCR induces VEGF and VEGF receptor 2 secretion in endothelial cells (168). Moreover, K1 expression in epithelial and endothelial cells also induces secretion of VEGF and the invasion factor MMP-9 (discussed below), as does KSHV infection of endothelial cells (114, 163).

Invasion and metastasis: Invasion and metastasis are multistep processes that begin with local invasion, due to cancer cells exceeding their occupied niche, resulting from hyperproliferation. Cancer cells that weakly adhere to neighboring cells easily escape and intravasate nearby blood vessels and lymph nodes and travel to distal sites through vasculature and lymphatics (169). Some cells escape these vessels and enter a new environment, often substantially different than the first, forming micro metastases; in the final stage, these grow into larger

masses that colonize the new niche, generating metastases (169). Activation of a developmental regulatory program termed “epithelial-mesenchymal transition” (EMT) bestows onto epithelial cells the ability to invade and metastasize (170, 171). EMT includes a transcriptional and signaling program, and a similar, “endothelial to mesenchymal” (EndMT) transition occurs in the context of KSHV infection (172). vFLIP and vGPCR activate the Notch signaling pathway, resulting in secretion of the mesenchymal marker membrane type-1 matrix metalloprotease (MT1-MMP), granting invasive properties to KSHV-positive cells. Significantly, MT1-MMP was found co-localized with LANA in KS biopsies. These data suggest that the presence of heterogeneous cell types within KS lesions results from viral proteins driving endmt within infected cells, moreover, bestowing them invasion capabilities, and the creation of a microenvironment that benefits viral dissemination.

Deregulation of cellular energetics: Recent evidence suggests that the reprogramming of cellular energetics and metabolism is an emerging hallmark of cancer (reviewed in (158)). Fueling the uncontrolled proliferation and cell division of tumor cells requires rewiring of normal cellular energetics. Normal cells, in aerobic conditions, utilize glucose to first generate pyruvate and ATP by glycolysis, and subsequent mitochondrial oxidative phosphorylation (OXPHOS). Anaerobic conditions result in a switch to glycolysis, which is relatively inefficient and generates smaller quantities of ATP, which may or may not be accompanied by reduced OXPHOS. Otto Warburg observed that cancer cells preferentially oxidize glucose by glycolysis even in aerobic conditions, limiting their energy

production; this phenomenon is termed the Warburg effect, or aerobic glycolysis (173). The Warburg effect is an adaptation of tumors growing in hypoxic conditions to generate ATP. KSHV infection of endothelial cells induced the Warburg effect, and glycolysis inhibition of latently-infected cells leads to apoptosis (174). Moreover, we reported that in KSHV-infected PEL, aerobic glycolysis fuels *de novo* lipid synthesis to generate precursors for daughter cells, explaining the significance of upregulating an energetically unfavorable biochemical process (175). This study also demonstrated that glycolysis and fatty acid synthesis (FAS) occur in a PI3K/AKT-dependent manner, providing a mechanism for metabolic reprogramming in PEL. Further, PEL viability was found to be susceptible to FAS inhibitors, revealing a new molecular therapeutic target.

Immune evasion: An ever-watchful immune system surveys the body for signs of nascent neoplasms, and eliminates such cells. The ability to escape immune surveillance is a frequent consequence of genetic instability and aberrant signaling in tumors. KSHV-associated tumors are even more able to hide from the immune system as viral protein expression can subvert various aspects of the innate and adaptive immune response. Viral proteins e.g. KSHV vIRFs, K3, K5, etc. Inhibit immune signaling, protecting the infected cell from host detection. For example, the K3 and K5 viral proteins can downregulate both class I and II major histocompatibility complexes (MHC), enhancing the immune-evasion capabilities of infected cells (176, 177). The KSHV vIRFs also contribute to immune evasion (reviewed in (178)). As discussed in previous sections,

apoptotic signaling resulting from immune detection is also potently inhibited by viral protein expression.

Tumor-promoting inflammatory microenvironment: Similar to non-viral tumors, KSHV-associated lesions are infiltrated by a large number of immune cells. KSHV-associated neoplasms are also characterized by elevated local and systemic levels of inflammatory cytokines and chemokines, further augmented by virally-encoded cytokines such as vIL-6, vMIPs/vCCLs and vOX2. KSHV infection also upregulates cyclooxygenase-2 (COX-2), an enzyme that converts arachidonic acid into prostaglandins, which are inflammation mediators (179). COX-2 is essential for survival of KSHV-infected cells, and viral genome maintenance, both of which are susceptible to COX-2 pharmacological inhibitors. Creation of an inflammatory environment is functionally significant, since it activates signaling in surrounding tissues, and also recruits readily-infectable cell types to facilitate viral dissemination.

EXPLOITING THE PI3K/AKT/mTOR PATHWAY TO TREAT KSHV-ASSOCIATED MALIGNANCIES

Individual KSHV proteins can activate PI3K/AKT/mTOR signaling in B cells and endothelial cells, and this pathway is important for both lytic and latent phases of the KSHV life cycle. Additionally, both KS and PEL display highly activated AKT and mTOR kinases (86, 119, 180). Because aberrant PI3K/AKT/mTOR signaling is a characteristic of almost all human cancers, a plethora of small molecule inhibitors exist that target various nodes of this pathway. These inhibitors include allosteric inhibitors such as rapamycin and

FK506, and also ATP-competitive small molecule kinase inhibitors that usually target the kinase activity of specific proteins.

Rapamycin is a macrolide that binds to FKBP12, a component of the mTOR signaling complex (mTORc), and is an allosteric inhibitor (181). Rapamycin is commonly used as an oral immunosuppressant for solid organ transplant recipients, as it inhibits the production and secretion of IL-2 in T cells, thus blocking T cell proliferation. Moreover, rapamycin blocks protein translation. Therefore, rapamycin and its derivative compounds called “rapalogs” are extensively studied for their therapeutic benefit in a variety of human cancers, including those associated with viral infection (182).

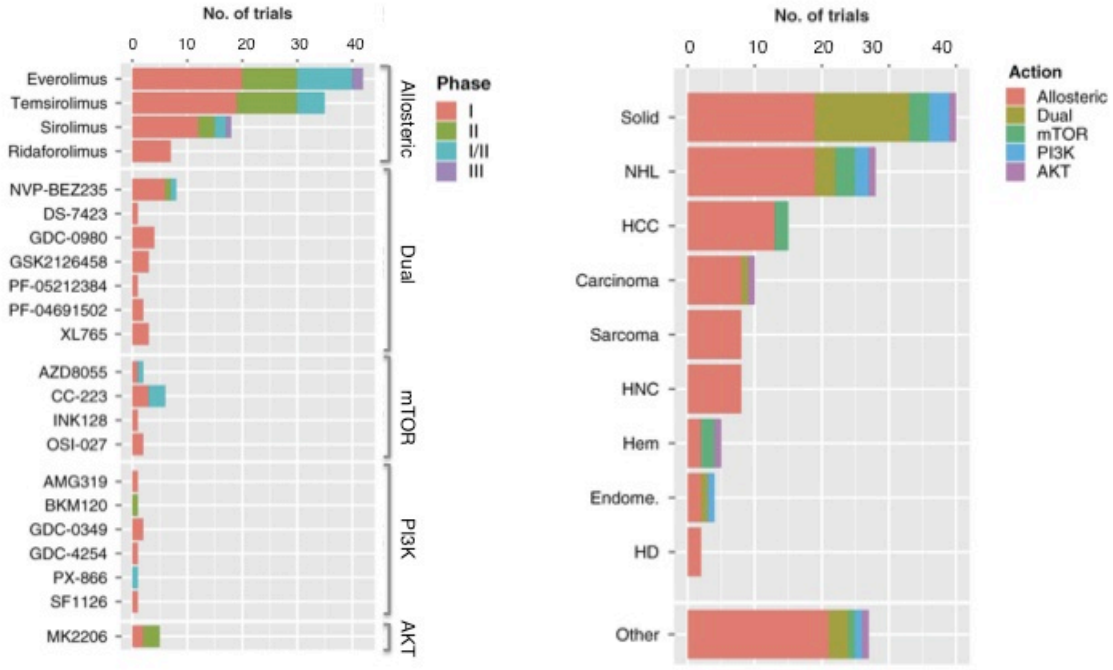

A B

Figure 4: Current NCI-registered clinical trials using inhibitors of the PI3K/AKT/mTOR pathway. (A) Stacked bar chart showing the number of trials (on the horizontal axis) for different inhibitors (on the vertical axis), grouped by mechanism of action. Different colors indicate trial phases. (B) Stacked bar chart showing number of trials (on the horizontal axis) for different cancer categories (on the vertical axis). Different colors indicate discrete classes of inhibitors. NHL: non-Hodgkin lymphoma; HCC: any liver cancer including hepatocellular carcinoma; HNC: head and neck cancer; Hem: hematopoietic malignancies including multicentric Castleman disease and leukemia; endome: endometrial cancer; HD: Hodgkin disease. Figure is adapted from (Dittmer et al, 2012).

Figure 4 graphically summarizes the various PI3K/AKT/mTOR targeted therapeutics currently under trial for viral cancers. Rapamycin treatment resolved transplant-associated Kaposi sarcoma (183), a seminal finding that has prompted many other studies which confirm that rapamycin is an effective anti-cancer drug for PEL (86). Specifically, rapamycin is effective at halting the proliferation of PEL in cell culture, and, in a xenograft model of PEL, rapamycin inhibits tumor formation and induces tumor regression (86). One drawback of rapamycin therapy is that it slows tumor growth (tumorstatic), rather than killing tumor cells (tumortoxic). Therefore, single agent therapy with rapamycin alone has limited benefit in a majority of cancers.

A class of AKT inhibitors called alkyllysophospholipids (for e.g. Miltefosine and Perifosine) also inhibited PEL cell proliferation both *in vitro* and *in vivo* (85). Moreover, NVP-BEZ235, a dual inhibitor of both PI3K and mTOR kinases, is a potent inhibitor of PEL cell proliferation and tumor formation in xenograft mouse models. NVP-BEZ235 treatment induced high levels of apoptosis in PEL (85).

Thus, it appears that the PI3K/AKT/mTOR signaling pathway is essential for the survival of both PEL and KS tumors. It is of critical importance to evaluate whether long-term treatment with small molecule inhibitors breeds resistance to pathway-focused inhibitors. Selective pressure resulting from these inhibitors could drive expression of viral proteins that may contribute to resistance. Therefore in the future, it will be important to investigate whether as yet uncharacterized KSHV proteins influence PI3K/AKT/mTOR signaling, both in the context of latency and lytic viral replication.

CONCLUSIONS

KSHV is an obligate intracellular parasite, and is a salient example of a successful pathogen. Viral manipulation of cellular pathways enhances the synthesis and secretion of growth factors and cytokines of both viral and cellular origin, which in turn supports angiogenesis and proliferation. These secreted growth factors and cytokines can also activate pro-survival, proliferative and angiogenic processes in uninfected or latently-infected cells (Figure 3). Thus, by manipulating cellular signaling, KSHV viral proteins create an environment beneficial for both lytic and latent phases of the viral life cycle. Given the central role it plays in cell survival and proliferation, it comes as no surprise that KSHV targets the PI3K/AKT/mTOR signaling pathway at multiple nodes, in order to induce and sustain a survival and proliferative signal that is advantageous for the virus.

CONFLICT OF INTEREST

The authors have no conflict of interest to disclaim.

REFERENCES

1. **Chang Y, Cesarman E, Pessin MS, Lee F, Culpepper J, Knowles DM, Moore PS.** 1994. Identification of herpesvirus-like DNA sequences in AIDS-associated Kaposi's sarcoma. Science **266:**1865-1869.

2. **Cesarman E, Chang Y, Moore PS, Said JW, Knowles DM.** 1995. Kaposi's sarcoma-associated herpesvirus-like DNA sequences in AIDS- related body-cavity-based lymphomas. N Engl J Med **332:**1186-1191.

3. **Gessain A, Sudaka A, Briere J, Fouchard N, Nicola MA, Rio B, Arborio M, Troussard X, Audouin J, Diebold J, de The G.** 1996. Kaposi sarcoma-associated herpes-like virus (human herpesvirus type 8) DNA sequences in multicentric Castleman's disease: is there any relevant association in non-human immunodeficiency virus-infected patients? Blood **87:**414-416.

4. **Murphy K, Travers P, Walport M, Janeway C.** 2008. Janeway's immunobiology, 7th ed. Garland Science, New York.

5. **Montecino-Rodriguez E, Dorshkind K.** 2012. B-1 B cell development in the fetus and adult. Immunity **36:**13-21.

6. **Green I, Espiritu E, Ladanyi M, Chaponda R, Wieczorek R, Gallo L, Feiner H.** 1995. Primary lymphomatous effusions in AIDS: a morphological, immunophenotypic, and molecular study. Mod Pathol **8:**39-45.

7. **Nador RG, Cesarman E, Chadburn A, Dawson DB, Ansari MQ, Sald J, Knowles DM.** 1996. Primary effusion lymphoma: a distinct clinicopathologic entity associated with the Kaposi's sarcoma-associated herpes virus. Blood **88:**645-656.

8. **Arvanitakis L, Mesri EA, Nador RG, Said JW, Asch AS, Knowles DM, Cesarman E.** 1996. Establishment and characterization of a primary effusion (body cavity-based) lymphoma cell line (BC-3) harboring kaposi's sarcoma-associated herpesvirus (KSHV/HHV-8) in the absence of Epstein-Barr virus. Blood. **88:**2648-2654.

9. **Cotter MAI, Robertson ES.** 1999. The latency-associated nuclear antigen tethers the Kaposi's sarcoma-associated herpesvirus genome to host chromosomes in body cavity-based lymphoma cells. Virology **264:**254-264.

10. **Ballestas ME, Chatis PA, Kaye KM.** 1999. Efficient persistence of extrachromosomal KSHV DNA mediated by latency- associated nuclear antigen. Science **284:**641-644.

11. **Schwam DR, Luciano RL, Mahajan SS, Wong L, Wilson AC.** 2000. Carboxy terminus of human herpesvirus 8 latency-associated nuclear antigen mediates dimerization, transcriptional repression, and targeting to nuclear bodies. J Virol **74:**8532-8540.

12. **Garber AC, Shu MA, Hu J, Renne R.** 2001. DNA binding and modulation of gene expression by the latency-associated nuclear antigen of Kaposi's sarcoma-associated herpesvirus. J Virol **75:**7882-7892.

13. **Cesarman E, Nador RG, Bai F, Bohenzky RA, Russo JJ, Moore PS, Chang Y, Knowles DM.** 1996. Kaposi's sarcoma-associated herpesvirus contains G protein-coupled receptor and cyclin D homologs which are expressed in Kaposi's sarcoma and malignant lymphoma. J Virol **70:**8218-8223.

14. **Ambinder RF, Cesarman E.** 2007. Clinical and pathological aspects of EBV and KSHV infection.

15. **Gaidano G, Gloghini A, Gattei V, Rossi MF, Cilia AM, Godeas C, Degan M, Perin T, Canzonieri V, Aldinucci D, Saglio G, Carbone A, Pinto A.** 1997. Association of Kaposi's sarcoma-associated herpesvirus-positive primary effusion lymphoma with expression of the CD138/syndecan-1 antigen. Blood. **90:**4894-4900.

16. **Luan SL, Boulanger E, Ye H, Chanudet E, Johnson N, Hamoudi RA, Bacon CM, Liu H, Huang Y, Said J, Chu P, Clemen CS, Cesarman E, Chadburn A, Isaacson PG, Du MQ.** 2010. Primary effusion lymphoma: genomic profiling revealed amplification of SELPLG and CORO1C encoding for proteins important for cell migration. J Pathol **222:**166-179.

17. **Laszik Z, Jansen PJ, Cummings RD, Tedder TF, McEver RP, Moore KL.** 1996. P-selectin glycoprotein ligand-1 is broadly expressed in cells of myeloid, lymphoid, and dendritic lineage and in some nonhematopoietic cells. Blood **88:**3010-3021.

18. **Roadcap DW, Clemen CS, Bear JE.** 2008. The role of mammalian coronins in development and disease. Subcell Biochem **48:**124-135.

19. **Roy D, Sin SH, Damania B, Dittmer DP.** 2011. Tumor suppressor genes FHIT and WWOX are deleted in primary effusion lymphoma (PEL) cell lines. Blood **118:**e32-39.

20. **Soulier J, Grollet L, Oksenhendler E, Cacoub P, Cazals-Hatem D, Babinet P, d'Agay MF, Clauvel JP, Raphael M, Degos L, et al.** 1995. Kaposi's sarcoma-associated herpesvirus-like DNA sequences in multicentric Castleman's disease. Blood **86:**1276-1280.

21. **Dupin N, Diss TL, Kellam P, Tulliez M, Du MQ, Sicard D, Weiss RA, Isaacson PG, Boshoff C.** 2000. HHV-8 is associated with a plasmablastic variant of Castleman disease that is linked to HHV-8-positive plasmablastic lymphoma. Blood **95:**1406-1412.

22. **Du MQ, Liu H, Diss TC, Ye H, Hamoudi RA, Dupin N, Meignin V, Oksenhendler E, Boshoff C, Isaacson PG.** 2001. Kaposi sarcoma-associated herpesvirus infects monotypic (IgM lambda) but polyclonal naive B cells in Castleman disease and associated lymphoproliferative disorders. Blood **97:**2130-2136.

23. **Dupin N, Fisher C, Kellam P, Ariad S, Tulliez M, Franck N, van Marck E, Salmon D, Gorin I, Escande JP, Weiss RA, Alitalo K, Boshoff C.** 1999. Distribution of human herpesvirus-8 latently infected cells in Kaposi's sarcoma, multicentric Castleman's disease, and primary effusion lymphoma. Proc Natl Acad Sci U S A **96:**4546-4551.

24. **Katano H, Suda T, Morishita Y, Yamamoto K, Hoshino Y, Nakamura K, Tachikawa N, Sata T, Hamaguchi H, Iwamoto A, Mori S.** 2000. Human

herpesvirus 8-associated solid lymphomas that occur in AIDS patients take anaplastic large cell morphology. Mod Pathol **13:**77-85.

25. **Parravicini C, Chandran B, Corbellino M, Berti E, Paulli M, Moore PS, Chang Y.** 2000. Differential viral protein expression in Kaposi's sarcoma-associated herpesvirus-infected diseases: Kaposi's sarcoma, primary effusion lymphoma, and multicentric Castleman's disease. Am J Pathol **156:**743-749.

26. **Jenner RG, Maillard K, Cattini N, Weiss RA, Boshoff C, Wooster R, Kellam P.** 2003. Kaposi's sarcoma-associated herpesvirus-infected primary effusion lymphoma has a plasma cell gene expression profile. Proc Natl Acad Sci U S A **100:**10399-10404.

27. **Hassman LM, Ellison TJ, Kedes DH.** 2011. KSHV infects a subset of human tonsillar B cells, driving proliferation and plasmablast differentiation. J Clin Invest **121:**752-768.

28. **Yoshizaki K, Matsuda T, Nishimoto N, Kuritani T, Taeho L, Aozasa K, Nakahata T, Kawai H, Tagoh H, Komori T, et al.** 1989. Pathogenic significance of interleukin-6 (IL-6/BSF-2) in Castleman's disease. Blood **74:**1360-1367.

29. **Vieira J, Huang ML, Koelle DM, Corey L.** 1997. Transmissible Kaposi's sarcoma-associated herpesvirus (human herpesvirus 8) in saliva of men with a history of Kaposi's sarcoma. J Virol **71:**7083-7087.

30. **Ballon G, Chen K, Perez R, Tam W, Cesarman E.** 2011. Kaposi sarcoma herpesvirus (KSHV) vFLIP oncoprotein induces B cell transdifferentiation and tumorigenesis in mice. J Clin Invest **121:**1141-1153.

31. **Cobaleda C, Busslinger M.** 2008. Developmental plasticity of lymphocytes. Curr Opin Immunol **20:**139-148.

32. **West JA, Gregory SM, Sivaraman V, Su L, Damania B.** 2011. Activation of plasmacytoid dendritic cells by Kaposi's sarcoma-associated herpesvirus. J Virol **85:**895-904.

33. **Akula SM, Naranatt PP, Walia NS, Wang FZ, Fegley B, Chandran B.** 2003. Kaposi's sarcoma-associated herpesvirus (human herpesvirus 8) infection of human fibroblast cells occurs through endocytosis. J Virol **77:**7978-7990.

34. **Greene W, Gao SJ.** 2009. Actin dynamics regulate multiple endosomal steps during Kaposi's sarcoma-associated herpesvirus entry and trafficking in endothelial cells. PLoS Pathog **5:**e1000512.

35. **Inoue N, Winter J, Lal RB, Offermann MK, Koyano S.** 2003. Characterization of entry mechanisms of human herpesvirus 8 by using an Rta-dependent reporter cell line. J Virol **77:**8147-8152.

36. **Jarousse N, Chandran B, Coscoy L.** 2008. Lack of heparan sulfate expression in B-cell lines: implications for Kaposi's sarcoma-associated herpesvirus and murine gammaherpesvirus 68 infections. J Virol **82:**12591-12597.

37. **Kaleeba JA, Berger EA.** 2006. Broad target cell selectivity of Kaposi's sarcoma-associated herpesvirus glycoprotein-mediated cell fusion and virion entry. Virology **354:**7-14.

38. **Kaleeba JA, Berger EA.** 2006. Kaposi's sarcoma-associated herpesvirus fusion-entry receptor: cystine transporter xCT. Science **311:**1921-1924.

39. **Kliche S, Kremmer E, Hammerschmidt W, Koszinowski U, Haas J.** 1998. Persistent infection of Epstein-Barr virus-positive B lymphocytes by human herpesvirus 8. J Virol **72:**8143-8149.

40. **Krishnan HH, Naranatt PP, Smith MS, Zeng L, Bloomer C, Chandran B.** 2004. Concurrent expression of latent and a limited number of lytic genes with immune modulation and antiapoptotic function by Kaposi's sarcoma-associated herpesvirus early during infection of primary endothelial and fibroblast cells and subsequent decline of lytic gene expression. J Virol **78:**3601-3620.

41. **Lagunoff M, Bechtel J, Venetsanakos E, Roy AM, Abbey N, Herndier B, McMahon M, Ganem D.** 2002. De novo infection and serial transmission of Kaposi's sarcoma-associated herpesvirus in cultured endothelial cells. J Virol **76:**2440-2448.

42. **Naranatt PP, Krishnan HH, Svojanovsky SR, Bloomer C, Mathur S, Chandran B.** 2004. Host gene induction and transcriptional reprogramming in Kaposi's sarcoma-associated herpesvirus (KSHV/HHV-8)-infected endothelial, fibroblast, and B cells: insights into modulation events early during infection. Cancer Res **64:**72-84.

43. **Rappocciolo G, Hensler HR, Jais M, Reinhart TA, Pegu A, Jenkins FJ, Rinaldo CR.** 2008. Human herpesvirus 8 infects and replicates in primary cultures of activated B lymphocytes through DC-SIGN. J Virol **82:**4793-4806.

44. **Rappocciolo G, Jenkins FJ, Hensler HR, Piazza P, Jais M, Borowski L, Watkins SC, Rinaldo CR, Jr.** 2006. DC-SIGN is a receptor for human herpesvirus 8 on dendritic cells and macrophages. J Immunol **176:**1741-1749.

45. **Renne R, Blackbourn D, Whitby D, Levy J, Ganem D.** 1998. Limited transmission of Kaposi's sarcoma-associated herpesvirus in cultured cells. J Virol **72:**5182-5188.

46. **Buchkovich NJ, Yu Y, Zampieri CA, Alwine JC.** 2008. The TORrid affairs of viruses: effects of mammalian DNA viruses on the PI3K-Akt-mTOR signalling pathway. Nat Rev Microbiol **6:**266-275.

47. **Wen KW, Damania B.** 2010. Kaposi sarcoma-associated herpesvirus (KSHV): molecular biology and oncogenesis. Cancer Lett **289:**140-150.

48. **Sun R, Lin SF, Gradoville L, Yuan Y, Zhu F, Miller G.** 1998. A viral gene that activates lytic cycle expression of Kaposi's sarcoma-associated herpesvirus. Proc Natl Acad Sci U S A **95:**10866-10871.

49. **Lukac DM, Kirshner JR, Ganem D.** 1999. Transcriptional activation by the product of open reading frame 50 of Kaposi's sarcoma-associated herpesvirus is required for lytic viral reactivation in B cells. J Virol **73:**9348-9361.

50. **Yu Y, Black JB, Goldsmith CS, Browning PJ, Bhalla K, Offermann MK.** 1999. Induction of human herpesvirus-8 DNA replication and transcription by butyrate and TPA in BCBL-1 cells. J Gen Virol **80 (Pt 1):**83-90.

51. **Mercader M, Taddeo B, Panella JR, Chandran B, Nickoloff BJ, Foreman KE.** 2000. Induction of HHV-8 lytic cycle replication by inflammatory cytokines produced by HIV-1-infected T cells. Am J Pathol **156:**1961-1971.

52. **Chang J, Renne R, Dittmer D, Ganem D.** 2000. Inflammatory cytokines and the reactivation of Kaposi's sarcoma-associated herpesvirus lytic replication. Virology **266:**17-25.

53. **Wilson SJ, Tsao EH, Webb BL, Ye H, Dalton-Griffin L, Tsantoulas C, Gale CV, Du MQ, Whitehouse A, Kellam P.** 2007. X box binding protein XBP-1s transactivates the Kaposi's sarcoma-associated herpesvirus (KSHV) ORF50 promoter, linking plasma cell differentiation to KSHV reactivation from latency. J Virol **81:**13578-13586.

54. **Yu F, Feng J, Harada JN, Chanda SK, Kenney SC, Sun R.** 2007. B cell terminal differentiation factor XBP-1 induces reactivation of Kaposi's sarcoma-associated herpesvirus. FEBS Lett **581:**3485-3488.

55. **Gregory SM, West JA, Dillon PJ, Hilscher C, Dittmer DP, Damania B.** 2009. Toll-like receptor signaling controls reactivation of KSHV from latency. Proc Natl Acad Sci U S A **106:**11725-11730.

56. **Hsieh AC, Truitt ML, Ruggero D.** 2011. Oncogenic AKTivation of translation as a therapeutic target. Br J Cancer **105:**329-336.

57. **Zoncu R, Efeyan A, Sabatini DM.** 2011. mTOR: from growth signal integration to cancer, diabetes and ageing. Nat Rev Mol Cell Biol **12:**21-35.

58. **Bunney TD, Katan M.** 2010. Phosphoinositide signalling in cancer: beyond PI3K and PTEN. Nat Rev Cancer **10:**342-352.

59. **De Luca A, Maiello MR, D'Alessio A, Pergameno M, Normanno N.** 2012. The RAS/RAF/MEK/ERK and the PI3K/AKT signalling pathways: role in cancer pathogenesis and implications for therapeutic approaches. Expert Opin Ther Targets **16 Suppl 2:**S17-27.

60. **Engelman JA, Luo J, Cantley LC.** 2006. The evolution of phosphatidylinositol 3-kinases as regulators of growth and metabolism. Nat Rev Genet **7:**606-619.

61. **Donahue AC, Fruman DA.** 2004. PI3K signaling controls cell fate at many points in B lymphocyte development and activation. Semin Cell Dev Biol **15:**183-197.

62. **Cantley LC, Neel BG.** 1999. New insights into tumor suppression: PTEN suppresses tumor formation by restraining the phosphoinositide 3-kinase/AKT pathway. Proc Natl Acad Sci U S A **96:**4240-4245.

63. **Manning BD, Cantley LC.** 2007. AKT/PKB signaling: navigating downstream. Cell **129:**1261-1274.

64. **Lawlor MA, Alessi DR.** 2001. PKB/Akt: a key mediator of cell proliferation, survival and insulin responses? J Cell Sci **114:**2903-2910.

65. **Cross DA, Alessi DR, Cohen P, Andjelkovich M, Hemmings BA.** 1995. Inhibition of glycogen synthase kinase-3 by insulin mediated by protein kinase B. Nature **378:**785-789.

66. **Datta SR, Dudek H, Tao X, Masters S, Fu H, Gotoh Y, Greenberg ME.** 1997. Akt phosphorylation of BAD couples survival signals to the cell- intrinsic death machinery. Cell **91:**231-241.

67. **del Peso L, Gonzalez-Garcia M, Page C, Herrera R, Nunez G.** 1997. Interleukin-3-induced phosphorylation of BAD through the protein kinase Akt. Science **278:**687-689.

68. **Cardone MH, Roy N, Stennicke HR, Salvesen GS, Franke TF, Stanbridge E, Frisch S, Reed JC.** 1998. Regulation of cell death protease caspase-9 by phosphorylation. Science **282:**1318-1321.

69. **Gera JF, Mellinghoff IK, Shi Y, Rettig MB, Tran C, Hsu JH, Sawyers CL, Lichtenstein AK.** 2004. AKT activity determines sensitivity to mammalian target of rapamycin (mTOR) inhibitors by regulating cyclin D1 and c-myc expression. J Biol Chem **279:**2737-2746.

70. **Zhou BP, Liao Y, Xia W, Spohn B, Lee MH, Hung MC.** 2001. Cytoplasmic localization of p21Cip1/WAF1 by Akt-induced phosphorylation in HER-2/neu-overexpressing cells. Nat Cell Biol **3:**245-252.

71. **Shin I, Yakes FM, Rojo F, Shin NY, Bakin AV, Baselga J, Arteaga CL.** 2002. PKB/Akt mediates cell-cycle progression by phosphorylation of p27(Kip1) at threonine 157 and modulation of its cellular localization. Nat Med **8:**1145-1152.

72. **Sun H, Lesche R, Li DM, Liliental J, Zhang H, Gao J, Gavrilova N, Mueller B, Liu X, Wu H.** 1999. PTEN modulates cell cycle progression and cell survival by regulating phosphatidylinositol 3,4,5,-trisphosphate and Akt/protein kinase B signaling pathway. Proc Natl Acad Sci U S A **96:**6199-6204.

73. **Karin M, Ben-Neriah Y.** 2000. Phosphorylation meets ubiquitination: the control of NF-[kappa]B activity. Annu Rev Immunol **18:**621-663.

74. **Ghosh S, May MJ, Kopp EB.** 1998. NF-kappa B and Rel proteins: evolutionarily conserved mediators of immune responses. Annu Rev Immunol **16:**225-260.

75. **Verma IM, Stevenson JK, Schwarz EM, Van Antwerp D, Miyamoto S.** 1995. Rel/NF-kappa B/I kappa B family: intimate tales of association and dissociation. Genes Dev **9:**2723-2735.

76. **Gustin JA, Korgaonkar CK, Pincheira R, Li Q, Donner DB.** 2006. Akt regulates basal and induced processing of NF-kappaB2 (p100) to p52. J Biol Chem **281:**16473-16481.

77. **Comb WC, Hutti JE, Cogswell P, Cantley LC, Baldwin AS.** 2012. p85alpha SH2 Domain Phosphorylation by IKK Promotes Feedback Inhibition of PI3K and Akt in Response to Cellular Starvation. Mol Cell **45:**719-730.

78. **de Oliveira DE, Ballon G, Cesarman E.** 2010. NF-kappaB signaling modulation by EBV and KSHV. Trends Microbiol **18:**248-257.

79. **Gingras AC, Gygi SP, Raught B, Polakiewicz RD, Abraham RT, Hoekstra MF, Aebersold R, Sonenberg N.** 1999. Regulation of 4E-BP1 phosphorylation: a novel two-step mechanism. Genes Dev **13:**1422-1437.

80. **Sarbassov DD, Guertin DA, Ali SM, Sabatini DM.** 2005. Phosphorylation and regulation of Akt/PKB by the rictor-mTOR complex. Science **307:**1098-1101.

81. **Dimmeler S, Fleming I, Fisslthaler B, Hermann C, Busse R, Zeiher AM.** 1999. Activation of nitric oxide synthase in endothelial cells by Akt-dependent phosphorylation. Nature **399:**601-605.

82. **Thomas DD, Ridnour LA, Isenberg JS, Flores-Santana W, Switzer CH, Donzelli S, Hussain P, Vecoli C, Paolocci N, Ambs S, Colton CA, Harris CC, Roberts DD, Wink DA.** 2008. The chemical biology of nitric oxide: implications in cellular signaling. Free Radic Biol Med **45:**18-31.

83. **Wieman HL, Wofford JA, Rathmell JC.** 2007. Cytokine stimulation promotes glucose uptake via phosphatidylinositol-3 kinase/Akt regulation of Glut1 activity and trafficking. Mol Biol Cell **18:**1437-1446.

84. **Duvel K, Yecies JL, Menon S, Raman P, Lipovsky AI, Souza AL, Triantafellow E, Ma Q, Gorski R, Cleaver S, Vander Heiden MG, MacKeigan JP, Finan PM, Clish CB, Murphy LO, Manning BD.** 2010. Activation of a metabolic gene regulatory network downstream of mTOR complex 1. Mol Cell **39:**171-183.

85. **Bhatt AP, Bhende PM, Sin SH, Roy D, Dittmer DP, Damania B.** 2010. Dual inhibition of PI3K and mTOR inhibits autocrine and paracrine proliferative loops in PI3K/Akt/mTOR-addicted lymphomas. Blood **115:**4455-4463.

86. **Sin SH, Roy D, Wang L, Staudt MR, Fakhari FD, Patel DD, Henry D, Harrington WJ, Jr., Damania BA, Dittmer DP.** 2007. Rapamycin is efficacious against primary effusion lymphoma (PEL) cell lines in vivo by inhibiting autocrine signaling. Blood **109:**2165-2173.

87. **Srinivasan L, Sasaki Y, Calado DP, Zhang B, Paik JH, DePinho RA, Kutok JL, Kearney JF, Otipoby KL, Rajewsky K.** 2009. PI3 kinase signals BCR-dependent mature B cell survival. Cell **139:**573-586.

88. **Hodson DJ, Turner M.** 2009. The role of PI3K signalling in the B cell response to antigen. Adv Exp Med Biol **633:**43-53.

89. **Beer-Hammer S, Zebedin E, von Holleben M, Alferink J, Reis B, Dresing P, Degrandi D, Scheu S, Hirsch E, Sexl V, Pfeffer K, Nurnberg B, Piekorz RP.** 2010. The catalytic PI3K isoforms p110gamma and p110delta contribute to B cell development and maintenance, transformation, and proliferation. J Leukoc Biol **87:**1083-1095.

90. **Chandran B.** 2010. Early events in Kaposi's sarcoma-associated herpesvirus infection of target cells. J Virol **84:**2188-2199.

91. **Krishnan HH, Sharma-Walia N, Streblow DN, Naranatt PP, Chandran B.** 2006. Focal adhesion kinase is critical for entry of Kaposi's sarcoma-associated herpesvirus into target cells. J Virol **80:**1167-1180.

92. **Veettil MV, Sharma-Walia N, Sadagopan S, Raghu H, Sivakumar R, Naranatt PP, Chandran B.** 2006. RhoA-GTPase facilitates entry of Kaposi's sarcoma-associated herpesvirus into adherent target cells in a Src-dependent manner. J Virol **80:**11432-11446.

93. **Sharma-Walia N, Naranatt PP, Krishnan HH, Zeng L, Chandran B.** 2004. Kaposi's sarcoma-associated herpesvirus/human herpesvirus 8 envelope glycoprotein gB induces the integrin-dependent focal adhesion kinase-Src-phosphatidylinositol 3-kinase-rho GTPase signal pathways and cytoskeletal rearrangements. J Virol **78:**4207-4223.

94. **Sharma-Walia N, Krishnan HH, Naranatt PP, Zeng L, Smith MS, Chandran B.** 2005. ERK1/2 and MEK1/2 induced by Kaposi's sarcoma-associated herpesvirus (human herpesvirus 8) early during infection of target cells are essential for expression of viral genes and for establishment of infection. J Virol **79:**10308-10329.

95. **Raghu H, Sharma-Walia N, Veettil MV, Sadagopan S, Caballero A, Sivakumar R, Varga L, Bottero V, Chandran B.** 2007. Lipid rafts of primary endothelial cells are essential for Kaposi's sarcoma-associated herpesvirus/human herpesvirus 8-induced phosphatidylinositol 3-kinase and RhoA-GTPases critical for microtubule dynamics and nuclear delivery of viral DNA but dispensable for binding and entry. J Virol **81:**7941-7959.

96. **Naranatt PP, Akula SM, Zien CA, Krishnan HH, Chandran B.** 2003. Kaposi's sarcoma-associated herpesvirus induces the phosphatidylinositol 3-kinase-PKC-zeta-MEK-ERK signaling pathway in target cells early during infection: implications for infectivity. J Virol **77:**1524-1539.

97. **Kerur N, Veettil MV, Sharma-Walia N, Sadagopan S, Bottero V, Paul AG, Chandran B.** 2010. Characterization of entry and infection of monocytic THP-1 cells by Kaposi's sarcoma associated herpesvirus (KSHV): role of heparan sulfate, DC-SIGN, integrins and signaling. Virology **406:**103-116.

98. **Lee H, Veazey R, Williams K, Li M, Guo J, Neipel F, Fleckenstein B, Lackner A, Desrosiers RC, Jung JU.** 1998. Deregulation of cell growth by the K1 gene of Kaposi's sarcoma- associated herpesvirus. Nat Med **4:**435-440.

99. **Jenner RG, Alba MM, Boshoff C, Kellam P.** 2001. Kaposi's sarcoma-associated herpesvirus latent and lytic gene expression as revealed by DNA arrays. J Virol **75:**891-902.

100. **Lagunoff M, Ganem D.** 1997. The structure and coding organization of the genomic termini of Kaposi's sarcoma-associated herpesvirus. Virology **236:**147-154.

101. **Lee BS, Connole M, Tang Z, Harris NL, Jung JU.** 2003. Structural analysis of the Kaposi's sarcoma-associated herpesvirus K1 protein. J Virol **77:**8072-8086.

102. **Wang L, Dittmer DP, Tomlinson CC, Fakhari FD, Damania B.** 2006. Immortalization of primary endothelial cells by the K1 protein of Kaposi's sarcoma-associated herpesvirus. Cancer Res **66:**3658-3666.

103. **Chandriani S, Xu Y, Ganem D.** 2010. The lytic transcriptome of Kaposi's sarcoma-associated herpesvirus reveals extensive transcription of noncoding regions, including regions antisense to important genes. J Virol **84:**7934-7942.

104. **Prakash O, Tang ZY, Peng X, Coleman R, Gill J, Farr G, Samaniego F.** 2002. Tumorigenesis and aberrant signaling in transgenic mice expressing the human herpesvirus-8 k1 gene. J Natl Cancer Inst **94:**926-935.

105. **Cuevas BD, Lu Y, Mao M, Zhang J, LaPushin R, Siminovitch K, Mills GB.** 2001. Tyrosine phosphorylation of p85 relieves its inhibitory activity on phosphatidylinositol 3-kinase. J Biol Chem **276:**27455-27461.

106. **Tomlinson CC, Damania B.** 2004. The K1 protein of Kaposi's sarcoma-associated herpesvirus activates the Akt signaling pathway. J Virol **78:**1918-1927.

107. **Lagunoff M, Majeti R, Weiss A, Ganem D.** 1999. Deregulated signal transduction by the K1 gene product of Kaposi's sarcoma-associated herpesvirus. Proc Natl Acad Sci U S A **96:**5704-5709.

108. **Wen KW, Damania B.** 2010. Hsp90 and Hsp40/Erdj3 are required for the expression and anti-apoptotic function of KSHV K1. Oncogene **29:**3532-3544.

109. **Sato S, Fujita N, Tsuruo T.** 2000. Modulation of Akt kinase activity by binding to Hsp90. Proc Natl Acad Sci U S A **97:**10832-10837.

110. **Gao SJ, Deng JH, Zhou FC.** 2003. Productive lytic replication of a recombinant Kaposi's sarcoma-associated herpesvirus in efficient primary infection of primary human endothelial cells. J Virol **77:**9738-9749.

111. **Asmuth DM, Kalish LA, Laycock ME, Murphy EL, Mohr BA, Lee TH, Gallarda J, Giachetti C, Dollard SC, van der Horst CM, Grant RM, Busch MP.** 2003. Absence of HBV and HCV, HTLV-I and -II, and human herpes virus-8 activation after allogeneic RBC transfusion in patients with advanced HIV-1 infection. Transfusion **43:**451-458.

112. **Zong JC, Ciufo DM, Alcendor DJ, Wan X, Nicholas J, Browning PJ, Rady PL, Tyring SK, Orenstein JM, Rabkin CS, Su IJ, Powell KF, Croxson M, Foreman KE, Nickoloff BJ, Alkan S, Hayward GS.** 1999. High-level variability in the ORF-K1 membrane protein gene at the left end of the Kaposi's sarcoma-associated herpesvirus genome defines four major virus subtypes and multiple variants or clades in different human populations. J Virol **73:**4156-4170.

113. **Zong J, Ciufo DM, Viscidi R, Alagiozoglou L, Tyring S, Rady P, Orenstein J, Boto W, Kalumbuja H, Romano N, Melbye M, Kang GH, Boshoff C, Hayward GS.** 2002. Genotypic analysis at multiple loci across Kaposi's sarcoma herpesvirus (KSHV) DNA molecules: clustering patterns, novel variants and chimerism. J Clin Virol **23:**119-148.

114. **Wang L, Wakisaka, N., Tomlinson, C.C., DeWire, S., Krall, S., Pagano, J.S. and B. Damania.** 2004. The Kaposi's Sarcoma-Associated Herpesvirus (KSHV/HHV8) K1 Protein Induces Expression of Angiogenic and Invasion Factors. Cancer Research.

115. **Lee BS, Lee SH, Feng P, Chang H, Cho NH, Jung JU.** 2005. Characterization of the Kaposi's sarcoma-associated herpesvirus K1 signalosome. J Virol **79:**12173-12184.

116. **Lee BS, Alvarez X, Ishido S, Lackner AA, Jung JU.** 2000. Inhibition of intracellular transport of B cell antigen receptor complexes by Kaposi's sarcoma-associated herpesvirus K1. J Exp Med **192:**11-21.

117. **Munger J, Bajad SU, Coller HA, Shenk T, Rabinowitz JD.** 2006. Dynamics of the cellular metabolome during human cytomegalovirus infection. PLoS Pathog **2:**e132.

118. **Bais C, Santomasso B, Coso O, Arvanitakis L, Raaka EG, Gutkind JS, Asch AS, Cesarman E, Gershengorn MC, Mesri EA.** 1998. G-protein-coupled receptor of Kaposi's sarcoma-associated herpesvirus is a viral oncogene and angiogenesis activator. Nature **391:**86-89.

119. **Montaner S, Sodhi A, Pece S, Mesri EA, Gutkind JS.** 2001. The Kaposi's sarcoma-associated herpesvirus G protein-coupled receptor promotes endothelial cell survival through the activation of Akt/protein kinase B. Cancer Res **61:**2641-2648.

120. **Guo HG, Sadowska M, Reid W, Tschachler E, Hayward G, Reitz M.** 2003. Kaposi's sarcoma-like tumors in a human herpesvirus 8 ORF74 transgenic mouse. J Virol **77:**2631-2639.

121. **Yang TY, Chen SC, Leach MW, Manfra D, Homey B, Wiekowski M, Sullivan L, Jenh CH, Narula SK, Chensue SW, Lira SA.** 2000. Transgenic expression of the chemokine receptor encoded by human herpesvirus 8 induces an angioproliferative disease resembling Kaposi's sarcoma. J Exp Med **191:**445-454.

122. **Montaner S, Sodhi A, Molinolo A, Bugge TH, Sawai ET, He Y, Li Y, Ray PE, Gutkind JS.** 2003. Endothelial infection with KSHV genes in vivo reveals that vGPCR initiates Kaposi's sarcomagenesis and can promote the tumorigenic potential of viral latent genes. Cancer Cell **3:**23-36.

123. **Rosenkilde MM, Kledal TN, Brauner-Osborne H, Schwartz TW.** 1999. Agonists and inverse agonists for the herpesvirus 8-encoded constitutively active seven-transmembrane oncogene product, ORF-74. J Biol Chem **274:**956-961.

124. **Sodhi A, Montaner S, Gutkind JS.** 2004. Viral hijacking of G-protein-coupled-receptor signalling networks. Nat Rev Mol Cell Biol **5:**998-1012.

125. **Rosenkilde MM, Kledal TN, Holst PJ, Schwartz TW.** 2000. Selective elimination of high constitutive activity or chemokine binding in the human herpesvirus 8 encoded seven transmembrane oncogene ORF74. J Biol Chem **275:**26309-26315.

126. **Gershengorn MC, Geras-Raaka E, Varma A, Clark-Lewis I.** 1998. Chemokines activate Kaposi's sarcoma-associated herpesvirus G protein- coupled receptor in mammalian cells in culture. J Clin Invest **102:**1469-1472.

127. **Sodhi A, Montaner S, Patel V, Zohar M, Bais C, Mesri EA, Gutkind JS.** 2000. The Kaposi's sarcoma-associated herpes virus G protein-coupled receptor up-regulates vascular endothelial growth factor expression and secretion through mitogen-activated protein kinase and p38 pathways acting on hypoxia-inducible factor 1alpha. Cancer Res **60:**4873-4880.

128. **Couty JP, Geras-Raaka E, Weksler BB, Gershengorn MC.** 2001. Kaposi's sarcoma-associated herpesvirus G protein-coupled receptor signals through multiple pathways in endothelial cells. J Biol Chem **276:**33805-33811.

129. **Schwarz M, Murphy PM.** 2001. Kaposi's sarcoma-associated herpesvirus g protein-coupled receptor constitutively activates nf-kappab and induces proinflammatory cytokine and chemokine production via a c-terminal signaling determinant. J Immunol **167:**505-513.

130. **Pati S, Foulke JS, Jr., Barabitskaya O, Kim J, Nair BC, Hone D, Smart J, Feldman RA, Reitz M.** 2003. Human herpesvirus 8-encoded vGPCR activates nuclear factor of activated T cells and collaborates with human immunodeficiency virus type 1 Tat. J Virol **77:**5759-5773.

131. **Jham BC, Ma T, Hu J, Chaisuparat R, Friedman ER, Pandolfi PP, Schneider A, Sodhi A, Montaner S.** 2011. Amplification of the angiogenic signal through the activation of the TSC/mTOR/HIF axis by the KSHV vGPCR in Kaposi's sarcoma. PLoS One **6:**e19103.

132. **Martin D, Galisteo R, Molinolo AA, Wetzker R, Hirsch E, Gutkind JS.** 2011. PI3Kgamma mediates kaposi's sarcoma-associated herpesvirus vGPCR-induced sarcomagenesis. Cancer Cell **19:**805-813.

133. **Polson AG, Wang D, DeRisi J, Ganem D.** 2002. Modulation of Host Gene Expression by the Constitutively Active G Protein-coupled Receptor of Kaposi's Sarcoma-associated Herpesvirus. Cancer Res **62:**4525-4530.

134. **Cannon M, Philpott NJ, Cesarman E.** 2003. The Kaposi's Sarcoma-Associated Herpesvirus G Protein-Coupled Receptor Has Broad Signaling Effects in Primary Effusion Lymphoma Cells. J Virol **77:**57-67.

135. **Cannon ML, Cesarman E.** 2004. The KSHV G protein-coupled receptor signals via multiple pathways to induce transcription factor activation in primary effusion lymphoma cells. Oncogene **23:**514-523.

136. **Murga C, Laguinge L, Wetzker R, Cuadrado A, Gutkind JS.** 1998. Activation of Akt/protein kinase B by G protein-coupled receptors. A role for alpha and beta gamma subunits of heterotrimeric G proteins acting through phosphatidylinositol-3-OH kinasegamma. J Biol Chem **273:**19080-19085.

137. **Montaner S, Sodhi A, Servitja JM, Ramsdell AK, Barac A, Sawai ET, Gutkind JS.** 2004. The small GTPase Rac1 links the Kaposi sarcoma-associated herpesvirus vGPCR to cytokine secretion and paracrine neoplasia. Blood **104:**2903-2911.

138. **Moore PS, Boshoff C, Weiss RA, Chang Y.** 1996. Molecular mimicry of human cytokine and cytokine response pathway genes by KSHV. Science **274:**1739-1744.

139. **Neipel F, Albrecht JC, Ensser A, Huang YQ, Li JJ, Friedman-Kien AE, Fleckenstein B.** 1997. Human herpesvirus 8 encodes a homolog of interleukin-6. J Virol **71:**839-842.

140. **Nicholas J, Ruvolo VR, Burns WH, Sandford G, Wan X, Ciufo D, Hendrickson SB, Guo HG, Hayward GS, Reitz MS.** 1997. Kaposi's sarcoma-associated human herpesvirus-8 encodes homologues of macrophage inflammatory protein-1 and interleukin-6. Nat Med **3:**287-292.

141. **Cannon JS, Nicholas J, Orenstein JM, Mann RB, Murray PG, Browning PJ, DiGiuseppe JA, Cesarman E, Hayward GS, Ambinder RF.** 1999. Heterogeneity of viral IL-6 expression in HHV-8-associated diseases. J Infect Dis **180:**824-828.

142. **Staskus KA, Sun R, Miller G, Racz P, Jaslowski A, Metroka C, Brett-Smith H, Haase AT.** 1999. Cellular tropism and viral interleukin-6 expression distinguish human herpesvirus 8 involvement in Kaposi's sarcoma, primary effusion lymphoma, and multicentric Castleman's disease. J Virol **73:**4181-4187.

143. **Osborne J, Moore PS, Chang Y.** 1999. KSHV-encoded viral IL-6 activates multiple human IL-6 signaling pathways. Hum Immunol **60:**921-927.

144. **Molden J, Chang Y, You Y, Moore PS, Goldsmith MA.** 1997. A Kaposi's sarcoma-associated herpesvirus-encoded cytokine homolog (vIL- 6) activates signaling through the shared gp130 receptor subunit. J Biol Chem **272:**19625-19631.

145. **Aoki Y, Yarchoan R, Braun J, Iwamoto A, Tosato G.** 2000. Viral and cellular cytokines in AIDS-related malignant lymphomatous effusions. Blood **96:**1599-1601.

146. **Aoki Y, Yarchoan R, Wyvill K, Okamoto S, Little RF, Tosato G.** 2001. Detection of viral interleukin-6 in Kaposi sarcoma-associated herpesvirus-linked disorders. Blood **97:**2173-2176.

147. **Aoki Y, Tosato G.** 1999. Role of vascular endothelial growth factor/vascular permeability factor in the pathogenesis of Kaposi's sarcoma-associated herpesvirus-infected primary effusion lymphomas. Blood **94:**4247-4254.

148. **Suthaus J, Stuhlmann-Laeisz C, Tompkins VS, Rosean TR, Klapper W, Tosato G, Janz S, Scheller J, Rose-John S.** 2012. HHV8 encoded viral IL-6 collaborates with mouse IL-6 in MCD-like development in mice. Blood.

149. **Morris VA, Punjabi AS, Lagunoff M.** 2008. Activation of Akt through gp130 receptor signaling is required for Kaposi's sarcoma-associated herpesvirus-induced lymphatic reprogramming of endothelial cells. J Virol **82:**8771-8779.

150. **Hong YK, Foreman K, Shin JW, Hirakawa S, Curry CL, Sage DR, Libermann T, Dezube BJ, Fingeroth JD, Detmar M.** 2004. Lymphatic reprogramming of blood vascular endothelium by Kaposi sarcoma-associated herpesvirus. Nat Genet **36:**683-685.

151. **Morris VA, Punjabi AS, Wells RC, Wittkopp CJ, Vart R, Lagunoff M.** 2012. The KSHV viral IL-6 homolog is sufficient to induce blood to lymphatic endothelial cell differentiation. Virology.

152. **Zhu FX, Yuan Y.** 2003. The ORF45 protein of Kaposi's sarcoma-associated herpesvirus is associated with purified virions. J Virol **77:**4221-4230.

153. **Zhu FX, King SM, Smith EJ, Levy DE, Yuan Y.** 2002. A Kaposi's sarcoma-associated herpesviral protein inhibits virus- mediated induction of type I interferon by blocking IRF-7 phosphorylation and nuclear accumulation. Proc Natl Acad Sci U S A **99:**5573-5578.

154. **Xie J, Pan H, Yoo S, Gao SJ.** 2005. Kaposi's sarcoma-associated herpesvirus induction of AP-1 and interleukin 6 during primary infection mediated by multiple mitogen-activated protein kinase pathways. J Virol **79:**15027-15037.

155. **Kuang E, Tang Q, Maul GG, Zhu F.** 2008. Activation of p90 ribosomal S6 kinase by ORF45 of Kaposi's sarcoma-associated herpesvirus and its role in viral lytic replication. J Virol **82:**1838-1850.

156. **Kuang E, Wu F, Zhu F.** 2009. Mechanism of sustained activation of ribosomal S6 kinase (RSK) and ERK by kaposi sarcoma-associated herpesvirus ORF45: multiprotein complexes retain active phosphorylated ERK AND RSK and protect them from dephosphorylation. J Biol Chem **284:**13958-13968.

157. **Hanahan D, Weinberg RA.** 2000. The hallmarks of cancer. Cell **100:**57-70.

158. **Hanahan D, Weinberg RA.** 2011. Hallmarks of cancer: the next generation. Cell **144:**646-674.

159. **Swanton C, Mann DJ, Fleckenstein B, Neipel F, Peters G, Jones N.** 1997. Herpes viral cyclin/Cdk6 complexes evade inhibition by CDK inhibitor proteins. Nature **390:**184-187.

160. **Sun Q, Matta H, Chaudhary PM.** 2003. The human herpes virus 8-encoded viral FLICE inhibitory protein protects against growth factor withdrawal-induced apoptosis via NF-kappa B activation. Blood **101:**1956-1961.

161. **Matta H, Chaudhary PM.** 2004. Activation of alternative NF-kappa B pathway by human herpes virus 8-encoded Fas-associated death domain-like IL-1 beta-converting enzyme inhibitory protein (vFLIP). Proc Natl Acad Sci U S A **101:**9399-9404.

162. **Thurau M, Marquardt G, Gonin-Laurent N, Weinlander K, Naschberger E, Jochmann R, Alkharsah KR, Schulz TF, Thome M, Neipel F, Sturzl M.** 2009. Viral inhibitor of apoptosis vFLIP/K13 protects endothelial cells against superoxide-induced cell death. J Virol **83:**598-611.

163. **Wang L, Damania B.** 2008. Kaposi's sarcoma-associated herpesvirus confers a survival advantage to endothelial cells. Cancer Res **68:**4640-4648.

164. **Knight JS, Cotter MA, 2nd, Robertson ES.** 2001. The latency-associated nuclear antigen of Kaposi's sarcoma-associated herpesvirus transactivates the telomerase reverse transcriptase promoter. J Biol Chem **276:**22971-22978.

165. **Nagy JA, Chang SH, Shih SC, Dvorak AM, Dvorak HF.** 2010. Heterogeneity of the tumor vasculature. Semin Thromb Hemost **36:**321-331.

166. **Baluk P, Hashizume H, McDonald DM.** 2005. Cellular abnormalities of blood vessels as targets in cancer. Curr Opin Genet Dev **15:**102-111.

167. **Jiang BH, Liu LZ.** 2009. PI3K/PTEN signaling in angiogenesis and tumorigenesis. Adv Cancer Res **102:**19-65.

168. **Bais C, Van Geelen A, Eroles P, Mutlu A, Chiozzini C, Dias S, Silverstein RL, Rafii S, Mesri EA.** 2003. Kaposi's sarcoma associated herpesvirus G protein-coupled receptor immortalizes human endothelial cells by activation of the VEGF receptor-2/ KDR. Cancer Cell **3:**131-143.

169. **Langley RR, Fidler IJ.** 2011. The seed and soil hypothesis revisited--the role of tumor-stroma interactions in metastasis to different organs. Int J Cancer **128:**2527-2535.

170. **Thiery JP.** 2002. Epithelial-mesenchymal transitions in tumour progression. Nat Rev Cancer **2:**442-454.

171. **Mani SA, Guo W, Liao MJ, Eaton EN, Ayyanan A, Zhou AY, Brooks M, Reinhard F, Zhang CC, Shipitsin M, Campbell LL, Polyak K, Brisken C, Yang J, Weinberg RA.** 2008. The epithelial-mesenchymal transition generates cells with properties of stem cells. Cell **133:**704-715.

172. **Cheng F, Pekkonen P, Laurinavicius S, Sugiyama N, Henderson S, Gunther T, Rantanen V, Kaivanto E, Aavikko M, Sarek G, Hautaniemi S, Biberfeld P, Aaltonen L, Grundhoff A, Boshoff C, Alitalo K, Lehti K, Ojala PM.** 2011. KSHV-initiated notch activation leads to membrane-type-1 matrix metalloproteinase-dependent lymphatic endothelial-to-mesenchymal transition. Cell Host Microbe **10:**577-590.

173. **O. Warburg KP, E. Negelein.** 1924. Ueber den Stoffwechsel der Tumoren; Biochemische Zeitschrift. " On metabolism of tumors" German. Reprinted in English by Constable, London, 1930 **152:**319-344.

174. **Delgado T, Carroll PA, Punjabi AS, Margineantu D, Hockenbery DM, Lagunoff M.** 2010. Induction of the Warburg effect by Kaposi's sarcoma herpesvirus is required for the maintenance of latently infected endothelial cells. Proc Natl Acad Sci U S A **107:**10696-10701.

175. **Bhatt AP, Jacobs SR, Freemerman AJ, Makowski L, Rathmell JC, Dittmer DP, Damania B.** 2012. Dysregulation of fatty acid synthesis and glycolysis in non-Hodgkin lymphoma. Proc Natl Acad Sci U S A.

176. **Ishido S, Wang C, Lee BS, Cohen GB, Jung JU.** 2000. Downregulation of major histocompatibility complex class I molecules by Kaposi's sarcoma-associated herpesvirus K3 and K5 proteins. J Virol **74:**5300-5309.

177. **Coscoy L, Ganem D.** 2000. Kaposi's sarcoma-associated herpesvirus encodes two proteins that block cell surface display of MHC class I chains by enhancing their endocytosis. Proc Natl Acad Sci U S A **97:**8051-8056.

178. **Jacobs SR, Damania B.** 2011. The Viral Interferon Regulatory Factors of KSHV: Immunosuppressors or Oncogenes? Front Immunol **2:**19.

179. **Sharma-Walia N, Paul AG, Bottero V, Sadagopan S, Veettil MV, Kerur N, Chandran B.** 2010. Kaposi's sarcoma associated herpes virus (KSHV) induced COX-2: a key factor in latency, inflammation, angiogenesis, cell survival and invasion. PLoS Pathog **6:**e1000777.

180. **Uddin S, Hussain AR, Al-Hussein KA, Manogaran PS, Wickrema A, Gutierrez MI, Bhatia KG.** 2005. Inhibition of phosphatidylinositol 3'-kinase/AKT signaling promotes apoptosis of primary effusion lymphoma cells. Clin Cancer Res **11:**3102-3108.

181. **Sawyers CL.** 2003. Will mTOR inhibitors make it as cancer drugs? Cancer Cell **4:**343-348.

182. **Dittmer DP, Bhatt AP, Damania B.** 2012. Rapalogs in viral cancers. Expert Opin Investig Drugs **21:**135-138.

183. **Stallone G, Schena A, Infante B, Di Paolo S, Loverre A, Maggio G, Ranieri E, Gesualdo L, Schena FP, Grandaliano G.** 2005. Sirolimus for Kaposi's sarcoma in renal-transplant recipients. N Engl J Med **352:**1317-1323.

CHAPTER 2: DUAL INHIBITION OF PI3K AND mTOR INHIBITS AUTOCRINE AND PARACRINE PROLIFERATIVE LOOPS IN PI3K/AKT/mTOR-ADDICTED LYMPHOMAS[3]

INTRODUCTION

The phosphatidylinositol 3-kinase (PI3K) signaling pathway plays a critical role in cell proliferation and cell survival (Figure 1). PI3K activation stimulates the production of phosphatidylinositol 3,4,5 tri-phosphate, which results in activation of the kinases, PDK1 and AKT. The lipid phosphatase and tensin homolog deleted on chromosome 10 (PTEN) protein is a negative regulator of this pathway. AKT kinase promotes cell survival by phosphorylating, and thereby inactivating, pro-apoptotic factors such as the FOXO transcription factor family, GSK-3b, Caspase-9 and Bad(1-4). Phosphorylation of Bad, and the FOXO transactivators prevent apoptosis. AKT also phosphorylates p27, a negative regulator of the cell cycle, thereby preventing cell cycle arrest. Additionally, AKT activation leads to phosphorylation and activation of the mammalian target of rapamycin (mTOR), a kinase that stimulates protein synthesis and cell proliferation.

---

[3] Aadra P Bhatt*, Prasanna M Bhende*, Sang-Hoon Sin, Debasmita Roy, Dirk P Dittmer and Blossom Damania. *APB and PMB contributed equally to this study. Copyright © Blood 2010 June 3; 115 (22): 4455-63

Activated mTOR protein can associate with raptor and mlst8/GbL to form the mTORc1 complex. The mTORc1 complex induces phosphorylation of p70 S6 kinase (S6K) leading to phosphorylation and activation of the ribosomal protein, S6. MTORc1 also inhibits 4E-BP1, a repressor of eukaryotic initiation factor eIF4e. This arm of the mTOR pathway is rapamycin-sensitive. In contrast, the mTORc2 complex, which consists of mTOR, mLST8/GβL, mSin1 and Rictor, is insensitive to the effects of rapamycin. MTORc2 functions in a feedback loop that phosphorylates and activates AKT by phosphorylation at Ser473(5). Hence, inhibitors of PI3K/AKT are likely to have broader effects than mTOR inhibitors.

The nutrient sensor, AMP activated kinase (AMPK), is a negative regulator of mTORc1(6). AMPK controls cellular homeostasis by regulating energy production within the cell. AMPK is activated when the cellular AMP/ATP balance drops, and this leads to activation of fatty acid oxidation in the liver, lipogenesis, stimulation of ketogenesis and inhibition of cholesterol synthesis. The net result of modulation of these pathways is the inhibition of mTOR, which results in attenuation of protein synthesis until cellular ATP reserves are sufficiently replenished. The glitazone class of drugs are known to activate AMPK(7, 8), leading us to hypothesize that AMPK activation may be of therapeutic value in treating mTOR-addicted lymphomas. Additionally, AMPK activation has previously been shown to inhibit some tumor types(8, 9).

We chose primary effusion lymphoma (PEL) as the target for our investigation, because PEL rely heavily on PI3K/AKT/mTOR signaling(10) and have a very poor prognosis, with reported median survival times of less than six

months(11). PEL is a variant of Non-Hodgkin lymphoma (NHL) and is infected with Kaposi sarcoma associated-herpesvirus (KSHV). KSHV is associated with multiple cancers in the human population: Kaposi sarcoma (KS), primary effusion lymphoma (PEL) and multicentric Castleman disease (MCD). The incidence of these cancers is highly increased in the context of HIV infection. We and others have previously shown that individual viral proteins like KSHV K1 activate the PI3K/AKT pathway in B cells and endothelial cells(12-16). Another viral protein, KSHV vGPCR, can also activate this pathway in endothelial and epithelial cells(17-21). KSHV-infected PEL display constitutive activation of the PI3K/AKT/mTOR pathway(10). No activating PI3K mutations have been reported in PEL, and only two PEL lines display PTEN mutations(22). This suggests that in PEL, constitutive activation of PI3K, AKT and mTOR kinases is due to the expression of viral proteins. We previously reported that treatment with rapamycin, an mTOR inhibitor, induces cell cycle arrest in PEL and may halt clinical progression(10). Rapamycin inhibits mTORc1, but not mTORc2. However, recent literature suggests there is increased mTORc2-mediated phosphorylation of AKT, which compensates for mTORc1 inhibition by rapamycin, in many cell types and tumors(23). Hence, single agent rapamycin therapy has had limited success in the clinic.

Here, we report the consequences of modulating AKT and AMPK kinases individually, as well as simultaneously inhibiting PI3K and mTOR kinases in PEL. All the compounds tested are either already FDA-approved or currently in clinical trials. We demonstrate that dual inhibition of PI3K and mTOR with a novel, orally

bioavailable compound, NVP-BEZ235, is more efficacious than single compounds in preventing PEL proliferation and tumor growth in mice. We are the first to report that the mechanism of action for NVP-BEZ235 involves the inhibition of autocrine and paracrine cytokine and growth factors, which may explain the heightened sensitivity of cytokine driven cancers to inhibitors of the PI3K/AKT/mTOR pathway.

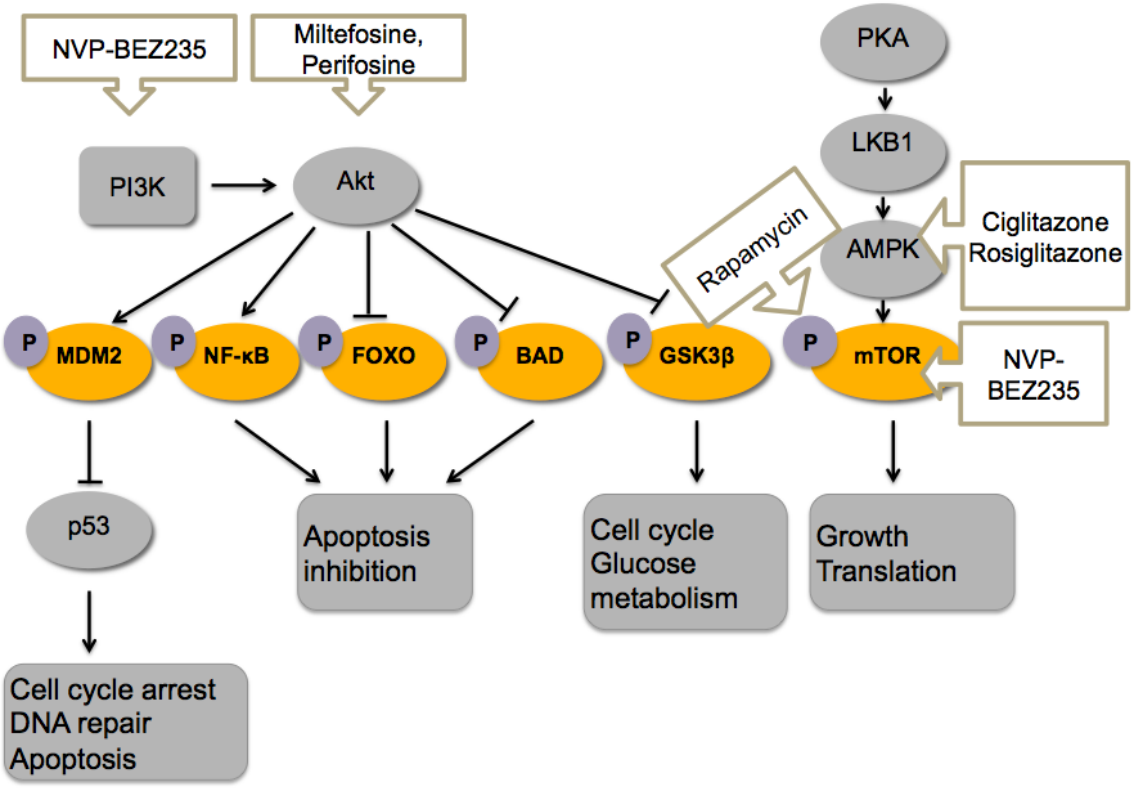

Figure 1: Schematic representation of cellular pathways leading to cell survival or cell death. The roles PI3K, AKT and AMPK play in signaling pathways important for

cell survival or cell death are shown. The influence of rapamycin, rosiglitazone, miltefosine, perifosine and NVP-BEZ235 on these pathways is also shown. Phosphorylation of proteins is indicated by "+p".

METHODS

Cell Culture

Patient-derived, PEL cell lines (BC-1, BCBL-1, BCLM, BCP-1, VG-1) were cultured in RPMI-1640 supplemented with 10% heat-inactivated fetal bovine serum, 100 IU/ml Penicillin G, 100 mg/ml Streptomycin (Mediatech), 0.075% sodium bicarbonate, 0.05 mm β-mercaptoethanol (Gibco) at 37°C in 5% CO_2. BC-1 is EBV(+)/KSHV(+), while the other cell lines are KSHV(+).

Inhibitors

Perifosine, miltefosine and rosiglitazone were purchased from Cayman Chemical. Ciglitazone was purchased from Calbiochem. We are grateful to Novartis for providing us with NVP-BEZ235.

MTS cell proliferation assay

To observe alterations in growth and proliferation, 2 X 10^5 PEL cells were treated with the therapeutic compounds at the indicated doses or with appropriate vehicle as a negative control. Cells were followed for 96 hours, and cell viability was determined by trypan blue exclusion performed in quadruplicate. Actively metabolic cells were quantified every 24 hours using the Cell Titer 96®

Aqueous One Solution Cell Proliferation Assay (Promega) according to the manufacturer's instructions. Absorbance was measured using fluostar OPTIMA (BMG Labtech). The absorbance measured at 485 or 490 nm indicates the number of metabolically active cells. The IC50 of NVP-BEZ235 was calculated by plotting the percent inhibition in proliferation in NVP-BEZ235 -treated cells compared to vehicle-treated cells (Y-axis) versus the log of the concentration of drug (X-axis). This was done using the statistical analysis program R. The dose of NVP-BEZ235 that reduced cell proliferation to 50% of vehicle-treated cells was calculated as the IC50 for NVP-BEZ235.

Western blots

Cells were treated with various compounds as indicated. After washing harvested cells with ice-cold PBS, cell lysates were prepared in a buffer containing 150 mm NaCl, 50 mm Tris-HCl (ph 8), 0.1% NP40, 50 mm NaF, 30 mm β-glycerophosphate, 1 mm Na_3VO_4 and 1x Complete Protease Inhibitor cocktail (Roche). Equal amounts of proteins were electrophoresed on a 10% SDS-PAGE denaturing gel, followed by transfer onto a Hybond™-ECL nitrocellulose membrane (GE Healthcare). Membranes were blocked with 5% fat-free milk for 1 hour at room temperature, followed by overnight incubation at 4°C in the indicated primary antibodies directed against either phosphorylated or total protein. The following primary antibodies against phosphorylated proteins were used: ampkα (Thr172), AKT (Ser473), AKT (Thr308), FOXO1 (Ser256), GSK3β

(Ser9), mTOR (Ser2448), S6K (Thr421/Ser424), S6 ribosomal protein (Ser235/236). After washing, the membrane was incubated with anti-rabbit igg conjugated to HRP. The results were visualized with the ECL Plus Western Blotting Detection System (GE Healthcare) according to the manufacturer's instructions.

Xenograft tumor model

PEL cells were washed in ice-cold phosphate-buffered saline (PBS, Mediatech), counted and diluted in 100 ml of PBS mixed with 100 ml of growth factor-depleted Matrigel (BD Biosciences)(10). $1x10^5$ to $7.5x10^5$ BC-1 cells were injected subcutaneously into the right flank of NOD.CB17- $Prkdc^{scid}$/J or CB17-$Prkdc^{scid}$/J mice (Jackson Laboratory, Taconic Inc.). The mice were monitored on alternate days for development of palpable tumors (~$2mm^3$), at which point drug or vehicle treatments were initiated, and were administered either intraperitoneally (miltefosine, perifosine) or by oral gavage (rosiglitazone, NVP-BEZ235) five days a week. Groups of five to seven mice were used to generate PEL tumors and treated with either vehicle or drug cocktail. Each biological experiment was repeated multiple times. For rosiglitazone, 0.25% methyl cellulose was used as vehicle, and 30 mg/kg or 60 mg/kg rosiglitazone was suspended in methyl cellulose. For perifosine and miltefosine, PBS was used as vehicle and 50mg/kg perifosine or miltefosine was dissolved in PBS. For NVP-BEZ235, the compound was dissolved in a 1:9 v/v mixture of 1-methyl-2-pyrrolidone (Fluka) and polyethylene glycol 300 (Sigma). A dose of 40 mg/kg of NVP-BEZ235 or equal volume of the vehicle was administered. Tumor diameters

were measured using digital calipers, and tumor volume was calculated as Volume = a X b X [MAX (a, b)]/2, with a and b being the long and short diameters of the tumor. The tumors were excised and fixed in formalin. Statistical analyses were performed using linear model fit by maximum likelihood with individual animals treated as random effect(24).

Immunohistochemistry

Tumors were excised, fixed in 10% neutral buffered Formalin for 5 days, paraffin-embedded and then 5 mm sections were prepared on slides. Slides were de-paraffinized using Histochoice Clearing Agent (Sigma) and re-hydrated using graded ethanol, followed by extensive washing with water. Endogenous peroxidase activity was quenched with 3% H_2O_2 in 10% methanol solution, and antigens were exposed by heating sections for 10 minutes in 1 mm EDTA (ph 8.0), and cooled to room temperature. Non-specific antigens were blocked using a blocking buffer (10% normal horse serum [Vector Labs], 5% BSA [Sigma], and 0.3% tritonx-100] for one hour at room temperature, followed by an overnight incubation at 4°C in blocking buffer containing the indicated antibodies: phospho-AMPK (Thr172, 1:50), phospho-p70 S6 kinase (Thr421/Ser424, 1:50), phospho-AKT (Ser473, 1:50), phospho-S6 (Ser235/236, 1:100), all from Cell Signaling Technology. Sections incubated in blocking buffer lacking primary antibody were used as negative controls. The next day, sections were washed in PBS, incubated with biotinylated goat anti-rabbit secondary antibody followed by one-hour incubation in pre-formed Avidin DH- biotinylated horseradish peroxidase H complexes (Vectastain ABC kit, Vector Labs), after which sections were stained

with Vector novared substrate, and washed. Sections were counterstained with hematoxylin (Invitrogen), dehydrated using graded alcohols, and mounted using Cytoseal XYL (Richard-Allan Scientific). Dried slides were imaged using a LEICA DM LA histology microscope and LEICA Firecam software.

Caspase-3 Assay

Levels of enzymatically active caspase-3 were quantified using the apoalert Caspase Fluorescent assay kit (Clontech), according to the manufacturer's directions. Briefly, $1X10^6$ BC-1 PEL cells were treated with 50 μM miltefosine, 50 μM Perifosine, or 20 nm NVP-BEZ235, as well as the respective vehicle controls. Cells were harvested and lysed 12 hours later. Equivalent micrograms of cell lysate for all samples were incubated with a fluorogenic caspase-3 substrate (DEVD-AFC). Cleavage of DEVD by caspase-3 releases AFC, the fluorescence of which was measured using a fluostar OPTIMA (BMG Labtech) fluorometer, with excitation and emission filter wavelengths set to 400 and 505 nm respectively.

Cytokine measurements

We measured the levels of thirty different cytokines in the growth medium supernatants of BC-1 PEL cells using a multi-analyte bead immunoassay (Invitrogen Cytokine human 30-plex panel) according to the manufacturer's guidelines. Briefly, diluted (1:2) culture supernatants were incubated with internally-dyed polystyrene beads coated with specific antibodies directed against one of the cytokines. Proteins in the culture supernatants bind to the

antibody-coated beads during a two-hour incubation, after which the beads are washed extensively. Biotinylated detector antibodies directed against specific proteins are added to the beads, where they bind to proteins derived from culture supernatants. After washing, streptavidin-conjugated R-phycoerythrin (Streptavidin-RPE) was added to the bead-culture supernatant-derived protein-detector antibody complexes. Unbound Streptavidin-RPE was washed off, and the bead complexes were analyzed using the Luminex Detection system. Cytokine concentrations in culture supernatants were extrapolated based on a standard curve generated using manufacturer-supplied standards of each cytokine analyte.

RESULTS

We used several compounds that are either FDA-approved or in clinical trials to target multiple arms of the PI3K/AKT/mTOR pathway (Figure 1). The glitazone class of drugs eg. Ciglitazone and rosiglitazone have been shown to activate AMPK(7, 8). Activated AMPK1 directly phosphorylates and activates TSC2(25, 26) leading to inactivation of Rheb and mTOR. We also used Perifosine and miltefosine, two alkylphospholipids, which have been shown to inhibit AKT(27). Perifosine is currently in clinical trials for solid tumors(28). Lastly, we evaluated a novel, orally bioavailable, dual inhibitor of PI3K and mTOR, NVP-BEZ235 (Novartis) (Figure 1).

The glitazones inhibit PEL growth in vitro

Ciglitazone and rosiglitazone are anti-diabetic compounds belonging to the thiazolidenedione class of drugs. Both activate AMPK via activation of PPARγ and adiponectin(7, 29, 30). We treated PEL cell lines with either 100 mM of ciglitazone or 150 mM and 200 mM of rosiglitazone for 96 hours(31), to determine the sensitivity of these compounds.

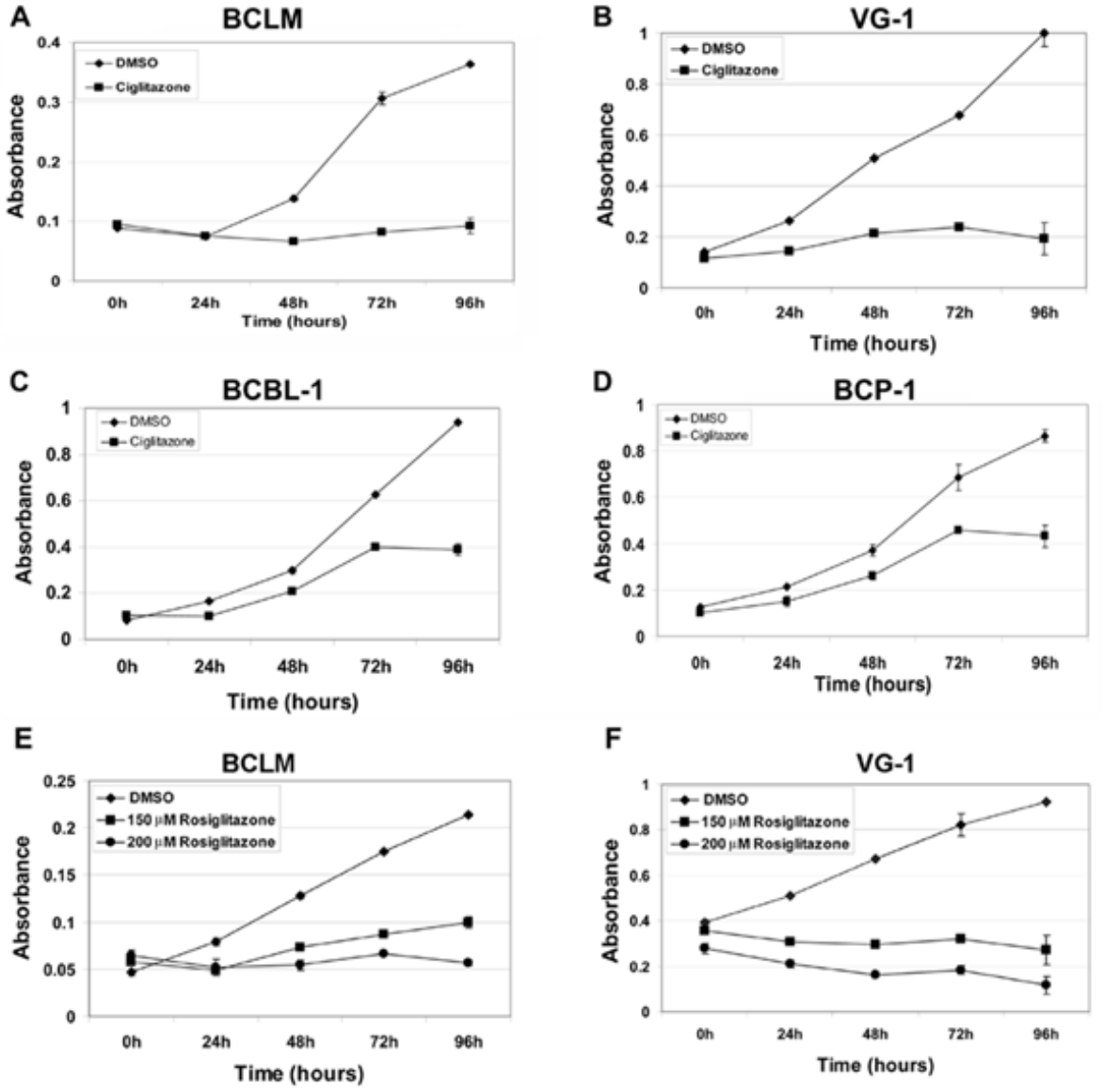

Figure 2: Inhibition of PEL cell proliferation induced by ciglitazone and rosiglitazone as measured by MTS assay. Shown in each panel (y-axis) is the absorbance at 490 nm in vehicle (DMSO) without drug ♦) or presence of 100μm ciglitazone (A-D, ■) or 150μm (E-F, ■) or 200μm rosiglitazone (E-F, ●) versus time in hours after drug treatment (x-axis). Each data point is the average of triplicate or quadruplicate measurements. Error bars represent the SD and in most cases, are smaller than the symbol.

Cell viability was measured using the MTS assay. Four different PEL cell lines treated with ciglitazone or rosiglitazone showed decreased viability compared to vehicle (DMSO) treated cells. Both 100mM ciglitazone and 200mM rosiglitazone displayed similar growth-inhibitory effects on BCLM and VG-1 (approximately four- and five-fold respectively). The inhibitory effects of ciglitazone were greater on BCLM and VG-1 than on BCBL-1 and BCP-1 (Figure 2). This reduced sensitivity to ciglitazone may be a consequence of *p53* mutations in BCBL-1 and BCP-1(32), which could prevent phosphorylated AMPK from exerting its full inhibitory effect. Indeed, a previous report showed that the stabilization and activation of AMPK induces p53-dependent apoptosis(33). AMPK phosphorylation was increased upon treatment of the PEL lines with either 100mM ciglitazone or 200mM rosiglitazone (Figure 3A) indicating that these compounds activated their target. As expected, there was a corresponding decrease in the phosphorylation of mTOR and its downstream targets, S6K, as well as S6 itself (Figure 3A).

Rosiglitazone delays PEL tumor growth in vivo

To investigate the effect of rosiglitazone on PEL growth *in vivo*, BC-1 cells were subcutaneously injected into NOD-SCID mice in the presence of growth factor-depleted Matrigel(10).

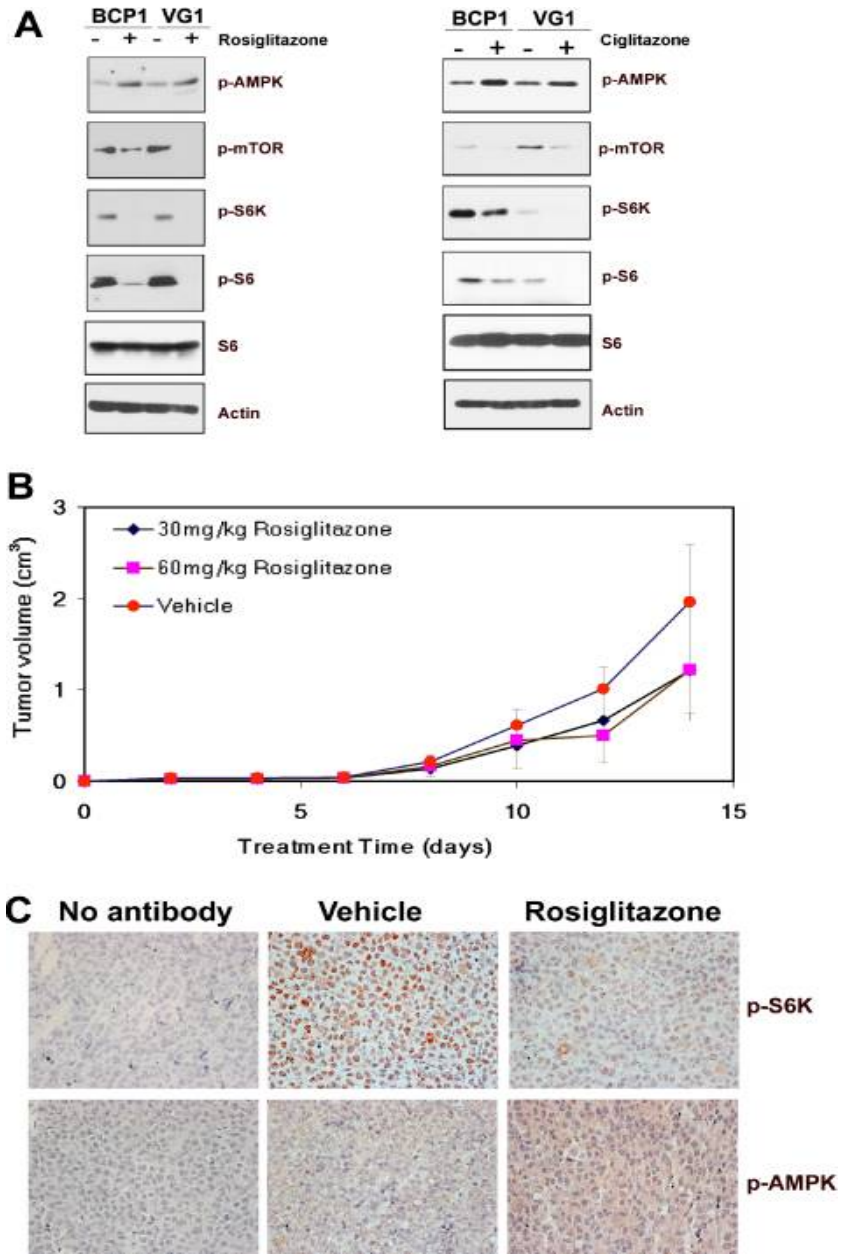

Figure 3. Effect of glitazone treatment on cellular signaling pathways and tumors in mice. **A)** Immunoblot analysis of protein extracts from the indicated cell lines exposed to DMSO (-) or 200 mM rosiglitazone for 72 h, or 100 mM ciglitazone for 96

h was performed to visualize the expression of phosphorylated AMPK (Ser172), mTOR (Ser 2448), S6K (T421/S424) or S6 (S235/236) proteins along with total S6 and b-actin as loading controls. **B)** Decrease in the average tumor size in mice treated with rosiglitazone compared to those treated with methyl cellulose (vehicle). Volumes of tumors in mice treated with either methyl cellulose as vehicle (n=5), 30 mg/kg of rosiglitazone (n=5), or 60 mg/kg of rosiglitazone (n=5), are plotted on the y-axis versus time in days post inoculation on the x-axis. Error bars indicate the standard deviation for each group of animals. **C)** Increase in phospho-AMPK (pAMPK; T172) and decrease in phospho-S6K (pS6K; T421/S424) in mouse xenograft tumors upon treatment with rosiglitazone. Immunohistochemistry of mouse xenograft tumors using antibodies specific for pAMPK and pS6K is shown. No staining was observed in the absence of a specific primary antibody (no antibody). Pictures are shown at 400X magnification.

Upon development of palpable tumors, the animals were randomized into groups of five and treated five days a week for the duration of the experiment with either 0.25% methyl cellulose (vehicle), or with 30 mg/kg or 60 mg/kg rosiglitazone suspended in methyl cellulose via oral gavage similar to previous reports(8). The animals were sacrificed after 14 days and tumors were harvested and measured. Both doses of rosiglitazone delayed tumor growth to some extent (Figure 3B), however the differences were not statistically significant. Immunohistochemistry showed that AMPK phosphorylation at Thr172 was increased in the rosiglitazone-treated mice compared to vehicle-treated mice (Figure 3C). S6K, a downstream effector of mTOR, was uniformly

phosphorylated at Thr421/Ser424 and detectable in tumors in mice treated with the vehicle (methylcellulose), but was virtually undetectable in tumors from mice treated with rosiglitazone (Figure 3C). This suggests that rosiglitazone delays tumor growth via activation of AMPK and inhibition of protein translation through mTOR.

Miltefosine and perifosine target AKT and inhibit proliferation of PEL in vitro

Miltefosine and perifosine are alkylphospholipids that inhibit activation of AKT(27). We treated BCLM, VG1, BC1 and BCBL-1 PEL cell lines with 10, 20, 30, 40 and 50 mM of miltefosine or perifosine over a 3-day period(27, 34). Figure 4A shows a representative MTS experiment using the VG-1 cell line and both drugs. perifosine was a more potent inhibitor of PEL growth compared to miltefosine at all concentrations. Perifosine treatment inhibited AKT and its downstream pro-apoptotic targets, FOXO1 and GSK-3β, comparable to the levels of the PI3K inhibitor, LY294002(13). The protein translation arm of the AKT pathway was also inhibited, as phosphorylation of mTOR (Ser2448), S6K (Thr421/Ser424), and the S6 ribosomal subunit (Ser235/236) were decreased (Figure 4B).

Miltefosine and Perifosine delay PEL tumor progression *in vivo*

We subcutaneously injected NOD-SCID mice with BC-1 cells suspended in growth factor-depleted Matrigel. Upon formation of palpable tumors, mice were randomized into groups of five, and injected intra-peritoneally five days a week

with 50 mg/kg of either miltefosine or perifosine dissolved in PBS, or equivalent volume of vehicle (PBS). Both miltefosine and perifosine inhibited the growth rate of tumors compared to vehicle-treated mice (Figure 4C). By day 14 post-treatment, there was an approximately 50% decrease in average tumor volume in perifosine- and miltefosine-treated mice, as compared to vehicle-treated mice ($p<0.04$). Tumor growth was also significantly retarded ($p<0.04$ for perifosine and $p\leq0.055$ for miltefosine by linear mixed effects model analysis). Immunohistochemical analyses (Figure 4D) displayed an overall reduction in staining for phosphorylated ribosomal S6 protein in tumor sections from miltefosine- and perifosine-treated mice compared to the PBS treated mice. This reduced phosphorylation correlated with the delay in tumor progression in drug-treated animals. Sections that were not incubated with primary antibody showed no phosphorylated S6 staining (Figure 4D).

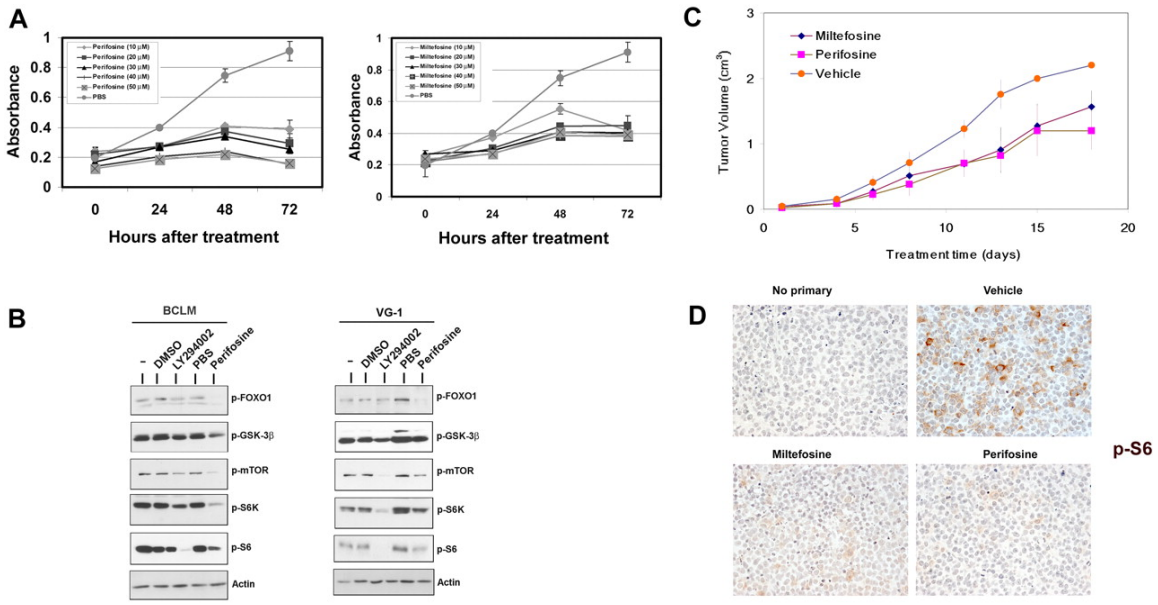

Figure 4. Effects of alkylphospholipids on PEL. A) Inhibition of PEL cell proliferation induced by miltefosine (right panel) and perifosine (left panel) as measured by MTS assay. Shown in each panel is the absorbance at 490 nm (y-axis) in the absence of drug (gray circles) or increasing, indicated doses of either miltefosine or perifosine, ranging from 10 mM to 50 mM. Treatment time is represented on the x-axis. Each datapoint is the average of triplicate or quadruplicate measurements. Error bars represent the standard deviation and in most cases are smaller than the symbol. B) Immunoblot analysis of extracts harvested from indicated PEL cell lines treated with DMSO (vehicle), the indicated drug, or untreated cells (-). Membranes were probed with antibodies raised specifically against the phosphorylated forms of FOXO1, GSK3b, mTOR, S6K or S6 proteins. Membranes were probed with anti-Actin antibody, as a loading control. C) Tumor progression is delayed in miltefosine-treated mice, and significantly delayed in perifosine-treated mice. Mice were treated with 50 mg/kg of miltefosine (n=5), perifosine (n=5) or vehicle (n=5) by intra-peritoneal injection, and followed for 20 days after formation of palpable tumors. Error bars indicate

the standard deviation for each group of animals. D) Tumors excised from miltefosine- and perifosine-treated mice display decreased phosphorylation of the ribosomal S6 protein, compared to vehicle controls. Staining is not observed in sections not incubated with primary antibody. Images are shown at 400X magnification.

NVP-BEZ235 treatment inhibits proliferation of PEL cell lines in vitro.

NVP-BEZ235 is an imidazo[4,5-c]quinoline derivative compound shown to inhibit PI3K and mTOR kinase activity both *in vitro* and *in vivo*(35, 36). NVP-BEZ235 inhibits the activity of these two kinases by binding, reversibly and competitively, to the ATP-binding cleft, thereby preventing phosphorylation and activation of downstream targets(10). We treated BCBL-1, BCP-1, BC-1 and VG-1 PEL cell lines with either 50 or 100 nm of NVP-BEZ235 and compared cell proliferation of drug-treated or mock-treated cells over a 36-hour time period using the MTS assay. Notably, BCBL-1 cells show partial resistance to 50 nm rapamycin,(10) yet the same cells remain sensitive to the dual inhibitor. Figure 5A shows representative cell proliferation profiles of the above-mentioned PEL cell lines. The concentration of NVP-BEZ235 required for inhibiting PEL cell proliferation by 50% was 5.68 ± 1.76 nm (Figure 5B) for the BC-1 cell line. The low inhibitory concentration of NVP-BEZ235 confirms the usefulness of this compound as a treatment for PEL, and suggests a favorable pharmacokinetic profile. We also performed MTS assays using a combination of 30μM perifosine and 50nm NVP-BEZ235 against PEL (Supplemental Figure 1). As expected,

because NVP-BEZ235 inhibits PI3K upstream of AKT, the combination of the AKT inhibitor perifosine and NVP-BEZ235 did not significantly affect BC-1 proliferation compared to NVP-BEZ235 alone.

To confirm the efficacy of NVP-BEZ235 against downstream targets of PI3K and mTOR, we tested the phosphorylation status of the downstream targets of these two kinases, using western blot analysis (Figure 5C). Treatment with NVP-BEZ235 for 24 hours induced marked reduction in phosphorylated mTOR (Ser2448) and FOXO1 (Ser256), both targets of the kinase activity of PI3K/AKT. Reduced phosphorylation of S6K (Thr421/Ser424), and the ribosomal S6 protein (Ser235/236), both targets of mTOR, reflects inhibition of mTOR by NVP-BEZ235. Importantly, reduction in the phosphorylation of AKT at Ser473, a feedback phosphorylation substrate of mTORc2, indicates that NVP-BEZ235 also inhibits mTORc2 activity (Figure 5C)(10). Thus, dual inhibition of PI3K and mTOR likely contributes to decreased cell proliferation by NVP-BEZ235.

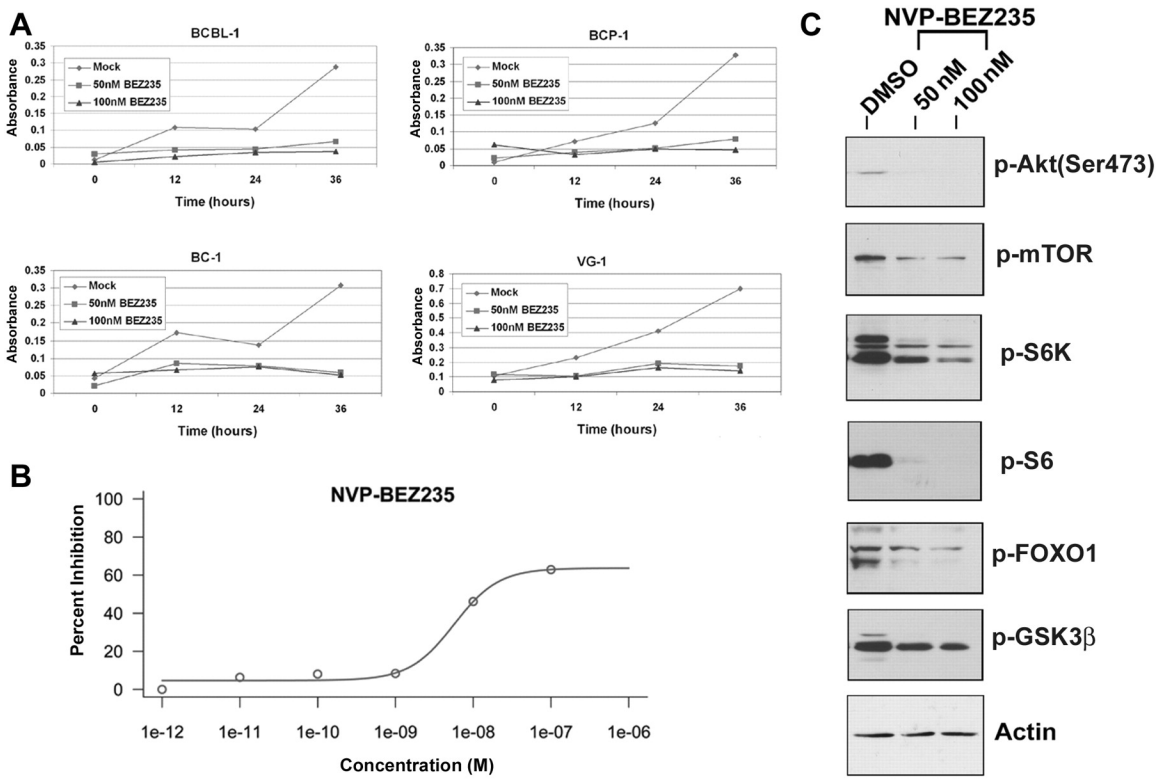

Figure 5. Low doses of NVP-BEZ235 inhibit the downstream targets of PI3K/mTOR pathway. A) Inhibition of proliferation of the indicated PEL cell lines upon treatment with NVP-BEZ235 as measured by MTS assay. Shown in each panel is the absorbance at 490 nm (y-axis) in the absence of drug (gray circles) or increasing, indicated doses of NVP-BEZ235. Treatment time is represented on the X-axis. Each datapoint is the average of triplicate or quadruplicate measurements. Error bars represent the standard deviation and in most cases are smaller than the symbol. B) The IC50 curve for NVP-BEZ235 showing an IC50 value of 5.68 ± 1.76 nm for BC-1 PEL cells. C) Immunoblot analysis of extracts harvested from indicated PEL cell lines treated with DMSO (vehicle) or increasing doses of NVP-BEZ235. Membranes were probed with antibodies raised specifically against the phosphorylated forms of

AKT (Ser473), mTOR, S6K, pS6, FOXO1 and GSK3β. Membranes were probed with anti-Actin antibody, as a loading control.

Dual Inhibition of PI3K and mTOR in PEL tumor progression *in vivo*

We subcutaneously injected NOD-SCID mice with BC-1 PEL cells suspended in growth factor-depleted Matrigel as described above. Upon formation of palpable tumors, mice were randomized to receive either orally administered 40 mg/kg of NVP-BEZ235 (n=7) or vehicle (n=6) five days a week. NVP-BEZ235 significantly inhibited the growth rate of tumors compared to vehicle-treated mice (Figure 6A). Following drug administration, NVP-BEZ235-treated mice displayed tumors with significantly smaller volumes compared to vehicle-treated mice ($p<0.0009$ by Linear mixed-effects model analysis). Immunohistochemical analyses of tumors derived from NVP-BEZ235-treated mice displayed an overall reduction in staining for phosphorylated ribosomal S6 (Ser235/236) protein and phosphorylated AKT (Ser473), compared to tumors from vehicle-treated mice (Figure 6B). Reduced phosphorylation of the S6 ribosomal protein suggests a reduction in protein translation, leading to delayed tumor progression in NVP-BEZ235-treated mice. Reduced phosphorylation of AKT at Ser473 confirms the inhibition of mTOR, which can phosphorylate AKT at Ser473 via the rapamycin-insensitive mTORc2 complex (Figure 6B).

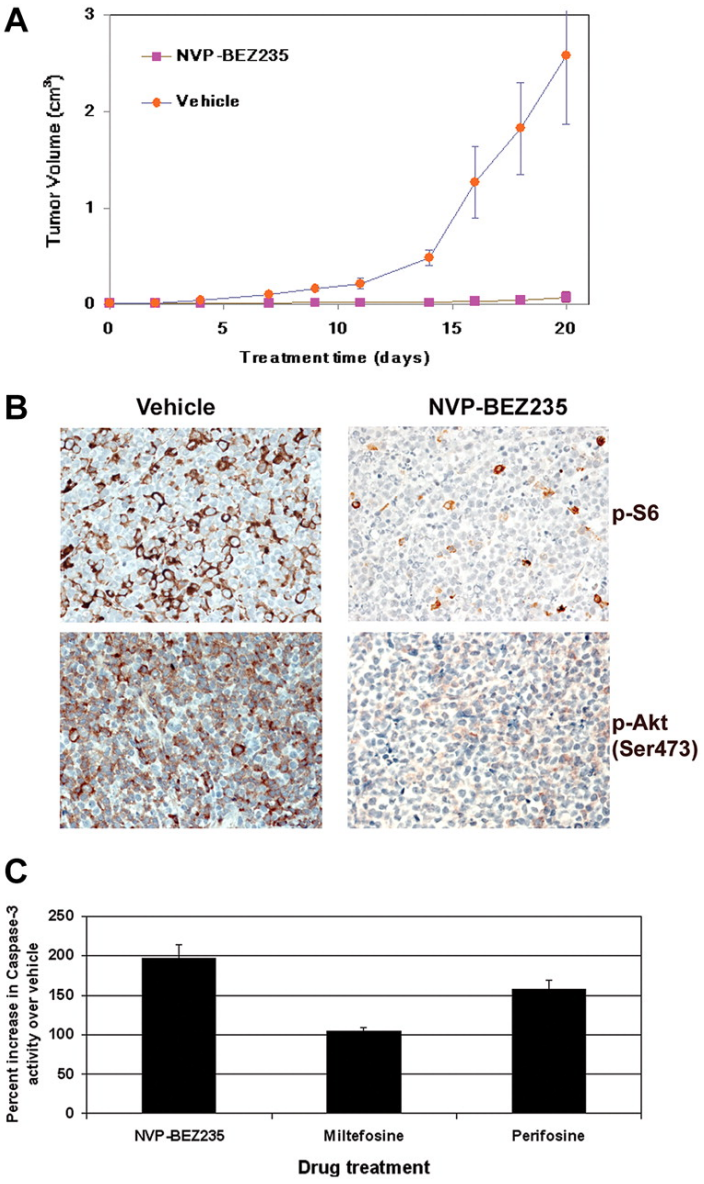

Figure 6. Treatment with NVP-BEZ235 delays tumor progression in vivo in a xenograft model of PEL. A) Tumor progression is significantly delayed ($p<0.0009$) in mice treated with 40 mg/kg NVP-BEZ235 administered by oral gavage. Mice were treated five times per week with NVP-BEZ235 (n=7) or vehicle (n=6) after the development of palpable tumors. Mice were followed for 20 days, at which point vehicle-treated mice were euthanized. NVP-BEZ235-treated mice had significantly smaller tumors. Error bars indicate the standard deviation for each group of animals.

B) Immunohistochemical analyses reveal decreased phosphorylation of ribosomal S6 protein and AKT (Ser473) in NVP-BEZ235 treated mice. No staining was observed in sections that had not been incubated with specific antibodies. C) PI3K/AKT inhibition induces apoptosis in PEL. $1X10^6$ BC-1 PEL cells were treated with either 50 μM miltefosine, 50 μM perifosine, or 20 nm NVP-BEZ235, and the appropriate vehicle controls. Cells were harvested and lysed 12 hours later. Equivalent micrograms of cell lysate for all samples were incubated with a fluorogenic caspase-3 substrate (DEVD-AFC). Caspase-3 cleavage of the fluorescent DEVD substrate was measured on a fluorometer. The percent of caspase-3 activity in BC-1 cells after incubation with perifosine, miltefosine or NVP-BEZ235 was calculated compared to vehicle treated cells. Percent increase in caspase-3 activity of drug treated cells compared to the respective vehicle control treated cells is displayed on the y-axis, and the specific inhibitor is shown on the x-axis.

PI3K/AKT inhibition triggers apoptosis in PEL cells

Activation of the PI3K and AKT kinases is important for cell survival. Since the inhibition of PI3K/AKT is known to induce apoptosis, we analyzed the levels of active caspase-3 in PEL treated with the AKT inhibitors, miltefosine or perifosine, and the PI3K inhibitor, NVP-BEZ235. BC-1 cells were treated with 50μM miltefosine, 50μM perifosine, 20nm NVP-BEZ235, or their respective vehicle controls for 24 hours. Cells were harvested and equivalent amount of cell lysates were measured for caspase-3 enzymatic activity as a marker of apoptosis. We found that NVP-BEZ235-treated BC-1 cells displayed substantially higher levels of activated caspase-3 compared to miltefosine- and perifosine-treated

cells (Figure 6C). The enhanced ability of NVP-BEZ235 to induce caspase-3-mediated cell death may explain why NVP-BEZ235 shows higher activity against PEL *in vitro* and *in vivo*. We also performed trypan blue staining to determine the number of live versus dead cells in PEL treated with 200μM Rosiglitazone, 50μM perifosine, 50μM miltefosine or NVP-BEZ235 (10 and 100nm) for various timepoints. We found that after a 24-hour drug treatment, NVP-BEZ235 and perifosine were more cytotoxic to PEL cells than rosiglitazone (Supplemental Figure 2).

Rosiglitazone, perifosine, and NVP-BEZ235 change the cytokine profile of PEL

PEL are highly sensitive to inhibition of autocrine growth factor signaling pathways(37). The cytokines IL-6 and IL-10, are particularly important for PEL growth(37), and our group has demonstrated that suppression of IL-6 and IL-10 translation by the mTOR inhibitor, rapamycin, inhibits PEL cell proliferation. We investigated the cytokine expression levels of the PEL cell line BC-1 using a 30-plex Luminex bead array technology (Figure 7). BC-1 PEL cells secrete high amounts of IL-6, IL-10, IP-10/CXCL10, hepatocyte growth factor (HGF), MIG/CXCL9, and vascular endothelial growth factor (VEGF). Treatment with the PI3K/mTOR dual inhibitor NVP-BEZ235 profoundly decreased secretion of all these cytokines ($p<0.001$ by post-hoc Tukey test), whereas miltefosine, Perifosine and rosiglitazone did not significantly alter the cytokine profile of PEL cells. Following NVP-BEZ235 treatment for 72 hours, IL-6 and IL-10 levels were

80% lower than vehicle control treated cells. Perifosine reduced IL-6 levels to 50% of control, whilst minimally altering IL-10 secretion. Levels of VEGF, MIG/CXCL9, HGF, and IP-10/CXCL10 were decreased between 50-70% by the dual inhibitor NVP-BEZ235 compared to the control, but were virtually unaffected by either perifosine or miltefosine. Interestingly, NVP-BEZ235 also reduced the transcript levels of some of the cytokines, such as VEGF (data not shown). Activation of PI3K has previously been shown to regulate VEGF transcription(38), and hence dual inhibition of PI3K and mTOR likely affects both mRNA transcript and protein levels of some of these cytokines. Curiously, rosiglitazone dramatically reduced the levels of IP-10 and HGF similar to that seen with NVP-BEZ235 treatment, without affecting the secretion levels of any other assayed cytokines. The difference in cytokine profile expression between NVP-BEZ235-treated cells and those treated with the other inhibitors, separates the *in vitro* proliferation inhibition phenotype from the tumor growth inhibition seen *in vivo*. Although all the inhibitors could prevent proliferation *in vitro*, NVP-BEZ235 was most efficacious at inhibiting tumor growth *in vivo,* likely due to the inhibition of multiple autocrine and paracrine growth factors. This suggests that cytokine profiling can be used to differentiate between different PI3K/AKT/mTOR pathway inhibitors.

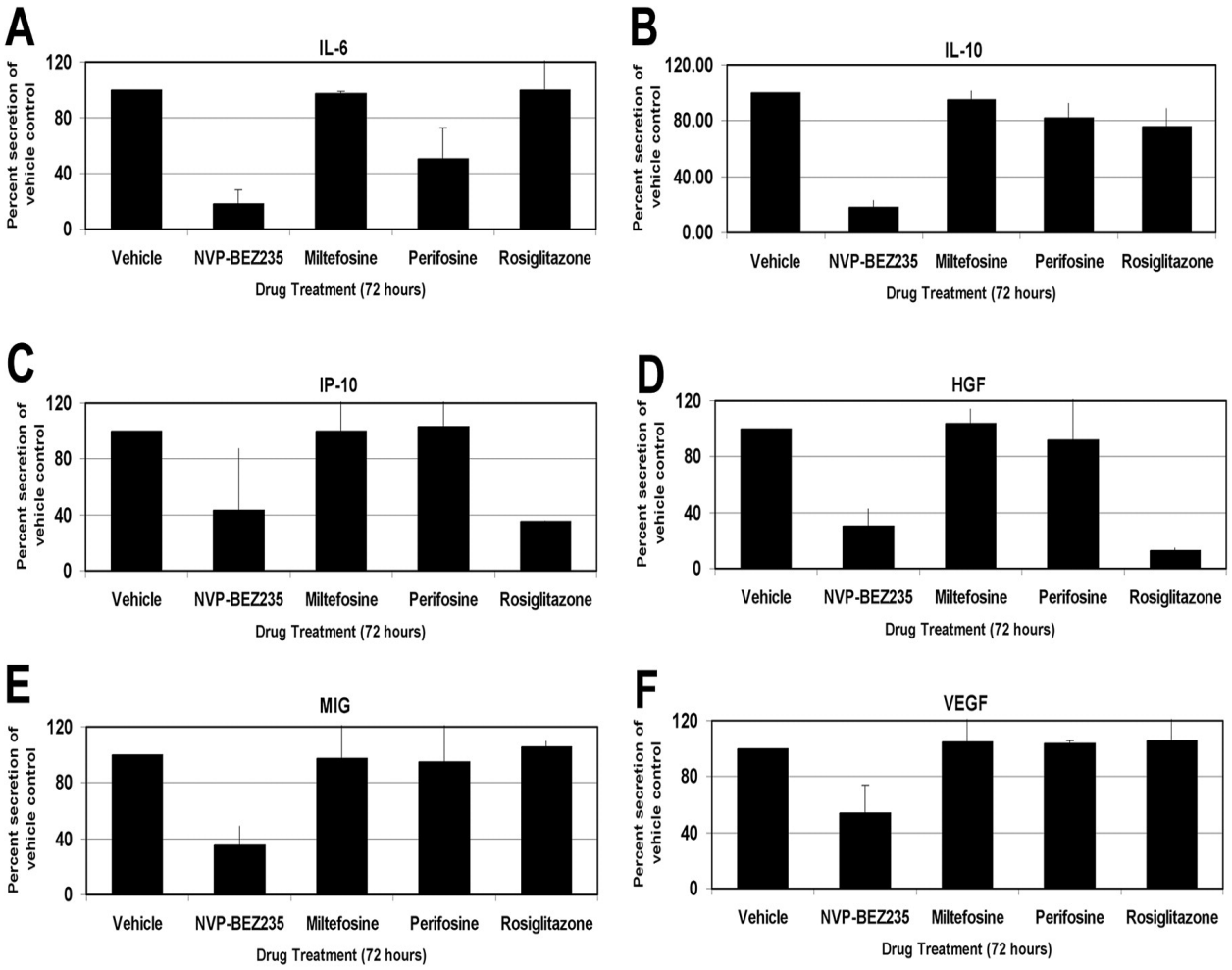

Figure 7. Profile of cellular cytokine levels following inhibition of PI3K/AKT/mTOR pathway members. IL-6, IL-10, IP-10, HGF, MIG and VEGF levels upon treatment with indicated compounds, or with vehicle control are displayed. Changes in cytokine levels are represented as percent change from vehicle-treated levels, which were set to 100%. Error bars indicated standard deviation. The PI3K/mTOR dual inhibitor NVP-BEZ235 dramatically reduces levels of the indicated cytokines secreted into the growth medium ($p<0.001$ by Tukey post-hoc test).

DISCUSSION

We, and others, have previously shown that individual KSHV viral proteins like K1 and vGPCR activate the PI3K/AKT pathway in B cells and endothelial cells(12-16). KSHV-infected PEL also display constitutive high-level activation of the PI3K/AKT/mTOR pathway(10). Our findings indicate that inhibiting the PI3K/AKT/mTOR pathway is an effective modality for treating PEL.

We determined that the glitazone class of drugs, which are known to activate AMPK, have limited efficacy. Ciglitazone and rosiglitazone induced dose-dependent inhibition of PEL growth *in vitro*. This correlated with AMPK activation and mTOR inhibition. Although effective in culture, AMPK activation by rosiglitazone only marginally reduced tumor growth in a xenograft model of PEL.

Miltefosine and perifosine are direct inhibitors of AKT. Both induced dose-dependent inhibition of PEL in culture, and also inhibited the downstream targets of AKT, such as mTOR, leading to reduced phosphorylation and activation of S6K and S6. Importantly, they also inhibited AKT targets that are not part of the mTOR pathway e.g. FOXO1, and are therefore expected to have a greater therapeutic impact than mTORc1 inhibitors alone. In our PEL xenograft model, perifosine reduced tumor volume and growth to a statistically significant extent, compared to vehicle treated mice. These two compounds therefore warrant further study for the treatment of PEL.

The dual PI3K/mTOR inhibitor, NVP-BEZ235(35, 36), was more effective than compounds that targeted only a single member of the PI3K/AKT/mTOR

pathway. Our results demonstrate that the PI3K/mTOR dual inhibitor, NVP-BEZ235, effectively inhibited the proliferation of PEL cell lines *in vitro* at a very low IC50 of 5.68 ± 1.76 nm.

NVP-BEZ235 efficacy was comparable across all PEL cell lines tested, even those that showed partial resistance to rapamycin(10), and was independent of p53 mutation status. BCBL-1, BC-1, BCP-1 and VG-1 showed comparable inhibition of proliferation suggesting that dual inhibition of PI3K and mTOR negates any survival advantage conferred by p53 mutations present in PEL cell lines.

The selective activity of NVP-BEZ235 on PI3K and mTOR was demonstrated by reduced phosphorylation of their downstream targets. Reduced phosphorylation of FOXO1 and GSK3b, the downstream targets of AKT, confirmed the inhibition of PI3K, whereas reduced phosphorylation of S6K and ribosomal S6 confirmed inhibition of mTOR. Importantly, there was an inhibition of phosphorylation of AKT at Ser473. This site is phosphorylated by the rapamycin-insensitive mTORc2, which is responsible for activating AKT in a feedback loop and has been implicated in rapamycin failure after prolonged treatment(39, 40). NVP-BEZ235 can prevent this feedback loop.

NVP-BEZ235 significantly ($p<0.009$) reduced tumor growth in our PEL xenograft model. Tumors excised from NVP-BEZ235-treated mice displayed reduced phosphorylation of both ribosomal S6 protein and AKT (Ser473), confirming *in vivo* inhibition of its targets. Importantly, this compound is orally

bioavailable, making it an attractive therapeutic molecule. Furthermore, NVP-BEZ235 treatment induced higher levels of apoptosis in PEL cells, as measured by caspase-3 activity, compared to the other PI3K/AKT inhibitors.

PEL is characterized by elevated IL-6 and IL-10 cytokine secretion(37). Our group has previously demonstrated that IL-10 may be used as a prognostic marker of PEL, and we have demonstrated that rapamycin treatment reduces IL-6 and IL-10 secretion in culture and *in vivo*(10). Using Luminex bead-based technology, we investigated the secretion profile of many cytokines following treatment with each of the compounds described in this study, or with the appropriate vehicle control. Six cytokines (IL-6, IL-10, IP-10, HGF, MIG and VEGF) were secreted to high levels in the growth medium of BC-1 cells consistent with earlier observations(41, 42). NVP-BEZ235 dramatically reduced secretion of all these cytokines 72 hours post-treatment. The other AKT/mTOR pathway inhibitors exhibited weaker, more differential phenotypes. Rosiglitazone significantly reduced secretion of IP-10 and HGF, but only modestly decreased IL-10 secretion, whereas all other cytokine profiles remained unaltered. The AKT inhibitor, perifosine, reduced IL-6 secretion by fifty percent, and that of IL-10 by twenty percent.

Only NVP-BEZ235 inhibited vascular endothelial growth factor (VEGF). VEGF is an angiogenic growth factor that is involved in tumor proliferation(43). Hepatocyte growth factor (HGF) has been implicated in tumorigenesis of diffused-large B cell lymphomas (DLBCL) and has been shown to activate AKT through PI3K(44). CXCL10/IP-10 and CXCL9/MIG are chemokines that attract T

lymphocytes and appear to antagonize angiogenesis(45). However, these chemokines also play a role in B lymphocyte migration and dissemination(46). Additionally, unlike normal B lymphocytes, Hodgkin lymphoma and several different types of NHL, including chronic lymphocytic leukemia, small lymphocytic lymphoma, follicular lymphoma, marginal zone B-cell lymphoma, and mantle cell lymphoma(47, 48) have been reported to express CXCL9/MIG and CXCL10/IP-10, and their cognate receptor CXCR3 as part of an autocrine loop. We surmise that these cytokines, chemokines, and growth factors play an important role in NHL in general, and that our results may therefore be applicable to other NHL beyond PEL.

In conclusion, the PI3K/AKT/mTOR axis is an important target in NHL because it regulates cell survival, protein translation, and as we show here, cytokine production. Dual inhibition of the PI3K and mTOR kinases inhibits the translation and secretion of the essential paracrine and autocrine cytokines required for growth. This is in addition to cell-intrinsic mTOR targets such as Myc and Cyclin D1(49). Inhibition of these cytokines is required for inhibiting PEL tumor growth *in vivo*. Thus, this dual inhibitor may prove therapeutic for tumors that are critically dependent on autocrine and paracrine growth factors for their survival.

REFERENCES

1. **Cross DA, Alessi DR, Cohen P, Andjelkovich M, Hemmings BA.** 1995. Inhibition of glycogen synthase kinase-3 by insulin mediated by protein kinase B. Nature **378:**785-789.

2. **Datta SR, Dudek H, Tao X, Masters S, Fu H, Gotoh Y, Greenberg ME.** 1997. Akt phosphorylation of BAD couples survival signals to the cell- intrinsic death machinery. Cell **91:**231-241.

3. **del Peso L, Gonzalez-Garcia M, Page C, Herrera R, Nunez G.** 1997. Interleukin-3-induced phosphorylation of BAD through the protein kinase Akt. Science **278:**687-689.

4. **Cardone MH, Roy N, Stennicke HR, Salvesen GS, Franke TF, Stanbridge E, Frisch S, Reed JC.** 1998. Regulation of cell death protease caspase-9 by phosphorylation. Science **282:**1318-1321.

5. **Manning BD, Cantley LC.** 2007. AKT/PKB signaling: navigating downstream. Cell **129:**1261-1274.

6. **Shaw RJ, Bardeesy N, Manning BD, Lopez L, Kosmatka M, DePinho RA, Cantley LC.** 2004. The LKB1 tumor suppressor negatively regulates mTOR signaling. Cancer Cell **6:**91-99.

7. **Fryer LG, Parbu-Patel A, Carling D.** 2002. The Anti-diabetic drugs rosiglitazone and metformin stimulate AMP-activated protein kinase through distinct signaling pathways. J Biol Chem **277:**25226-25232.

8. **Panigrahy D, Singer S, Shen LQ, Butterfield CE, Freedman DA, Chen EJ, Moses MA, Kilroy S, Duensing S, Fletcher C, Fletcher JA, Hlatky L, Hahnfeldt P, Folkman J, Kaipainen A.** 2002. PPARgamma ligands inhibit primary tumor growth and metastasis by inhibiting angiogenesis. J Clin Invest **110:**923-932.

9. **Girnun GD, Naseri E, Vafai SB, Qu L, Szwaya JD, Bronson R, Alberta JA, Spiegelman BM.** 2007. Synergy between PPARgamma ligands and platinum-based drugs in cancer. Cancer Cell **11:**395-406.

10. **Sin SH, Roy D, Wang L, Staudt MR, Fakhari FD, Patel DD, Henry D, Harrington WJ, Jr., Damania BA, Dittmer DP.** 2007. Rapamycin is efficacious against primary effusion lymphoma (PEL) cell lines in vivo by inhibiting autocrine signaling. Blood **109:**2165-2173.

11. **Boulanger E, Gerard L, Gabarre J, Molina JM, Rapp C, Abino JF, Cadranel J, Chevret S, Oksenhendler E.** 2005. Prognostic factors and outcome of human herpesvirus 8-associated primary effusion lymphoma in patients with AIDS. J Clin Oncol **23:**4372-4380.

12. **Wang L, Damania B.** 2008. Kaposi's sarcoma-associated herpesvirus confers a survival advantage to endothelial cells. Cancer Res **68:**4640-4648.

13. **Tomlinson CC, Damania B.** 2004. The K1 protein of Kaposi's sarcoma-associated herpesvirus activates the Akt signaling pathway. J Virol **78:**1918-1927.

14. **Tomlinson CC, Damania B.** 2008. Critical role for endocytosis in the regulation of signaling by the Kaposi's sarcoma-associated herpesvirus K1 protein. J Virol **82:**6514-6523.

15. **Wang L, Wakisaka, N., Tomlinson, C.C., DeWire, S., Krall, S., Pagano, J.S. and B. Damania.** 2004. The Kaposi's Sarcoma-Associated Herpesvirus (KSHV/HHV8) K1 Protein Induces Expression of Angiogenic and Invasion Factors. Cancer Research.

16. **Wang L, Dittmer DP, Tomlinson CC, Fakhari FD, Damania B.** 2006. Immortalization of primary endothelial cells by the K1 protein of Kaposi's sarcoma-associated herpesvirus. Cancer Res **66:**3658-3666.

17. **Bais C, Van Geelen A, Eroles P, Mutlu A, Chiozzini C, Dias S, Silverstein RL, Rafii S, Mesri EA.** 2003. Kaposi's sarcoma associated herpesvirus G protein-coupled receptor immortalizes human endothelial cells by activation of the VEGF receptor-2/ KDR. Cancer Cell **3:**131-143.

18. **Sodhi A, Montaner S, Patel V, Gomez-Roman JJ, Li Y, Sausville EA, Sawai ET, Gutkind JS.** 2004. Akt plays a central role in sarcomagenesis induced by Kaposi's sarcoma herpesvirus-encoded G protein-coupled receptor. Proc Natl Acad Sci U S A **101:**4821-4826.

19. **Sodhi A, Chaisuparat R, Hu J, Ramsdell AK, Manning BD, Sausville EA, Sawai ET, Molinolo A, Gutkind JS, Montaner S.** 2006. The TSC2/mTOR pathway drives endothelial cell transformation induced by the Kaposi's sarcoma-associated herpesvirus G protein-coupled receptor. Cancer Cell **10:**133-143.

20. **Montaner S, Sodhi A, Pece S, Mesri EA, Gutkind JS.** 2001. The Kaposi's sarcoma-associated herpesvirus G protein-coupled receptor promotes endothelial cell survival through the activation of Akt/protein kinase B. Cancer Res **61:**2641-2648.

21. **Sodhi A, Montaner S, Patel V, Zohar M, Bais C, Mesri EA, Gutkind JS.** 2000. The Kaposi's sarcoma-associated herpes virus G protein-coupled receptor up-regulates vascular endothelial growth factor expression and secretion through mitogen-activated protein kinase and p38 pathways acting on hypoxia-inducible factor 1alpha. Cancer Res **60:**4873-4880.

22. **Boulanger E, Marchio A, Hong SS, Pineau P.** 2009. Mutational analysis of TP53, PTEN, PIK3CA and CTNNB1/beta-catenin genes in human herpesvirus 8-associated primary effusion lymphoma. Haematologica **94:**1170-1174.

23. **Jacinto E, Loewith R, Schmidt A, Lin S, Ruegg MA, Hall A, Hall MN.** 2004. Mammalian TOR complex 2 controls the actin cytoskeleton and is rapamycin insensitive. Nat Cell Biol **6:**1122-1128.

24. **Faraway. J.** 2006. Extending the Linear Model with R. Chapman and Hall/CRC.

25. **Inoki K, Zhu T, Guan KL.** 2003. TSC2 mediates cellular energy response to control cell growth and survival. Cell **115:**577-590.

26. **Inoki K, Ouyang H, Zhu T, Lindvall C, Wang Y, Zhang X, Yang Q, Bennett C, Harada Y, Stankunas K, Wang CY, He X, MacDougald OA, You M, Williams BO, Guan KL.** 2006. TSC2 integrates Wnt and energy signals via a coordinated phosphorylation by AMPK and GSK3 to regulate cell growth. Cell **126:**955-968.

27. **Ruiter GA, Zerp SF, Bartelink H, van Blitterswijk WJ, Verheij M.** 2003. Anti-cancer alkyl-lysophospholipids inhibit the phosphatidylinositol 3-kinase-Akt/PKB survival pathway. Anticancer Drugs **14:**167-173.

28. **LoPiccolo J, Blumenthal GM, Bernstein WB, Dennis PA.** 2008. Targeting the PI3K/Akt/mTOR pathway: effective combinations and clinical considerations. Drug Resist Updat **11:**32-50.

29. **Yamauchi T, Waki H, Kamon J, Murakami K, Motojima K, Komeda K, Miki H, Kubota N, Terauchi Y, Tsuchida A, Tsuboyama-Kasaoka N, Yamauchi N, Ide T, Hori W, Kato S, Fukayama M, Akanuma Y, Ezaki O, Itai A, Nagai R, Kimura S, Tobe K, Kagechika H, Shudo K, Kadowaki T.** 2001. Inhibition of RXR and PPARgamma ameliorates diet-induced obesity and type 2 diabetes. J Clin Invest **108:**1001-1013.

30. **Han S, Roman J.** 2006. Rosiglitazone suppresses human lung carcinoma cell growth through PPARgamma-dependent and PPARgamma-independent signal pathways. Mol Cancer Ther **5:**430-437.

31. **Heaney AP, Fernando M, Yong WH, Melmed S.** 2002. Functional PPAR-gamma receptor is a novel therapeutic target for ACTH-secreting pituitary adenomas. Nat Med **8:**1281-1287.

32. **Petre CE, Sin SH, Dittmer DP.** 2007. Functional p53 signaling in Kaposi's sarcoma-associated herpesvirus lymphomas: implications for therapy. J Virol **81:**1912-1922.

33. **Okoshi R, Ozaki T, Yamamoto H, Ando K, Koida N, Ono S, Koda T, Kamijo T, Nakagawara A, Kizaki H.** 2008. Activation of AMP-activated protein kinase induces p53-dependent apoptotic cell death in response to energetic stress. J Biol Chem **283:**3979-3987.

34. **Hideshima T, Catley L, Yasui H, Ishitsuka K, Raje N, Mitsiades C, Podar K, Munshi NC, Chauhan D, Richardson PG, Anderson KC.** 2006. Perifosine, an oral bioactive novel alkylphospholipid, inhibits Akt and induces in vitro and in vivo cytotoxicity in human multiple myeloma cells. Blood **107:**4053-4062.

35. **Maira SM, Stauffer F, Brueggen J, Furet P, Schnell C, Fritsch C, Brachmann S, Chene P, De Pover A, Schoemaker K, Fabbro D, Gabriel D, Simonen M, Murphy L, Finan P, Sellers W, Garcia-Echeverria C.** 2008. Identification and characterization of NVP-BEZ235, a new orally available dual phosphatidylinositol 3-kinase/mammalian target of rapamycin inhibitor with potent in vivo antitumor activity. Mol Cancer Ther **7:**1851-1863.

36. **Serra V, Markman B, Scaltriti M, Eichhorn PJ, Valero V, Guzman M, Botero ML, Llonch E, Atzori F, Di Cosimo S, Maira M, Garcia-Echeverria C, Parra JL, Arribas J, Baselga J.** 2008. NVP-BEZ235, a dual PI3K/mTOR inhibitor, prevents PI3K signaling and inhibits the growth of cancer cells with activating PI3K mutations. Cancer Res **68:**8022-8030.

37. **Aoki Y, Yarchoan R, Braun J, Iwamoto A, Tosato G.** 2000. Viral and cellular cytokines in AIDS-related malignant lymphomatous effusions. Blood **96:**1599-1601.

38. **Kang J, Rychahou PG, Ishola TA, Mourot JM, Evers BM, Chung DH.** 2008. N-myc is a novel regulator of PI3K-mediated VEGF expression in neuroblastoma. Oncogene **27:**3999-4007.

39. **Bayascas JR, Alessi DR.** 2005. Regulation of Akt/PKB Ser473 phosphorylation. Mol Cell **18:**143-145.

40. **Sarbassov DD, Guertin DA, Ali SM, Sabatini DM.** 2005. Phosphorylation and regulation of Akt/PKB by the rictor-mTOR complex. Science **307:**1098-1101.

41. **Drexler HG, Meyer C, Gaidano G, Carbone A.** 1999. Constitutive cytokine production by primary effusion (body cavity-based) lymphoma-derived cell lines. Leukemia **13:**634-640.

42. **Capello D, Gaidano G, Gallicchio M, Gloghini A, Medico E, Vivenza D, Buonaiuto D, Fassone L, Avanzi GC, Saglio G, Prat M, Carbone A.** 2000. The tyrosine kinase receptor met and its ligand HGF are co-expressed and functionally active in HHV-8 positive primary effusion lymphoma. Leukemia **14:**285-291.

43. **Lohela M, Bry M, Tammela T, Alitalo K.** 2009. VEGFs and receptors involved in angiogenesis versus lymphangiogenesis. Curr Opin Cell Biol **21:**154-165.

44. **Tjin EP, Groen RW, Vogelzang I, Derksen PW, Klok MD, Meijer HP, van Eeden S, Pals ST, Spaargaren M.** 2006. Functional analysis of HGF/MET signaling and aberrant HGF-activator expression in diffuse large B-cell lymphoma. Blood **107:**760-768.

45. **Sgadari C, Farber JM, Angiolillo AL, Liao F, Teruya-Feldstein J, Burd PR, Yao L, Gupta G, Kanegane C, Tosato G.** 1997. Mig, the monokine induced by interferon-gamma, promotes tumor necrosis in vivo. Blood **89:**2635-2643.

46. **Pals ST, de Gorter DJ, Spaargaren M.** 2007. Lymphoma dissemination: the other face of lymphocyte homing. Blood **110:**3102-3111.

47. **Teichmann M, Meyer B, Beck A, Niedobitek G.** 2005. Expression of the interferon-inducible chemokine IP-10 (CXCL10), a chemokine with proposed anti-neoplastic functions, in Hodgkin lymphoma and nasopharyngeal carcinoma. J Pathol **206:**68-75.

48. **Jones D, Benjamin RJ, Shahsafaei A, Dorfman DM.** 2000. The chemokine receptor CXCR3 is expressed in a subset of B-cell lymphomas and is a marker of B-cell chronic lymphocytic leukemia. Blood **95:**627-632.

49. **Gera JF, Mellinghoff IK, Shi Y, Rettig MB, Tran C, Hsu JH, Sawyers CL, Lichtenstein AK.** 2004. AKT activity determines sensitivity to mammalian target of rapamycin (mTOR) inhibitors by regulating cyclin D1 and c-myc expression. J Biol Chem **279:**2737-2746.

CHAPTER 3

DYSREGULATION OF FATTY ACID SYNTHESIS AND GLYCOLYSIS IN NON-HODGKIN LYMPHOMA[4]

INTRODUCTION

Primary effusion lymphoma (PEL) is a subtype of B cell non-Hodgkin lymphoma (B-NHL), which has a poor prognosis, with a median survival time of six months (1). PEL display elevated levels of activated phosphatidylinositol 3-kinase (PI3K), AKT and mammalian target of rapamycin (mTOR) kinases (2). All PEL are infected with Kaposi sarcoma-associated herpesvirus (KSHV) and hence represent a tightly defined sub-type of B-NHL. In addition to PEL, KSHV is also associated with Kaposi sarcoma (KS) and multicentric Castleman's disease (MCD) (3, 4). Our group and others have previously shown that KSHV viral proteins such as K1 and vGPCR can activate the PI3K/AKT/mTOR pathway in B lymphocytes and endothelial cells (5-9) and that the reliance of PEL on the PI3K/AKT/mTOR pathway can be exploited to treat PEL using inhibitors of this pathway (2, 10).

---

[4] Aadra P Bhatt, Sarah R Jacobs, Alex J Freemerman, Liza Makowski, Jeffrey C Rathmell, Dirk P Dittmer and Blossom Damania. Copyright © Proceedings of the National Academy of Sciences United States. 2012 July 17; 109 (29): 11818-23

The ability of cancer cells to selectively induce aerobic glycolysis in order to generate ATP was first reported by Otto Warburg (11). Glycolysis generates fewer ATP per molecule of glucose compared to oxidative phosphorylation, and produces lactate, which is excreted (Fig. 1A). Recent studies indicate that upregulated aerobic glycolysis in cancer cells exerts a protective effect against apoptosis (12). Moreover, the requirement for high rates of macromolecular synthesis required by rapidly proliferating cancer cells is met by upregulating glycolysis (13).

The PI3K/AKT/mTOR signaling pathway is essential for the control of cell proliferation and protein translation, and also regulates anabolic activities within the cell (14). PI3K/AKT signaling is known to regulate glycolysis by controlling the expression and localization of the glucose transporter GLUT1 (15), hexokinase, and transcriptional control of glycolytic enzymes (16). PI3K activation results in PDK1 and subsequently AKT activation, which is necessary for the induction of glycolytic enzymes (17-19). AKT also activates the mTOR signaling complex, which regulates protein translation. Under nutrient abundant conditions, mTOR activation stimulates aerobic glycolysis as well as *de novo* lipid synthesis, mediated *via* mobilization of the SREBP group of transcription factors (20). SREBP1 can induce the transcription of fatty acid synthase (FASN), which is a multi-enzyme complex responsible for synthesizing cellular lipids. FASN is expressed in the liver, and present at low levels in other tissues. Many human cancers express high levels of FASN (21, 22), and FASN is posited to be a metabolic oncogene (23). Moreover, aberrant PI3K signaling resulting from

receptor tyrosine kinase hyperactivation in cancer cells has been demonstrated to drive FASN expression via constitutive SREBP-1c activity (24, 25).

In this work, we describe the metabolic sequelae of PI3K/AKT/mTOR pathway activation on the metabolism of B-NHL, with a focus on PEL. We demonstrate that most B-NHL, including PEL are highly glycolytic and actively synthesize fatty acids, compared to healthy donor-derived primary B cells. Further, we demonstrate that PEL display elevated levels of FASN compared to primary B cells, and that the glycolysis and FAS pathways in PEL are interlinked, and dependent on PI3K/AKT/mTOR activation.

MATERIALS & METHODS

Cell isolation and culture

Primary B cells were isolated by negative selection from donor buffy coats using the B cell isolation kit II (Miltenyi) as per the manufacturer's directions. Cells were cultured at 37°C with 5% CO_2 in filter-sterilized RPMI-1640 supplemented with 10% FBS, 100 U/ml each of penicillin and streptomycin, 0.075% $nahco_3$ and 0.05 mm 2-mercaptoethanol. Purity of the isolated B cells was determined by staining with phycoerythrin-conjugated anti-CD19 antibodies (Miltenyi) and analyzed on a macsquant® VYB (Miltenyi). Purity ranged from 89-98% (data not shown). Primary effusion lymphoma (PEL) cell lines were cultured in identical media and culture conditions as previously described (26). Lymphoblast cell line were generated by infecting freshly isolated primary human

B cells with Epstein-Barr virus (EBV), using previously described protocols (27). Follicular lymphoma cells were cultured as previously described (28). CA46, a Burkitt lymphoma cell line, was purchased from ATCC and maintained in RPMI-1640 supplemented with 20% FBS and 100 U/ml penicillin and streptomycin. All cell lines were cultured in PEL growth medium for every experiment.

Chemical compounds

2-deoxy-D-glucose (2DG), C75 and lipopolysaccharide (LPS) were purchased from Sigma Aldrich. LY294002 was purchased from Calbiochem. 2DG was suspended in H_2O, C75 and LY294002 in DMSO, and LPS in phosphate-buffered saline. All cells were treated for indicated time periods. For visualizing intracellular lipids, the lipophilic dye Nile Red (AAT Bioquest), was used per the manufacturer's direction. A Nikon Eclipse Ti microscope equipped with NIS Elements imaging software was used to acquire images.

Cell Viability Assays

To determine the susceptibility of both cell types to various inhibitors, 2 x 10^5 PEL or primary B cells were cultured in growth medium containing compounds at increasing concentrations, or the appropriate vehicle controls, for indicated lengths of time. Cell viability was determined in quadruplicate by trypan blue exclusion. Proliferation was measured using the Cell Titer 96Aqueous One Solution (Promega) and apoptosis was measured using the ApoAlert Caspase-3 assay (Clontech), both according to the manufacturer's instructions, and absorbance was measured using a Fluostar OPTIMA (BMG Labtech) plate

reader. Additionally, cell viability was also measured using forward and side scatter parameters from flow cytometry performed on a MACSquant® VYB (Miltenyi).

Immunoblotting

Following indicated treatments, cells were washed with ice-cold PBS and then lysed in a buffer containing 150 mm NaCl, 50 mm Tris-HCl (ph 8), 0.1% NP40, 50 mm NaF, 30 mm β-glycerophosphate, 1 mm Na_3VO_4, and 1× Complete Protease Inhibitor cocktail (Roche Diagnostics). Protein concentration was determined by Bradford assay, and equal amounts of proteins were separated using SDS-PAGE, transferred onto Hybond-ECL nitrocellulose membranes (GE Healthcare), blocked and incubated in appropriate antibodies overnight at 4°C. The antibodies used were against Fatty Acid Synthase, phospho-AKT Ser^{473} (Cell Signal Technology), and Ku 70/80 as a loading control (a generous gift of Dale Ramsden, PhD; University of North Carolina at Chapel Hill). Blots were incubated in appropriate secondary antibodies conjugated to horseradish peroxidase, and bands were visualized using chemiluminescence (GE Corporation). Densitometry was performed using NIH Image J.

Measurement of glycolytic flux

Glycolytic flux was measured as previously described (29). Briefly, 2 x 10^6 cells of each type were incubated with indicated compounds for 72 h, after which cells were washed twice in PBS and starved for 30 min by suspension in glucose-free Krebs solution, followed by a 1 h pulse with 10 μCi of D-[5-^{3}H](N)-

glucose (Perkin-Elmer) and non-labeled glucose, adjusted to a final glucose concentration of 10 mM. Equal volume of 0.2 M HCl was added to all samples to stop the reaction after which [^{3}H]-H_2O generated via glycolysis was separated from the D-[5-^{3}H](N)-glucose bolus by evaporation-mediated equilibration in sealed chambers. Levels of [^{3}H]-H_2O were measured on a liquid scintillation counter (Wallac), and glycolytic flux was determined by normalizing CPM to the total protein input. These and all subsequently described data were analyzed using a two-tailed type II Student's *t*-test for significance; *p* values are indicated at appropriate locations within figure legends.

Measurement of lipid synthesis and analysis of newly synthesized lipid classes.

Lipid synthesis was measured as previously described (30). Briefly, 1 X 10^6 B cells were incubated with indicated compounds for 72 h; 12 h prior to harvest and subsequent analysis, growth medium of all cells was supplemented with D-[U-$^{14}C_6$]-glucose, after which cells were collected, washed thrice with PBS and then lysed by vortexing in 0.5% NP-40 in water. Lipids were extracted by sequentially mixing in 1 ml methanol, 2 x 1 ml $ChCl_3$ and 1 ml H_2O, with extensive vortexing after addition of each solvent. To resolve aqueous and organic phases, tubes were centrifuged for 10 min at 2000 x g in a tabletop centrifuge. The organic phase was transferred to a fresh tube and excess $chcl_3$ was evaporated. Extracted lipids were dissolved in 100 ml of $chcl_3$, and counted using scintillation fluid (Scintisafe) in a liquid scintillation counter (Wallac). CPM was normalized to the total protein input. Analysis of lipid components was

performed by the UNC Nutrition and Obesity Research Center using previously described methods (31).

Measurement of fatty acid oxidation

Fatty acid oxidative capacity was determined by measuring 1-^{14}C-oleate oxidation to CO_2 as previously described (32). Briefly, 1 x 10^6 B cells were incubated with indicated compounds for 72 h, after which cells were resuspended in normal growth media supplemented with 12.5 mm HEPES (ph 7.4) and 500 μm 1-^{14}C-oleate (Perkin Elmer) complexed with 0.5% BSA (Sigma) and incubated for 2 h at 37°C. A result of 1-^{14}C-oleate oxidation is release of radiolabeled bicarbonate into the growth medium, which was collected at the end of 2 h and transferred to custom wells. Medium was acidified with $HClO_4$ and resulting $^{14}CO_2$ was captured in 1N NaOH over 1 h and counted using liquid scintillation (Wallac). Specific activity was calculated following normalization of CPM to protein content.

Metabolic profiling

Glycolytic and fatty acid metabolite profiles were obtained to assess the relative distribution of various intra- and extracellular metabolites of PEL and primary B cells by culturing all cells for three days in growth media described above at a starting concentration of 1 x 10^6 cells/ml, after which cells were washed twice in PBS and cell pellets were flash-frozen. The conditioned growth media of cultured cells was also collected after centrifugation and flash frozen. Further sample preparation, metabolic profiling, peak identification and curation

was performed by Metabolon, Inc. (Durham, NC) using previously described methods (33).

Profiling of fatty acid oxidation intermediates

1 x 10^7 PEL or primary B cells were cultured for 36 h in growth media supplemented with 1 mM L-carnitine, after which cells were placed in fresh media containing indicated compounds for a further 72 h. Cells were harvested, washed in PBS and then snap-frozen. Cell pellets were resuspended in ddH_2O and lysed on ice for 15 min, followed by sonication and centrifugation at 13,000 x g for 15 min at 4°C. Supernatants were quantified for protein concentration and stored at -80°C. Profiling of cell lysates by tandem MS was performed as previously described (34).

Bioinformatics

Hierarchical clustering and principal component analysis was conducted using the R programming environment (version 2.13.2) package factominer.

RESULTS

PEL display elevated aerobic glycolysis

To determine the minimum glucose (Glc) requirement of PEL cells, 2 x 10^5 PEL cells were cultured in Glc-free media with defined amounts of D-Glc, and cell survival was monitored using two independent techniques: trypan blue exclusion (Fig. 1B, left panel) and MTS assay (Fig. 1B, right panel). Viability of

BCP-1, a representative PEL cell line, decreased when the D-Glc concentration of growth medium was lowered, and the reduction in cell viability correlated with a dose-dependent decrease in Glc concentration (Fig. 1B). These data were similar in other PEL lines tested, including BC-1, BCBL-1, BCLM and VG-1. Thus, PEL are dependent on Glc for survival.

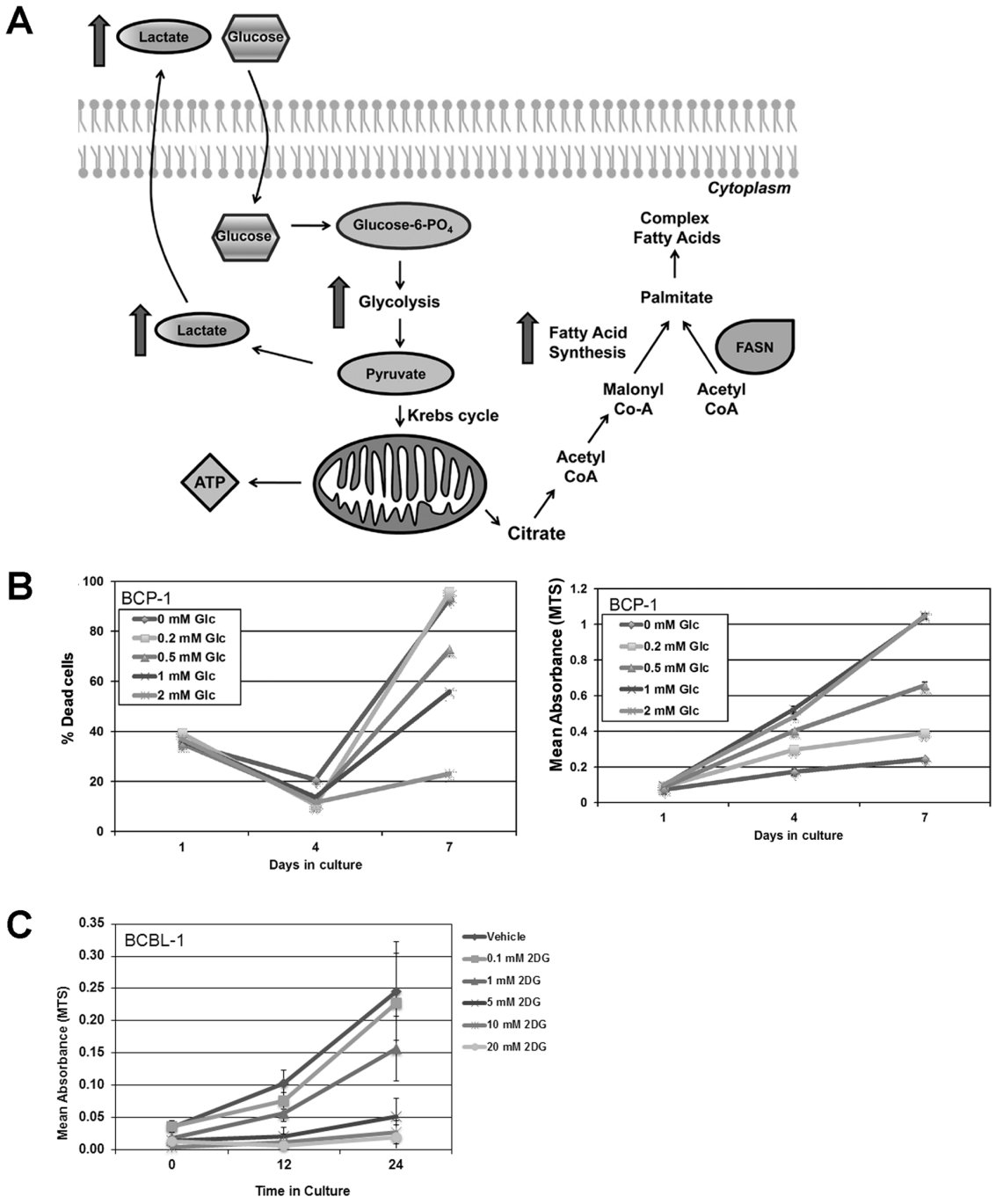

Figure 1: Glycolysis and fatty acid synthesis pathways. **(A)** Once glucose (Glc) is transported into the cell, hexokinase rapidly phosphorylates Glc into Glc-6-phosphate, which participates in glycolysis to generate 2 ATP. Pyruvate, the end product of

glycolysis, is converted into lactate by lactate dehydrogenase and is secreted. Alternatively, pyruvate can be further oxidized in the mitochondrion via the Krebs cycle to yield 36 ATP per molecule of Glc. Citrate, an intermediate metabolite, can exit the Krebs cycle and be transported into the cytoplasm, where it can be broken down into acetyl-CoA. Acetyl-CoA is converted into malonyl-CoA by acetyl-CoA carboxylase, which is the commitment step of fatty acid synthesis (FAS). Acetyl- and malonyl-CoA, in a series of reactions, are combined by Fatty Acid Synthase (FASN), a multi-enzyme polypeptide, to yield palmitate (C16), which is then elongated or desaturated into other fatty acids. These fatty acids can be used to further synthesize other macromolecules and lipids necessary for dividing cells. **(B)** BCP-1, a representative PEL, is sensitive to Glc deprivation from growth medium, which normally has 2 mm glucose. Reduction of Glc concentration in growth medium reduces BCP-1 proliferation as determined by MTS assay (right panel), and increases the percentage of dead cells, as visualized by trypan blue exclusion (left panel). **(C)** BCBL-1, another representative PEL, is susceptible to 2DG added to normal growth medium, in a dose-dependent manner. Error bars are ± SEM, and data is representative of multiple independent experiments.

Next, 2 x 10^5 PEL cells were treated with increasing concentrations of the inhibitor 2-deoxy-D-glucose (2DG), a D-Glc mimetic that cannot be metabolized by glycolytic enzymes, thereby inhibiting glycolysis. Cells were cultured in fully-supplemented media, which contains 2 mm D-Glc, containing increasing doses of 2DG for 0, 12 or 24 hours and then analyzed by MTS assay. 2DG inhibited the proliferation of BCBL-1, a representative PEL, in a dose-dependent manner (Fig. 1C), indicating that inhibition of glycolysis is sufficient to reduce PEL cell viability.

Since PEL are heavily reliant upon Glc, glycolysis was compared between PEL and primary B cells. Intra- and extracellular levels of Glc and lactate were measured from primary B-lymphocytes isolated from six individual healthy donors and six different PEL cell lines: BC-1, BC-3, BCBL-1, BCP-1, JSC-1 and VG-1. Averaged intensities of intracellular metabolites were normalized to total cellular protein, and extracellular metabolite intensities were normalized to the total volume of spent media. When compared to primary B cells, PEL displayed decreased levels of intracellular Glc and elevated levels of intracellular lactate (Fig. 2A) indicative of upregulated glycolytic flux. Analysis of the spent growth media from equivalent numbers of cells revealed higher levels of extracellular lactate and pyruvate in the growth medium of PEL cells, compared to primary B cells (Fig. 2B). PEL media had a concurrent decrease in extracellular D-Glc, confirming enhanced Glc uptake and increased glycolysis in PEL compared to primary B cells.

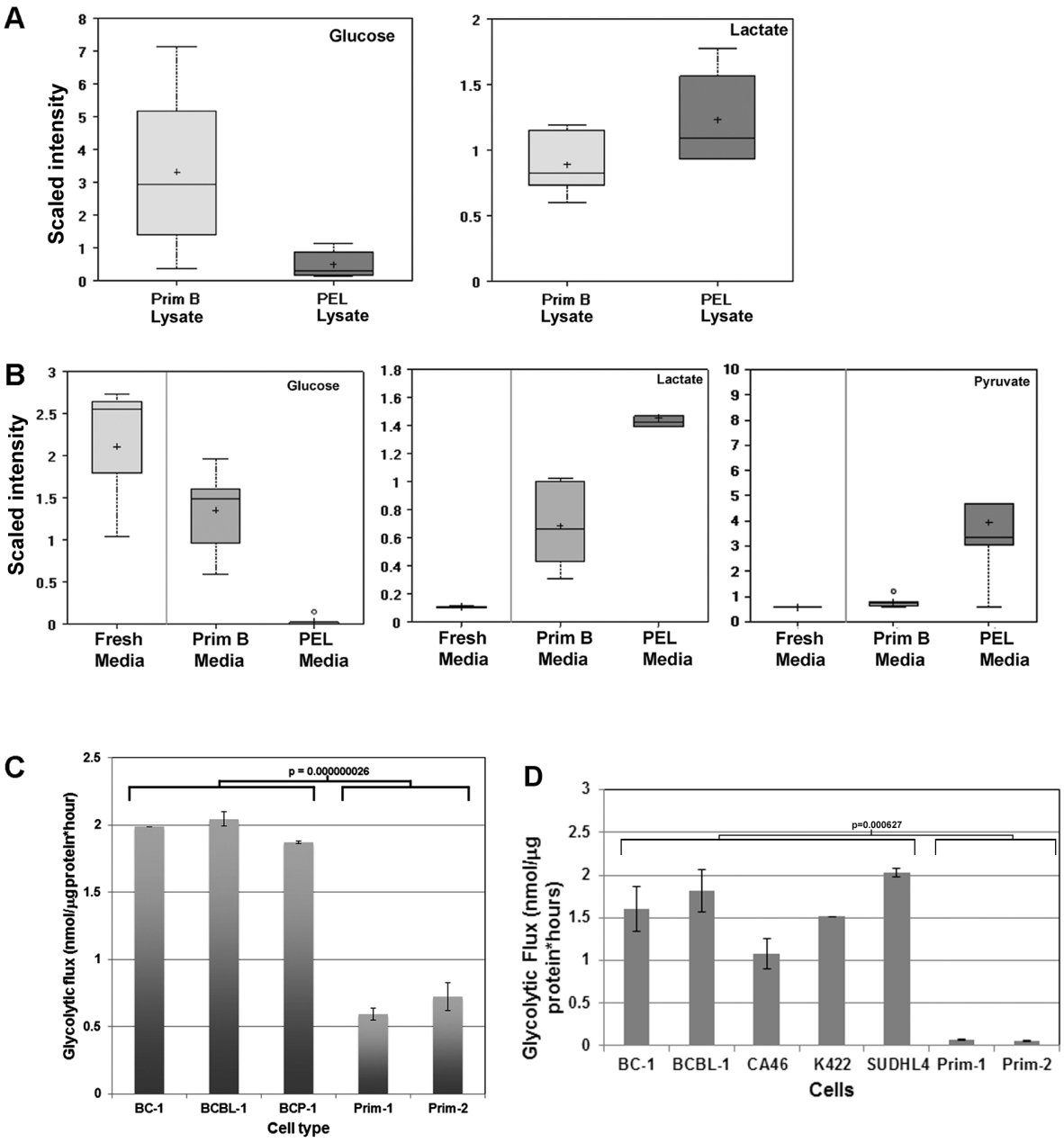

Figure 2. PEL upregulate glycolysis. The protein-normalized relative intensities ("scaled intensities") of intra- and extracellular concentrations of glycolytic intermediates, represented as box and whisker plots, is significantly different between PEL and primary B cells. Data is the combined average of six different

primary B cells derived from 6 healthy donors and six PEL lines. **(A)** Intracellular levels of free Glc are lower while that of lactate are higher in PEL, as compared to primary B cells. **(B)** The spent media of PEL contains lower concentration of Glc and increased levels of lactate and pyruvate compared to the spent media of primary B cells. **(C)** Equal numbers of PEL and primary cells were cultured for 24 h, and glycolytic flux was measured. PEL cells exhibit significantly increased (*p≤ 0.01)* glycolysis compared to primary human B cells. **(D)** Equal numbers of PEL, BL (CA46), FL (K422 and SUDHL4) and primary B cells were cultured for 24 h, and glycolytic flux was measured. All B-NHL have significantly (p value =0.000627) higher glycolytic flux compared to primary B cells. Data are normalized to total input protein. Error bars are ± SEM, data is one representative of >5 independent experiments.

We also measured the glycolytic flux of both B-NHL and primary B cells. Cells were pulsed with 10 μCi of D-[5-^{3}H](N)-glucose. [^{3}H]-H_2O generated through glycolysis was measured, and glycolytic flux was determined by normalizing CPM to the total protein input. We found that glycolytic flux was significantly increased (*p≤0.001)* up to four-fold in PEL cells compared to primary human B cells; Fig. 2C shows a representative panel of PEL and primary B cells. Fig. 2D shows a comparison between two PEL lines BC-1 and BCBL-1, the Burkitt lymphoma (BL) cell line CA46, and the follicular lymphoma (FL) lines K422 and SUDHL4, in comparison with two primary B cells derived from different donors than in Fig. 2C. CA46, K422 and SUDHL4 are all EBV- and KSHV-

negative. We found that glycolysis is highly upregulated in all of these B-NHL lines, compared to primary B cells.

Upregulation of fatty acid synthesis (FAS) in PEL

Fatty acid synthase (FASN) is a multi-functional protein complex responsible for synthesizing all cellular fatty acids. Aberrant FASN over-expression can be a metabolic signature of some human cancers (21, 23). We analyzed equivalent amounts of lysate of various PEL cell lines and primary B cells by immunoblotting to compare the relative expression of FASN protein. As shown in Fig. 3A, FASN was highly expressed in every PEL cell line analyzed (Fig. 3A), while FASN expression was barely detectable in lysates from primary B cells. PEL and primary B cells were also stained with the lipophilic dye Nile Red, and visualized using fluorescence microscopy (Fig. 4). PEL cells contain many cytoplasmic lipid droplets that are absent in primary B cells, indicative of intracellular lipid accumulation. To determine whether FASN protein expression correlated with activation of fatty acid synthesis (FAS), we determined the rate at which *de novo* FAS occurs in PEL and primary B cells, by measuring the degree of incorporation of radiolabeled Glc into the cellular lipid fraction. Radioactive counts from the extracted lipid fraction of each cell type were normalized to the total protein content of the cell pellet. We found that PEL synthesize fatty acids from Glc at a substantially higher rate ($p=0.012$) compared to primary cells (Fig. 3B).

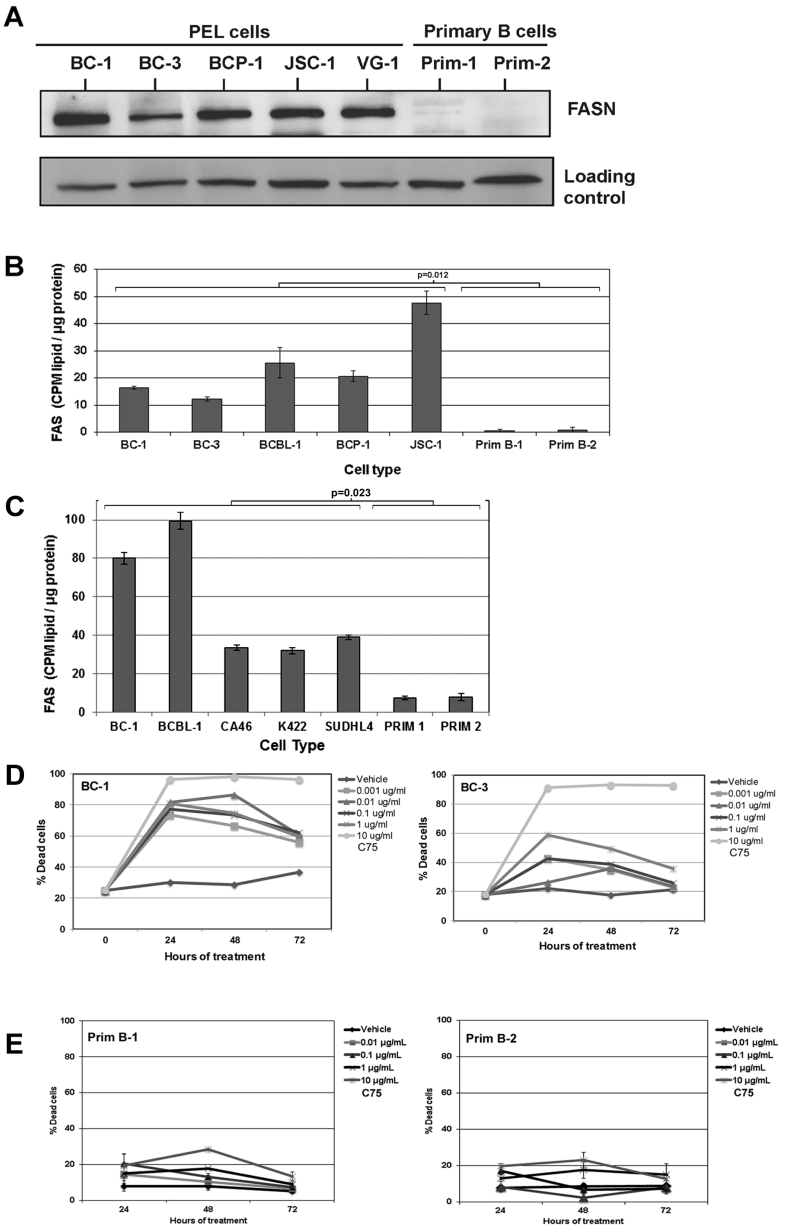

Figure 3. FAS is a critical and essential metabolic pathway for the proliferation of PEL. **(A)** PEL express higher levels of fatty acid synthase (FASN) compared to primary B cells. Ku80 is shown as a loading control. **(B)** The rate of FAS in PEL is significantly higher (*p=0.012*) compared to primary B cells. **(C)** PEL (BC-1 and BCBL-1) have higher FAS rates compared to BL (CA46) and FL (K422 and SUDHL4). Collectively, all B-NHL have a higher FAS rate compared to primary B

cells. Data are normalized to total input protein, and is one representative of multiple independent experiments. Error bars are ± SEM. **(D)** Inhibition of FAS using varying concentrations of the FASN inhibitor, C75, leads to a dose-dependent increase in cell death in BC-1 and BC-3 PEL cells, as measured by trypan blue exclusion. **(E)** Inhibition of FAS using C75 leads to a small amount of cell death in primary B cells from two donors, as measured by trypan blue exclusion. Error bars are ± SEM.

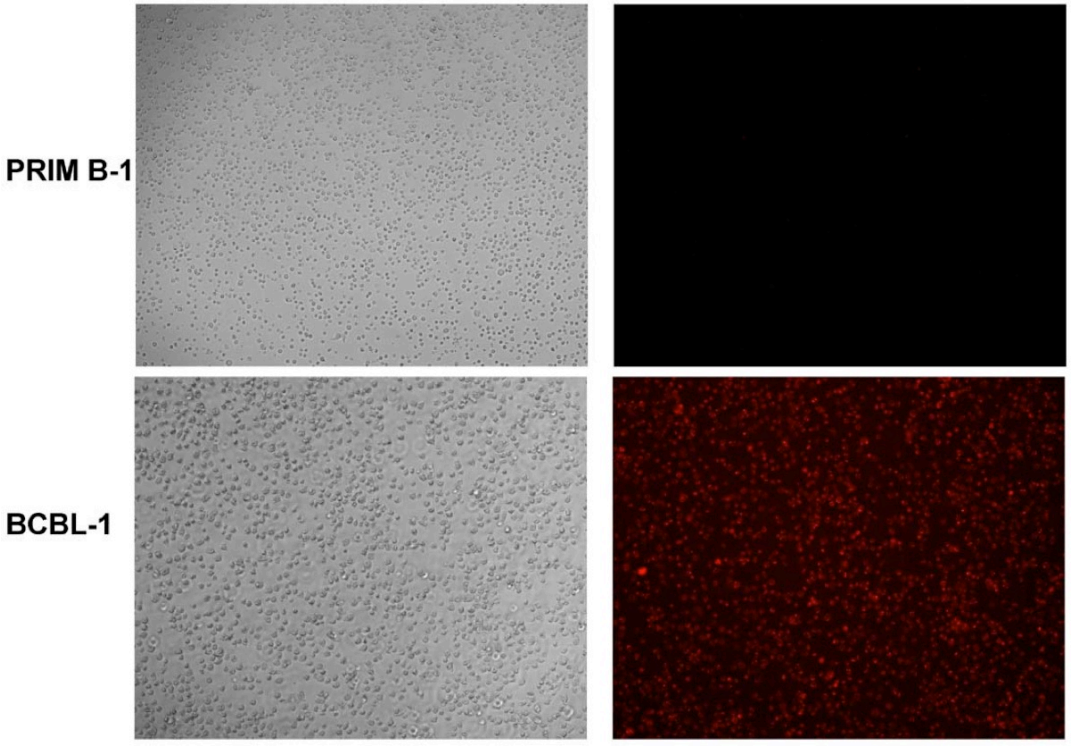

Figure 4: PEL cells display intracellular lipid droplets. BCBL-1 and primary B cells were stained with the lipophilic dye, Nile Red. Stained cells were visualized using a Nikon Eclipse Ti microscope (Ex/Em = 552/636 nm, or bright field) at 10X magnification under identical settings. The Nikon Eclipse is equipped with NIS Elements imaging software. Fluorescence in PEL is attributed to the large amount of intracellular lipid, while the primary B cells do not exhibit the same degree of fluorescence.

We also compared the FAS rates of other B-NHL cell lines (CA46, K422 and SUDHL4) to FAS rates of primary B cells (Fig. 3C), and found that upregulated FAS is a phenotype shared by all the B-NHL lines we tested, with significantly (*p= 0.023*) elevated FAS rates compared to primary B cells. Interestingly, PEL generally exhibited higher rates of FAS compared to the other B-NHL tested.

Increased FAS levels could be a consequence of reduced catabolism or increased synthesis. We therefore measured the rate of fatty acid oxidation (FAO) using previously described methods (32) and described in the methods section. Fig. 5 demonstrates that FAO rates are not significantly different between PEL and primary B cells. Thus, FAS seems to be the dominant fatty acid metabolic pathway upregulated in PEL.

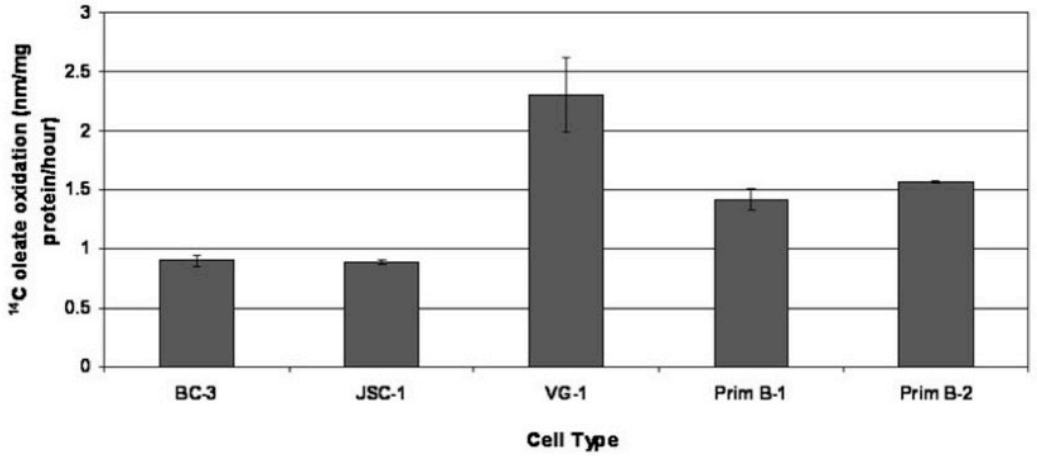

Figure 5: FAO levels do not significantly differ between PEL and primary B cells. PEL and primary B cells oxidize the radiolabeled fatty acid ^{14}C-Oleate, at similar rates. Data is normalized to total input protein and error bars are ±SEM

To establish the importance of increased FAS for PEL survival, we inhibited FAS with C75, a FASN inhibitor (35, 36). When treated with increasing doses of C75, PEL cells displayed a dose-dependent increase in cell death, as measured by trypan blue exclusion (Fig. 3D). BC-1 and BC-3 are shown as representative PEL. In contrast, primary B cells were minimally affected (Fig. 3E). Fig. 6A and 6B respectively demonstrate that both Burkitt (CA46) and follicular (SUDHL4) lymphoma cell lines are susceptible to C75, however, the degree of susceptibility is not as great as that of PEL. FAS inhibition by C75 resulted in activation of pro-apoptotic caspase-3 in all B-NHL (Fig. 6C).

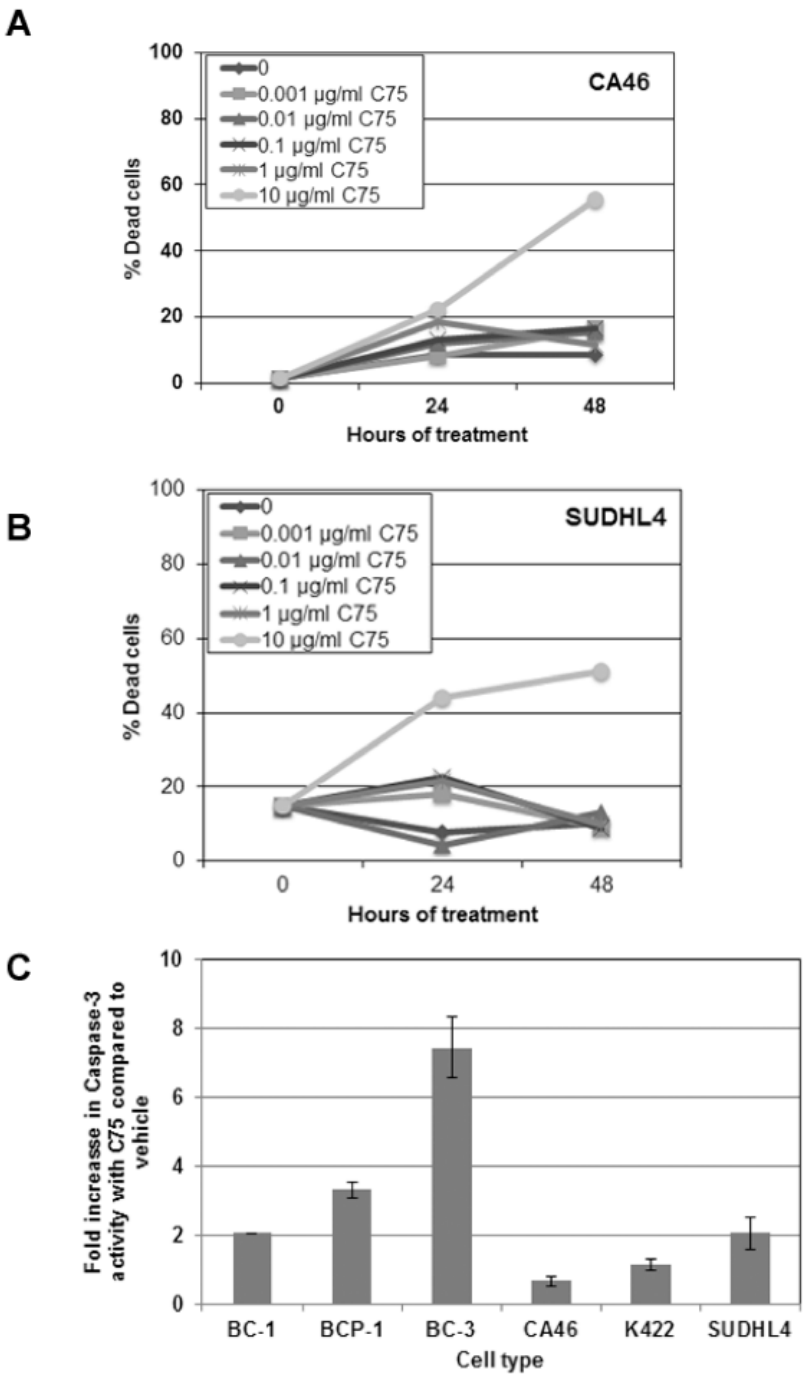

Figure 6: B-NHL are susceptible to the FAS inhibitor C75. (A) CA46 and (B) SUDHL4 B-NHL are susceptible to C75. C75 treatment leads to about 50% reduction in proliferation of these two lines, in contrast with >90% cell death of PEL, at the same dose (10 μg/ml). (C) C75 induces apoptosis in B-NHL.

B lymphocytes isolated from circulating peripheral blood are normally in a resting state. PEL are lymphoma cells, and hence proliferate continuously in the absence of specific stimulus. To rule out the possibility that differentials in glycolysis and FAS were a consequence of proliferation rather than the transformed phenotype, we measured glycolytic flux, FAS rates and FASN expression in activated primary B cells. Primary B cells were treated for 48h with either PBS as vehicle, or 10 mg/ml lipopolysaccharide (LPS) to stimulate B cell proliferation as previously reported (37), after which proliferation was confirmed using the MTS assay (Fig. 7A). The rates of glycolysis (Fig. 7B) and lipid synthesis (Fig. 7C) were quantified and compared to PEL (BC-1 and BCBL-1). LPS-stimulated B cells proliferated more than unstimulated B cells, as expected (Fig. 7A and Fig. 8C). This was accompanied by a doubling in the rate of glycolysis, although the increased glycolytic rate was still significantly lower ($p \leq 0.01$) than that of vehicle-treated PEL cells (Fig. 7B). Interestingly, LPS-stimulated primary B cells did not change their rates of FAS compared to vehicle-treated primary B cells (Fig. 7C), and this rate of FAS was significantly lower than that of an equivalent number of vehicle-treated BC-1 and BCBL-1 PEL cells ($p \leq 0.05$). LPS stimulation of PEL did not further increase glycolysis or FAS compared to vehicle-treated PEL (Fig. 8A and B). Furthermore, immunoblot analysis of cell lysates revealed that FASN expression in primary B cells was slightly increased upon LPS-stimulation (Fig 7D); however, FASN expression in stimulated primary B cells was still five-fold lower than that of unstimulated

(vehicle-treated) PEL cells. These data suggest that FASN activity is an independent phenotype of PEL rather than a consequence of increased proliferation index and that upregulated lipid synthesis observed in PEL cells is a metabolic signature of PEL.

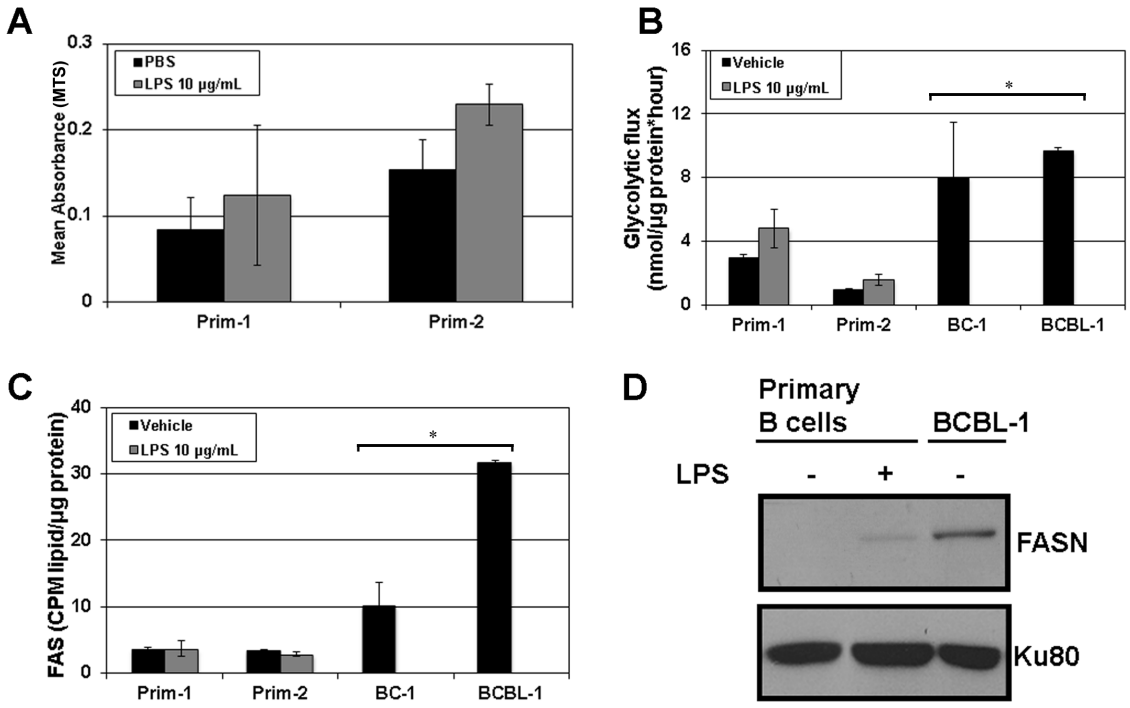

Figure 7. LPS-driven proliferation of primary B cells is not linked to the rate of FAS as is evident in untreated PEL. **(A)** Stimulation of primary B cells with 10 μg/ml of LPS leads to an increase in proliferation as measured by MTS assay. **(B)** Glycolysis is minimally upregulated in LPS-stimulated proliferating primary B cells, but the rates are significantly lower (* indicates $p \leq 0.05$) than those of vehicle-treated PEL. **(C)** FAS is not upregulated in LPS-stimulated primary B cells and the rates of FAS are significantly lower (* indicates $p \leq 0.01$) than those seen in untreated PEL. Error bars are ± SEM. **(D)** There is a slight increase in

FASN expression in LPS-stimulated proliferating primary B cells, but these levels are 5 times lower than seen in untreated PEL (quantified using densitometry). Ku80 is a loading control.

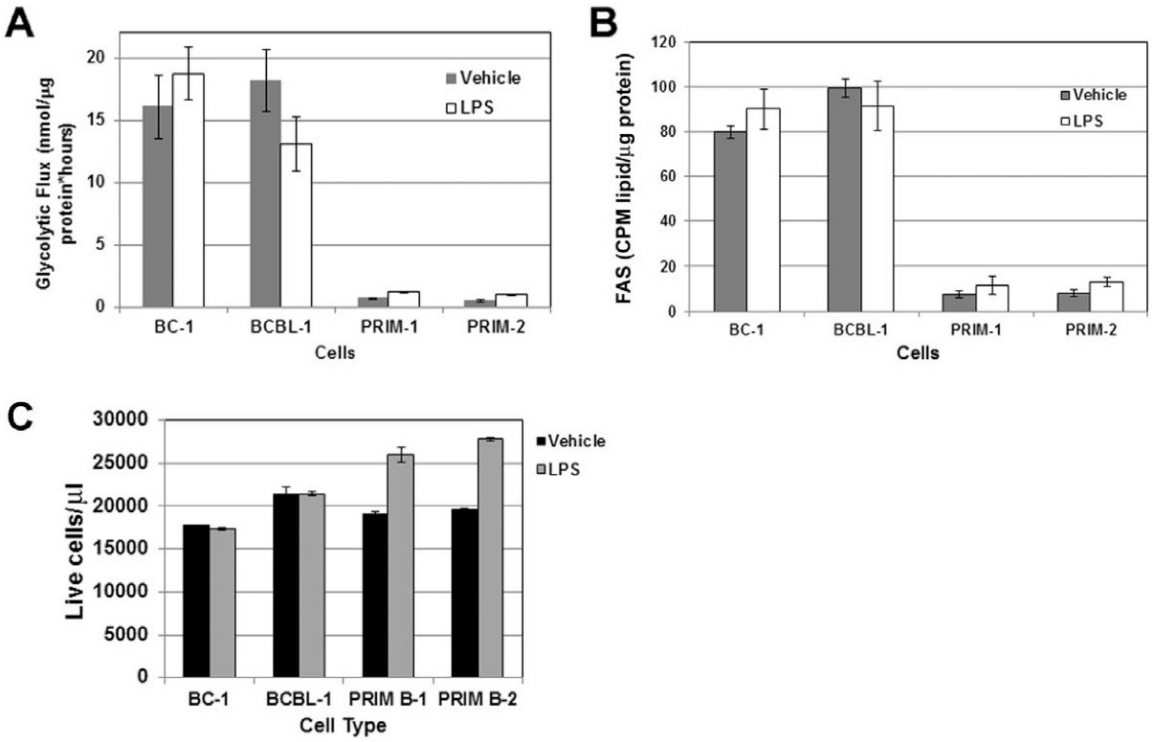

Figure 8: LPS-driven proliferation of primary B cells. (A) Glycolysis is minimally upregulated in LPS-stimulated primary B cells but the rates are significantly lower than those of vehicle-treated PEL. Error bars are ±SEM. (B) FAS is not significantly upregulated in LPS-stimulated primary B cells, and the rates of FAS are significantly lower than those seen in untreated PEL. Error bars are ±SEM. (C) Primary B cells proliferate upon treatment with LPS over a period of 48h, whereas PEL cell proliferation remains unchanged post-LPS stimulation.

PEL have a distinct lipid synthesis profile compared to primary B cells

We identified the major classes of lipids resulting from FAS by culturing primary B and PEL cells in medium supplemented with D-[U-$^{14}C_6$]-Glc; lipids derived from D-[U-$^{14}C_6$]-Glc were identified using thin-layer chromatography, as previously described (31). Table 1 demonstrates that the PEL and primary B cells have different amounts of *de novo* synthesized lipids that are derived from Glc. We found that phosphatidylcholine, phosphatidylethanolamine, phosphatidylinositol, phosphatidylserine and sphingomyelin, the major components of eukaryotic cell walls, are preferentially and abundantly synthesized by PEL, compared to primary B cells. Interestingly, PEL cells also had high intracellular levels of *de novo* Glc-derived triglycerides. The ratio of *de novo* lipids and triglycerides synthesized using glucose precursors is much higher in PEL compared to primary B cells.

	^{14}C incorporation (cpm)				
Lipid class	**BC-1**	**BC-3**	**BCBL-1**	**Donor 1**	**Donor 2**
Phosphatidylcholine	1215.0	1463.8	1926.6	118.8	67.8
Phosphatidylethanolamine	269.7	458.5	475.4	45.8	23.0
Phosphatidylinositol	95.4	99.0	123.4	20.9	14.9
Phosphatidylserine	242.5	430.0	444.7	47.3	24.5
Sphingomyelin	138.2	298.5	361.8	34.9	25.4
Triacylglycerol	523	726.4	418.5	45.8	31.0
1,2-Diacylglycerol	58.3	146.3	58.1	23.1	15.8
1,3-Diacylglycerol	60.2	72.4	50.1	13.6	14.4
Free fatty acids	44.7	81.0	63.8	22.5	20.3

Table 1: Summary of ^{14}C-glucose derived lipids, newly synthesized by PEL, compared to primary B cells.

BIOCHEMICAL COMPOUND	TYPE	PUBCHEM ID	PRIM B-1 Primary B cells	PRIM B-2 Primary B cells	PRIM B-3 Primary B cells	PRIM B-4 Primary B cells	PRIM B-5 Primary B cells	PRIM B-6 Primary B cells	BC-1 PEL cell line	BCBL-1 PEL cell line	BCP-1 PEL cell line	JSC-1 PEL cell line	VG-1 PEL cell line
10-heptadecenoate (17:1n7)	Lipid	5312435	2.154	2.343	2.142	1.595	1.302	0.671	0.389	0.386	0.409	0.571	0.725
adrenate (22:4n6)	Lipid	5282844	1.971	4.090	1.775	2.308	0.993	1.007	0.071	0.039	0.253	0.093	0.178
arachidonate (20:4n6)	Lipid	444899	0.972	2.607	2.683	2.164	1.418	1.091	0.084	0.083	0.108	0.219	0.271
cis-vaccenate (18:1n7)	Lipid	5282761	1.028	1.708	1.000	2.589	2.732	1.181	0.638	0.533	0.944	0.735	0.730
dihomo-linoleate (20:2n6)	Lipid	6439848	1.058	1.503	1.430	1.700	0.942	1.262	0.502	0.352	0.334	0.392	0.367
dihomo-linolenate (20:3n3 or n6)	Lipid	5312529	0.843	1.699	1.634	1.384	1.168	1.157	0.159	0.138	0.185	0.283	0.260
docosahexaenoate (DHA; 22:6n3)	Lipid	445580	0.881	1.818	1.821	2.447	1.496	0.840	0.294	0.309	0.430	0.764	1.119
docosapentaenoate (n3 DPA; 22:5n3)	Lipid		0.992	2.146	1.919	2.085	1.346	1.008	0.175	0.162	0.237	0.418	0.816
linoleate (18:2n6)	Lipid	5280450	1.100	1.352	1.747	1.616	1.514	1.087	0.260	0.260	0.299	0.417	0.454
linolenate [alpha or gamma; (18:3n3 or 6)]	Lipid		1.365	1.810	2.407	1.879	1.841	0.827	0.293	0.294	0.404	0.561	0.518
oleate (18:1n9)	Lipid	445639	2.042	1.068	1.420	1.714	2.123	0.875	0.647	0.708	1.138	0.730	0.932
2-hydroxystearate	Lipid	69417	2.275	1.879	2.166	1.966	1.449	0.551	0.141	0.164	0.462	0.356	0.195
carnitine	Lipid	288	0.640	1.653	1.301	0.807	0.994	1.260	0.585	0.882	1.366	1.198	1.006
coenzyme A	Cofactors and vitamins	317	0.666	0.666	0.666	0.666	0.666	0.666	0.841	1.000	1.110	0.666	2.019
acetylcarnitine	Lipid	7045767	0.891	0.778	1.023	0.727	1.028	1.114	0.546	0.977	1.466	1.030	3.240
glucose	Carbohydrate	79025	7.136	3.772	2.066	0.366	1.385	5.161	1.144	0.399	0.169	0.189	0.856
glucose-6-phosphate (G6P)	Carbohydrate		0.207	0.207	0.207	0.207	0.207	0.207	3.160	1.000	0.207	0.308	1.701
Isobar: fructose 1,6-diphosphate, glucose 1,6-diphosphate	Carbohydrate		0.609	0.609	0.609	0.609	0.609	0.609	3.334	1.363	0.816	0.609	1.184
malate	Energy	525	0.456	0.456	0.456	0.456	0.456	0.456	0.585	1.161	1.487	0.456	1.000
1-arachidonoylglycerophosphoethanolamine*	Lipid		0.231	2.017	2.590	2.572	0.561	1.000	0.284	0.403	0.409	0.231	1.699
1-arachidonoylglycerophosphoinositol*	Lipid		0.554	0.554	0.554	0.554	0.554	0.554	0.968	0.554	0.750	1.032	3.033
1-oleoylglycerophosphoethanolamine	Lipid	9547071	0.227	0.227	0.227	0.227	0.227	0.227	1.599	1.000	0.967	0.815	2.708
1-oleoylglycerophosphoinositol*	Lipid		0.761	0.761	0.761	0.761	0.761	0.761	0.761	1.000	1.610	0.919	1.366
1-palmitoylglycerol (1-monopalmitin)	Lipid	14900	2.935	2.474	0.394	1.758	0.896	1.846	0.604	0.724	0.743	0.394	1.000
1-palmitoylglycerophosphocholine	Lipid	86554	20.396	0.137	4.038	33.143	0.137	1.089	0.137	0.160	0.455	0.183	2.619
1-palmitoylglycerophosphoethanolamine	Lipid	9547069	0.899	0.899	0.899	0.899	0.899	0.899	2.035	0.914	0.935	0.899	4.046
1-palmitoylglycerophosphoinositol*	Lipid		0.684	0.684	0.684	0.684	0.684	0.684	1.214	1.150	1.000	0.684	0.762
1-palmitoylplasmenylethanolamine*	Lipid		1.156	1.855	1.370	0.635	0.483	0.954	1.391	0.559	0.535	1.046	0.302
1-stearoylglycerophosphocholine	Lipid	497299	6.652	0.035	1.796	7.818	0.035	0.035	0.035	0.035	0.080	0.035	0.204
1-stearoylglycerophosphoethanolamine	Lipid	9547068	0.942	2.686	2.181	2.213	0.850	0.825	1.058	0.784	0.697	0.474	1.103
1-stearoylglycerophosphoinositol	Lipid		0.482	0.482	1.345	1.842	0.746	0.999	1.292	0.482	0.649	0.914	1.001
2-oleoylglycerophosphoethanolamine*	Lipid		0.759	0.759	0.759	0.759	0.759	0.759	1.028	0.819	1.000	0.759	3.476
2-oleoylglycerophosphoinositol*	Lipid		0.457	0.457	0.457	0.457	0.457	2.741	0.457	0.504	1.297	0.905	1.095
lactate	Carbohydrate	612	0.598	0.914	1.193	1.152	0.736	0.732	1.565	1.118	1.774	1.067	0.932
Isobar: fructose 1,6-diphosphate, glucose 1,6-diphosphate-media	Carbohydrate		0.609	0.609	0.609	0.609	0.609	0.609	3.334	1.363	0.816	0.609	1.184
dihydroxyacetone phosphate (DHAP)	Carbohydrate	4643300	0.775	0.775	0.775	0.775	0.775	0.775	1.851	0.874	0.775	0.775	1.126
lactate-media	Carbohydrate	612	0.311	0.435	0.595	0.736	1.023	1.000	1.397	1.447	1.391	1.396	1.469
pyruvate-media	Carbohydrate	107735	0.752	0.627	0.718	0.789	0.566	1.211	3.194	3.515	3.031	0.569	4.679
glucose-media	Carbohydrate	79025	1.970	1.603	1.556	1.428	0.592	0.961	0.148	0.020	0.002	0.001	0.006

Table 2: List of scaled PEL and B cell metabolite intensities that were subject to hierarchical clustering and principal component analysis.

Glycolysis and Fatty Acid Synthesis are intimately linked in B-NHL

We measured both glycolytic flux and rates of FAS in an equivalent number of both PEL and primary B cells, in the presence of 1 mm 2DG (glycolysis inhibitor), or 10 μg/ml C75 (FAS inhibitor) for 72h. As shown in Fig 9A, 2DG inhibited glycolysis in both cell types, as expected. However, C75 also reduced glycolysis to levels similar to that seen following 2DG treatment (Fig.9A). In the converse experiment, Fig. 9B demonstrates that while C75 expectedly and potently inhibits the rate of FAS, 2DG also reduces FAS in PEL. This suggests that Glc is utilized for both glycolysis and FAS in PEL and suggests that upregulation of glycolysis is a mechanism to generate intermediates that can be used for the synthesis of fatty acids (13, 38). In contrast, the rate of FAS in primary B cells remained static and independent of 2DG treatment (Fig. 9B). In PEL, inhibition of FAS decreased the rate of glycolysis, and conversely, inhibition of glycolysis blocked FAS. This suggests that both glycolysis and FAS are intimately linked in PEL and inhibition of one pathway impacts the other. Moreover, these two pathways are linked in other B-NHL subsets as well. Fig. 9C demonstrates that FAS inhibition reduces glycolytic flux in the FL cell line, SUDHL4, and Fig. 9D indicates that glycolysis inhibition potently reduces FAS not only in B-NHL lines, but also in an EBV-positive lymphoblastoid cell line (EBV-LCL).

Thirty-nine glycolysis and FAS intermediates (listed in Table 1) from five PEL cell lines and six primary B cell samples were analyzed and the data were subjected to unsupervised clustering (Fig. 9E) and principal component analysis

(PCA) (Fig. 9F). PEL and primary B cells clearly segregated into two distinct groups as represented in the dendrogram (Fig. 9E) or along component 2 in the PCA (Fig. 9F). The dissimilarity between the PEL cluster and the primary B cell cluster was much greater than among primary B cell cultures alone or among the PEL.

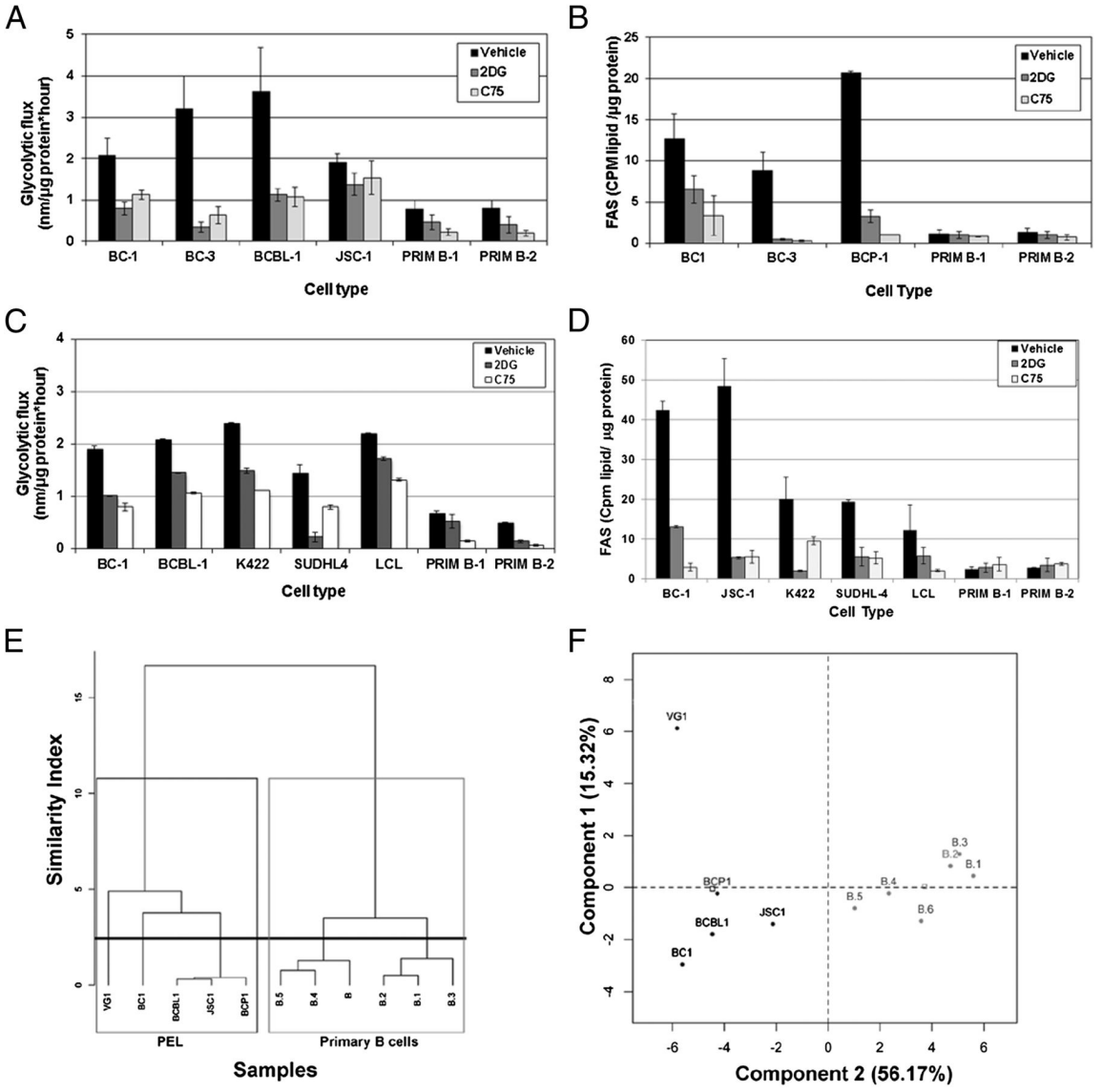

Figure 9: Glycolysis and FAS are intimately linked in B-NHL. (*A*) PEL and primary B cells treated for 72 h with 10 μg/mL C75 show a significant decrease in glycolysis ($P \leq 0.05$ for all comparisons), similar to 1 mM 2DG-treated cells (positive control). Error bars are ± SEM. (*B*) PEL cells treated for 72 h with 1 mM 2DG have decreased FAS ($P \leq 0.05$), and with 10 μg/mL C75 (positive control) have significantly decreased FAS ($P \leq 0.05$). Primary B cells display minimal FAS activity, which is not down-regulated with inhibitors. Error bars are ± SEM; data are representative of more than three independent experiments. (*C*) B-NHL (including PEL), LCL, and primary B cells treated for 72 h with 10 μg/mL C75 show a reduction in glycolysis comparable with 2DG-treated cells. (*D*) Glycolysis inhibition of B-NHL (including PEL) and LCL with 2DG substantially reduces FAS to a rate similar to the FASN inhibitor C75, but does not impact FAS in primary B cells. (*E* and *F*) A dendrogram of hierarchical clustering (*E*) and principal component analysis (*F*) of relative intensities of metabolic intermediates of glycolysis and FAS demonstrates that PEL and primary B cells display distinct metabolic profiles.

PI3K/AKT is required for increased glycolysis and fatty acid synthesis in PEL

PI3K/AKT signaling is known to regulate glycolysis, and previous reports indicate that PI3K inhibition reduces glycolytic flux and induces cell cycle arrest in diffuse large B cell lymphomas (39). We investigated whether inhibiting PI3K using LY294002 would alter glycolysis and FAS in PEL. We first determined a dose of LY294002 (1 μM) that was not significantly cytotoxic to PEL cell lines over the course of 72h (Fig. 9). Next, equivalent numbers of PEL and primary B cells were treated with either 1 μM of LY294002 or DMSO for 72h, after which the rates of glycolysis and FAS were measured as described above. As expected, LY294002 dramatically (*p≤0.01)* reduced the glycolytic flux in both PEL and primary B cells (Fig. 10). We also found that LY294002 significantly (*p≤0.05)* decreased the rates at which PEL cells incorporated radiolabeled Glc into lipids via FAS (Fig. 10B). However, the primary B cells were unaffected (Fig. 10B). Moreover, as shown in Fig 10C, LY294002 treatment resulted in a dose-dependent reduction of FASN expression in PEL, as previously reported for prostate cancer (40), providing a potential mechanism for the dramatic reduction in FAS in PEL upon PI3K inhibition. Collectively, these data indicate that not only does PI3K/AKT inhibition in PEL decrease FASN expression, but it also diminishes glycolytic flux, thereby preventing Glc incorporation into newly synthesized fatty acids.

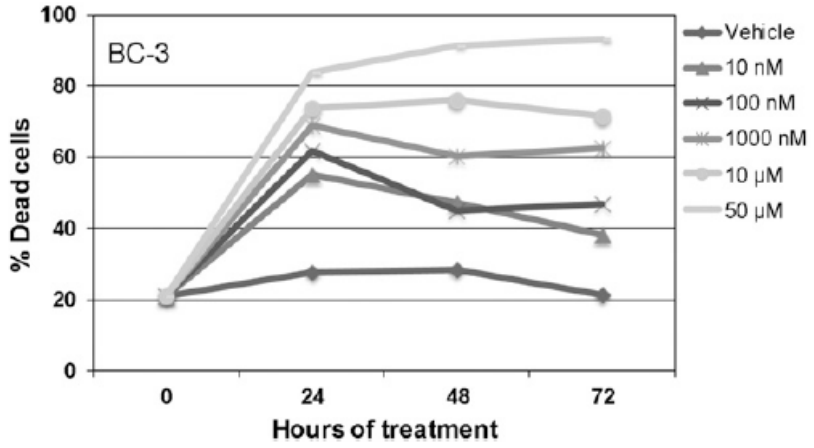

Figure 10: PI3K inhibition of PEL. To determine a non-cytotoxic dose of LY294002, the drug was added to cells at different concentrations, ranging from 10 nM to 50 µM for 72h. Cell death was measured by trypan blue exclusion, and represented as percent of total cells counted.

FAS inhibition leads to an accumulation of carnitine.

To examine the degree of FAO efficiency within B cell lymphomas and primary B cells, we compared the relative distribution of FAO intermediates derived from PEL (BC-1, JSC-1 and VG-1) and primary B cells from two healthy donors. All data are normalized to protein content and are shown in Fig. S6A, B, C. The overall levels of free carnitine are lower in PEL compared to primary B cells (Fig. 10A). Lowered carnitine levels in colon cancer cells have been shown to inhibit the generation of apoptosis-inducing O_2^- radicals (41). Treatment of PEL and primary B cells with the FAS inhibitor C75 resulted in a decrease in cellular free carnitine in both cell types, however, the magnitude of reduction was greater

in PEL (31% reduction) compared to primary B cells (13.5% reduction), which might reflect the fact that PEL are more sensitive to C75 than primary B cells.

We also measured the relative levels of distinct acyl-carnitine intermediates of FAO by MS. We found that many of the even-chained acyl-carnitines were increased in PEL compared to primary B cells (Figs. S6B and S6C), indicative of incomplete oxidation of fatty acids (34). In contrast, primary B cells display higher amounts of C3 and C5 acyl-carnitines, which suggest a reliance on oxidation of amino acids rather than fatty acids (34).

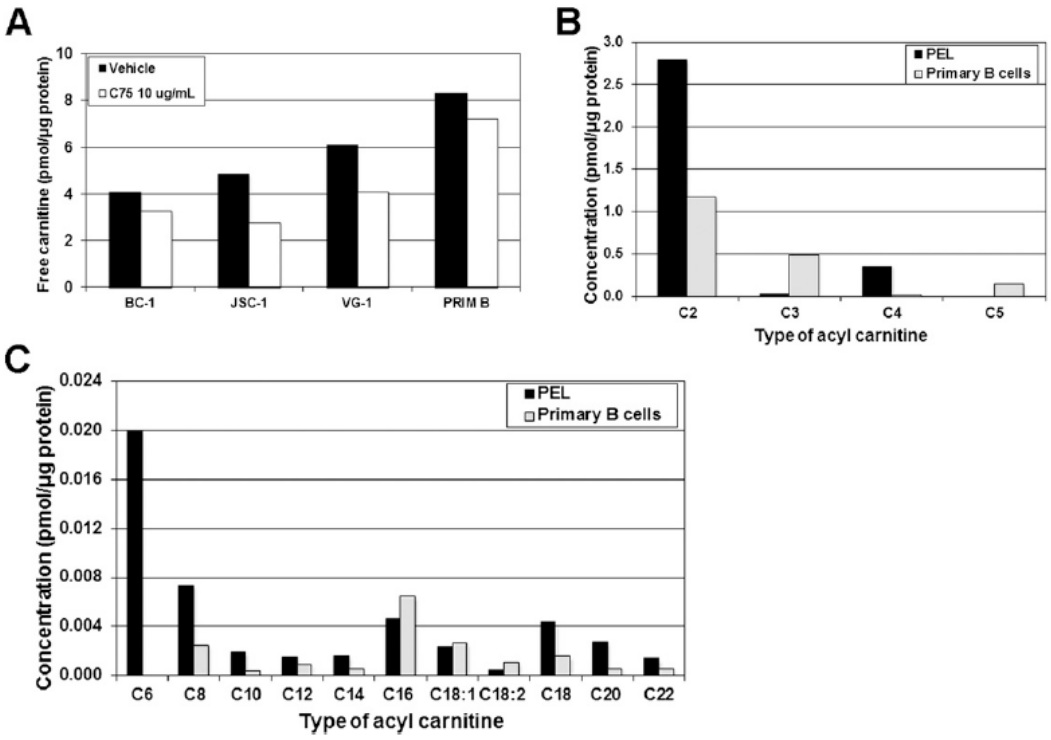

Figure 11: Levels of free carnitine and FAO intermediates differ between PEL and primary B cells. (A and B) Tandem mass spectrometric analysis was used to determine the relative intensities of carnitine and acyl-carnitine intermediates within PEL and primary B cells. (A) Levels of free carnitine (normalized to total

cellular protein) in PEL are slightly lower than in primary B cells. Two different primary B-cell donors were combined for this analysis. FAS inhibition with C75 (open bars) decreases free carnitine in both PEL and primary B cells, however, the magnitude of decrease is greater in PEL compared with primary B cells. (B and C) Relative distribution of intracellular acyl-carnitines reveals that PEL (black bars) have higher levels of even-chained acyl-carnitine intermediates compared with primary B cells (gray bars). Further, higher levels of C3 and C5 acyl-carnitine intermediates are found in primary B cells compared with PEL (Fig 11 B).

Combination of LY294002 and C75 is most effective at inhibiting PEL proliferation

Overall, our findings suggest that FAS is upregulated in PEL and other B-NHL. The above experiments indicate that the PI3K inhibitor, LY294002, blocks glycolysis and FAS in PEL (Fig. 10). Therefore we sought to determine whether a combination of LY294002 and C75 would enhance PEL cell death. We treated PEL cells with increasing doses of LY294002 and C75 for 72h, and measured cell survival by trypan blue exclusion. As seen in Fig. 12, either drug alone reduced cell viability in a dose-dependent manner. However, combined treatment with 10 μM LY294002 and 10 μg/ml of C75 led to death of approximately 75% of PEL cells (*p≤0.05)* in culture. These data confirm that FAS inhibition may be an efficacious treatment modality for PEL, particularly when combined with existing PI3K-targeted chemotherapeutics.

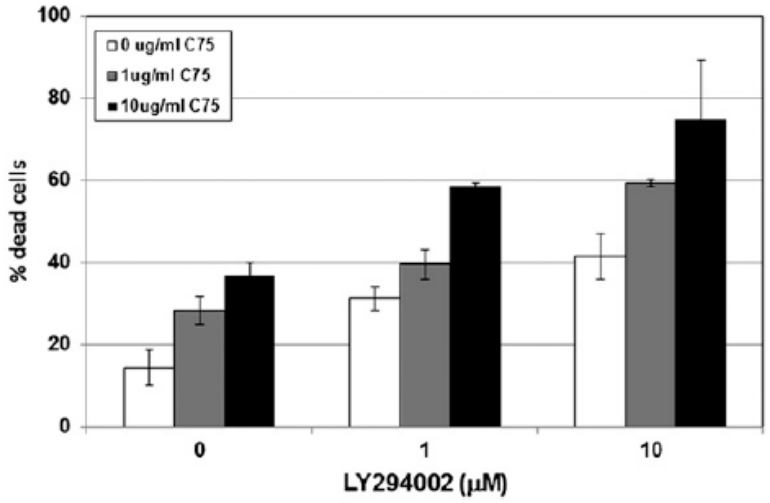

Figure 12: FAS inhibition increases susceptibility of PEL to the PI3K inhibitor LY294002. PEL are sensitive to LY294002 in a dose-dependent manner, as measured by trypan blue exclusion. Addition of C75 significantly incrreases the number of dead cells, with maximal death when PEL are treated with 10 μM LY294002 and 10 μg/mL C75. For the comparison between PEL treated with only LY294002 vs. LY294002 plus C75: $P \leq 0.05$

DISCUSSION

We report that PEL and other B-NHL display increased glycolytic activity. PEL are highly sensitive to Glc withdrawal and the glycolysis inhibitor, 2DG. Lactate, a byproduct of glycolysis, is present in high levels in the growth media of PEL. These data are in line with clinical observations of elevated serum levels of lactate dehydrogenase (LDH) correlating with poor prognosis in patients with lymphomas (42). LDH converts pyruvate, the end product of glycolysis, into lactate. Our flux measurements confirm upregulated rates of glycolysis in B-NHL cells as compared to primary B cells from healthy donors. Additionally, KSHV infection of endothelial cells was previously shown to increase glycolysis (43).

We found that PEL express high levels of FASN, whereas FASN expression or biosynthetic activity in human primary B cells was barely detectable. We report that FAS inhibition by C75 reduced the viability of PEL and other B-NHL, while primary B cells remain largely unaffected by C75 treatment. Moreover, C75 also sensitized PEL cells to the PI3K inhibitor LY294002. This might be a case of oncogene addiction where cancer cells are highly sensitive to inactivation of a pathway that they depend on (44), while normal cells are not sensitive to this inactivation. The PEL proliferate continuously, and when FAS is inhibited, the cells end up undergoing apoptosis because there is a lack of lipid-derived building blocks required to make daughter cells. This provides the opportunity to use molecular targeted therapy against B-NHL that preferentially kill B-NHL while sparing primary B cells.

Notably, despite heightened FAS, PEL cells displayed FAO rates that were not significantly different than those of primary B cells. In primary cells, FAS and FAO are carefully counter-regulated, since FAS utilizes ATP, whereas FAO generates ATP (45). Thus, concurrent FAS and FAO within the same cell, as exhibited by PEL, would be an energetically futile occurrence. However, coordinate regulation of FAS and FAO appears to be lost in PEL, which have highly upregulated rates of FAS, whereas FAO rates remain quite similar to primary B cells. Elevated FAS rates in PEL contribute to an abundance of *de novo* synthesized, Glc-derived triglycerides and phospholipids, suggesting that newly-generated fatty acids are rapidly incorporated into membrane lipids and triglyceride stores to accommodate the dramatic proliferative rates of lymphoma cells. Precursors derived from other biochemical pathways such as glutaminolysis, can input into FAS. However, their relevance in the context of B-NHL remains to be determined. Our data indicate that upregulated FAS is a characteristic of B-NHL, and that FASN might be an efficacious therapeutic target against B-NHL, while sparing normal, primary B cells.

We report that glycolysis and FAS are intertwined in PEL and other B-NHL since inhibition of glycolysis affected FAS and *vice versa*. The fact that inhibition of glycolysis causes a reduction in FAS demonstrates that glycolysis fuels the synthesis of fatty acids in PEL and B-NHL by providing acetyl-CoA intermediates. Conversely, FAS inhibition may result in decreased glycolysis, if the cells sense that the glycolytic intermediates required to fuel FAS are unnecessary, due to

decreased FASN biosynthetic activity. Thus, these two metabolic pathways appear to be linked in B-NHL.

Fatty acids are essential for subsequent synthesis of macromolecules and cell membranes, both of which are necessary for rapidly dividing cancer cells. Interestingly, primary B cells stimulated to proliferate with LPS upregulated glycolysis, along with a concurrent expression of FASN; however, in proliferating primary B cells, the rate of neither pathway was comparable to the high degree of glycolysis and FAS taking place in untreated PEL. These data suggest that enhanced FAS and upregulated FASN expression is an advantageous metabolic adaptation of PEL and other B-NHL. In concordance with our observations, several groups have reported instances of hypertriglyceridemia and hyperlipidemia in patients with leukemia and lymphoma (46, 47) and clinical remission of disease was shown to coincide with plasma lipid and triglyceride levels returning to baseline. PI3K/AKT pathway activation in PEL contributes to the increase in both glycolysis and FAS, since treatment of PEL with a non-cytotoxic dose of the PI3K inhibitor LY294002, reduced the rate of glycolysis as well as FASN expression, thus diminishing the rate of FAS. However, in primary B cells, LY294002 decreased glycolytic flux, but did not affect the rate of FAS.

Collectively, our data suggest that hyperactivated FAS is essential for the growth advantage of B-NHL. Further, these data indicate that combining existing therapeutics targeting the PI3K/AKT/mTOR pathway with FAS inhibitors may be an efficacious therapeutic strategy for non-Hodgkin lymphomas.

REFERENCES

1. **Boulanger E, Gerard L, Gabarre J, Molina JM, Rapp C, Abino JF, Cadranel J, Chevret S, Oksenhendler E.** 2005. Prognostic factors and outcome of human herpesvirus 8-associated primary effusion lymphoma in patients with AIDS. J Clin Oncol **23:**4372-4380.

2. **Sin SH, Roy D, Wang L, Staudt MR, Fakhari FD, Patel DD, Henry D, Harrington WJ, Jr., Damania BA, Dittmer DP.** 2007. Rapamycin is efficacious against primary effusion lymphoma (PEL) cell lines in vivo by inhibiting autocrine signaling. Blood **109:**2165-2173.

3. **Chang Y, Cesarman E, Pessin MS, Lee F, Culpepper J, Knowles DM, Moore PS.** 1994. Identification of herpesvirus-like DNA sequences in AIDS-associated Kaposi's sarcoma. Science **266:**1865-1869.

4. **Cesarman E, Chang Y, Moore PS, Said JW, Knowles DM.** 1995. Kaposi's sarcoma-associated herpesvirus-like DNA sequences in AIDS- related body-cavity-based lymphomas. N Engl J Med **332:**1186-1191.

5. **Wang L, Wakisaka N, Tomlinson CC, DeWire SM, Krall S, Pagano JS, Damania B.** 2004. The Kaposi's sarcoma-associated herpesvirus (KSHV/HHV-8) K1 protein induces expression of angiogenic and invasion factors. Cancer Res **64:**2774-2781.

6. **Tomlinson CC, Damania B.** 2004. The K1 protein of Kaposi's sarcoma-associated herpesvirus activates the Akt signaling pathway. J Virol **78:**1918-1927.

7. **Wang L, Dittmer DP, Tomlinson CC, Fakhari FD, Damania B.** 2006. Immortalization of primary endothelial cells by the K1 protein of Kaposi's sarcoma-associated herpesvirus. Cancer Res **66:**3658-3666.

8. **Sodhi A, Montaner S, Patel V, Gomez-Roman JJ, Li Y, Sausville EA, Sawai ET, Gutkind JS.** 2004. Akt plays a central role in sarcomagenesis induced by Kaposi's sarcoma herpesvirus-encoded G protein-coupled receptor. Proc Natl Acad Sci U S A **101:**4821-4826.

9. **Bais C, Van Geelen A, Eroles P, Mutlu A, Chiozzini C, Dias S, Silverstein RL, Rafii S, Mesri EA.** 2003. Kaposi's sarcoma associated herpesvirus G protein-coupled receptor immortalizes human endothelial cells by activation of the VEGF receptor-2/ KDR. Cancer Cell **3:**131-143.

10. **Bhatt AP, Bhende PM, Sin SH, Roy D, Dittmer DP, Damania B.** 2010. Dual inhibition of PI3K and mTOR inhibits autocrine and paracrine proliferative loops in PI3K/Akt/mTOR-addicted lymphomas. Blood **115:**4455-4463.

11. **Warburg O.** 1956. On respiratory impairment in cancer cells. Science **124:**269-270.

12. **Hsu PP, Sabatini DM.** 2008. Cancer cell metabolism: Warburg and beyond. Cell **134:**703-707.
13. **Young CD, Anderson SM.** 2008. Sugar and fat - that's where it's at: metabolic changes in tumors. Breast Cancer Res **10:**202.

14. **Manning BD, Cantley LC.** 2007. AKT/PKB signaling: navigating downstream. Cell **129:**1261-1274.

15. **Wieman HL, Wofford JA, Rathmell JC.** 2007. Cytokine stimulation promotes glucose uptake via phosphatidylinositol-3 kinase/Akt regulation of Glut1 activity and trafficking. Mol Biol Cell **18:**1437-1446.

16. **Elstrom RL, Bauer DE, Buzzai M, Karnauskas R, Harris MH, Plas DR, Zhuang H, Cinalli RM, Alavi A, Rudin CM, Thompson CB.** 2004. Akt stimulates aerobic glycolysis in cancer cells. Cancer Res **64:**3892-3899.

17. **Majumder PK, Febbo PG, Bikoff R, Berger R, Xue Q, McMahon LM, Manola J, Brugarolas J, McDonnell TJ, Golub TR, Loda M, Lane HA, Sellers WR.** 2004. mTOR inhibition reverses Akt-dependent prostate intraepithelial neoplasia through regulation of apoptotic and HIF-1-dependent pathways. Nat Med **10:**594-601.

18. **Lum JJ, Bui T, Gruber M, Gordan JD, DeBerardinis RJ, Covello KL, Simon MC, Thompson CB.** 2007. The transcription factor HIF-1alpha plays a critical role in the growth factor-dependent regulation of both aerobic and anaerobic glycolysis. Genes Dev **21:**1037-1049.

19. **Majewski N, Nogueira V, Bhaskar P, Coy PE, Skeen JE, Gottlob K, Chandel NS, Thompson CB, Robey RB, Hay N.** 2004. Hexokinase-mitochondria interaction mediated by Akt is required to inhibit apoptosis in the presence or absence of Bax and Bak. Mol Cell **16:**819-830.

20. **Duvel K, Yecies JL, Menon S, Raman P, Lipovsky AI, Souza AL, Triantafellow E, Ma Q, Gorski R, Cleaver S, Vander Heiden MG, MacKeigan JP, Finan PM, Clish CB, Murphy LO, Manning BD.** 2010. Activation of a metabolic gene regulatory network downstream of mTOR complex 1. Mol Cell **39:**171-183.

21. **Kuhajda FP.** 2000. Fatty-acid synthase and human cancer: new perspectives on its role in tumor biology. Nutrition **16:**202-208.

22. **Vazquez-Martin A, Colomer R, Brunet J, Lupu R, Menendez JA.** 2008. Overexpression of fatty acid synthase gene activates HER1/HER2 tyrosine kinase receptors in human breast epithelial cells. Cell Prolif **41:**59-85.

23. **Flavin R, Peluso S, Nguyen PL, Loda M.** 2010. Fatty acid synthase as a potential therapeutic target in cancer. Future Oncol **6:**551-562.

24. **Yoon S, Lee MY, Park SW, Moon JS, Koh YK, Ahn YH, Park BW, Kim KS.** 2007. Up-regulation of acetyl-CoA carboxylase alpha and fatty acid synthase by

human epidermal growth factor receptor 2 at the translational level in breast cancer cells. J Biol Chem **282:**26122-26131.

25. **Yang YA, Han WF, Morin PJ, Chrest FJ, Pizer ES.** 2002. Activation of fatty acid synthesis during neoplastic transformation: role of mitogen-activated protein kinase and phosphatidylinositol 3-kinase. Exp Cell Res **279:**80-90.

26. **Roy D, Dittmer DP.** 2011. Phosphatase and tensin homolog on chromosome 10 is phosphorylated in primary effusion lymphoma and Kaposi's sarcoma. Am J Pathol **179:**2108-2119.

27. **Roskrow MA, Suzuki N, Gan Y, Sixbey JW, Ng CY, Kimbrough S, Hudson M, Brenner MK, Heslop HE, Rooney CM.** 1998. Epstein-Barr virus (EBV)-specific cytotoxic T lymphocytes for the treatment of patients with EBV-positive relapsed Hodgkin's disease. Blood **91:**2925-2934.

28. **Bhende PM, Park SI, Lim MS, Dittmer DP, Damania B.** 2010. The dual PI3K/mTOR inhibitor, NVP-BEZ235, is efficacious against follicular lymphoma. Leukemia **24:**1781-1784.

29. **Rathmell JC, Farkash EA, Gao W, Thompson CB.** 2001. IL-7 enhances the survival and maintains the size of naive T cells. J Immunol **167:**6869-6876.

30. **Deberardinis RJ, Lum JJ, Thompson CB.** 2006. Phosphatidylinositol 3-kinase-dependent modulation of carnitine palmitoyltransferase 1A expression regulates lipid metabolism during hematopoietic cell growth. J Biol Chem **281:**37372-37380.

31. **Teng YW, Mehedint MG, Garrow TA, Zeisel SH.** 2011. Deletion of betaine-homocysteine S-methyltransferase in mice perturbs choline and 1-carbon metabolism, resulting in fatty liver and hepatocellular carcinomas. J Biol Chem **286:**36258-36267.

32. **Muoio DM, Way JM, Tanner CJ, Winegar DA, Kliewer SA, Houmard JA, Kraus WE, Dohm GL.** 2002. Peroxisome proliferator-activated receptor-alpha regulates fatty acid utilization in primary human skeletal muscle cells. Diabetes **51:**901-909.

33. **Reitman ZJ, Jin G, Karoly ED, Spasojevic I, Yang J, Kinzler KW, He Y, Bigner DD, Vogelstein B, Yan H.** 2011. Profiling the effects of isocitrate dehydrogenase 1 and 2 mutations on the cellular metabolome. Proc Natl Acad Sci U S A **108:**3270-3275.

34. **Newgard CB, An J, Bain JR, Muehlbauer MJ, Stevens RD, Lien LF, Haqq AM, Shah SH, Arlotto M, Slentz CA, Rochon J, Gallup D, Ilkayeva O, Wenner BR, Yancy WS, Jr., Eisenson H, Musante G, Surwit RS, Millington DS, Butler MD, Svetkey LP.** 2009. A branched-chain amino acid-related metabolic signature that differentiates obese and lean humans and contributes to insulin resistance. Cell Metab **9:**311-326.

35. **Kuhajda FP, Pizer ES, Li JN, Mani NS, Frehywot GL, Townsend CA.** 2000. Synthesis and antitumor activity of an inhibitor of fatty acid synthase. Proc Natl Acad Sci U S A **97:**3450-3454.

36. **Rendina AR, Cheng D.** 2005. Characterization of the inactivation of rat fatty acid synthase by C75: inhibition of partial reactions and protection by substrates. Biochem J **388:**895-903.

37. **Armerding D, Sachs DH, Katz DH.** 1974. Activation of T and B lymphocytes in vitro. III. Presence of Ia determinants on allogeneic effect factor. J Exp Med **140:**1717-1722.

38. **Vander Heiden MG, Cantley LC, Thompson CB.** 2009. Understanding the Warburg effect: the metabolic requirements of cell proliferation. Science **324:**1029-1033.

39. **Faber AC, Dufort FJ, Blair D, Wagner D, Roberts MF, Chiles TC.** 2006. Inhibition of phosphatidylinositol 3-kinase-mediated glucose metabolism coincides with resveratrol-induced cell cycle arrest in human diffuse large B-cell lymphomas. Biochem Pharmacol **72:**1246-1256.

40. **Van de Sande T, De Schrijver E, Heyns W, Verhoeven G, Swinnen JV.** 2002. Role of the phosphatidylinositol 3'-kinase/PTEN/Akt kinase pathway in the overexpression of fatty acid synthase in LNCaP prostate cancer cells. Cancer Res **62:**642-646.

41. **Wenzel U, Nickel A, Daniel H.** 2005. Increased carnitine-dependent fatty acid uptake into mitochondria of human colon cancer cells induces apoptosis. J Nutr **135:**1510-1514.

42. **Schneider RJ, Seibert K, Passe S, Little C, Gee T, Lee BJ, 3rd, Mike V, Young CW.** 1980. Prognostic significance of serum lactate dehydrogenase in malignant lymphoma. Cancer **46:**139-143.

43. **Delgado T, Carroll PA, Punjabi AS, Margineantu D, Hockenbery DM, Lagunoff M.** 2010. Induction of the Warburg effect by Kaposi's sarcoma herpesvirus is required for the maintenance of latently infected endothelial cells. Proc Natl Acad Sci U S A **107:**10696-10701.

44. **Weinstein IB, Joe AK.** 2006. Mechanisms of disease: Oncogene addiction--a rationale for molecular targeting in cancer therapy. Nat Clin Pract Oncol **3:**448-457.

45. **Nelson DLC, M.M.** 2005. Lehninger Principles of Biochemistry, 4 ed. Worth Publishers, New York, NY.

46. **Moschovi M, Trimis G, Apostolakou F, Papassotiriou I, Tzortzatou-Stathopoulou F.** 2004. Serum lipid alterations in acute lymphoblastic leukemia of childhood. J Pediatr Hematol Oncol **26:**289-293.

47. **Spiegel RJ, Schaefer EJ, Magrath IT, Edwards BK.** 1982. Plasma lipid alterations in leukemia and lymphoma. Am J Med **72:**775-782.

CHAPTER 4: THE KSHV VIRAL PROTEIN KINASE ACTIVATES THE PI3K/AKT/mTOR SIGNALING PATHWAY

INTRODUCTION

Viruses have a relatively small genetic payload, yet engage in complex, interweaving relationships with their eukaryotic hosts. Viral proteins hijack host cell machinery in order to replicate, disseminate and propagate. Additionally, large DNA viruses like KSHV also encode proteins that are functional mimics of homologous cellular proteins. The repertoire of KSHV mimics of cellular proteins includes cytokines (e.g. vIL-6,) (1) cell cycle control proteins (e.g. vCyclin) (2), anti-apoptotic proteins (e.g. vFLIP) (3), and immune-modulatory proteins (e.g K1, a B cell receptor homolog) (4). In addition, some viral proteins possess domains with enzymatic function homologous to eukaryotic enzymes, such deubiquitinase activity of ORF64 (5), and the kinase activity of ORF36, also known as viral protein kinase (6). Thus, viral proteins capable of post-translational modifications alter the cellular proteome.

Protein kinases (PKs) are enzymes that catalyze the transfer of phosphate groups from energetic nucleotide triphosphates such as ATP or GTP, onto specific residues of substrate proteins. Phosphorylation of the target protein generates a conformation change, which alters its properties, such as location, enzymatic activity and association with other cellular proteins, resulting in a functional change in the associated biological pathway. PKs are subdivided into serine/threonine (S/T) or tyrosine (Y) kinases, depending on their substrate specificity. The human genome codes for about 500 PKs, and up to 30% of all cellular proteins are modified by kinases (7). Kinases regulate most cellular pathways and are essential players in transducing signals within the cell. PKs phosphorylate these specific residues in their target substrates. These residues are flanked by specific, often conserved amino acid sequences called consensus sequences; kinases generally phosphorylate groups of substrates sharing consensus sequences. Most PKs have conserved catalytic sites: an N-terminus glycine-rich stretch proximal to a lysine, which is essential for binding ATP, and a catalytic loop consisting of an aspartic acid which imparts catalytic activity to the kinase. There are seven classes of protein kinases: AGC, CaM , CK1, CMGC, STE, TK and TKL kinases.

Herpesviruses are large, enveloped viruses with double-stranded DNA genomes. The human herpesviruses (HHV) are divided into three families, α, β and ɣ. Herpes simplex virus 1 and 2 (HSV1 and HSV2) and Varicella Zoster virus (VZV) are α-herpesviruses. Human cytomegalovirus, roseolaviruses (HHV6) and HHV7 are examples of β-herpesviruses. Epstein-Barr virus (EBV) and Kaposi’s

sarcoma-associated herpesvirus (KSHV) are ɣ-herpesviruses. KSHV was the eighth human herpesvirus identified, and is linked to Kaposi's sarcoma, primary effusion lymphoma and multicentric Castleman's disease.

α-herpesviruses encode the Us3 kinase family, which inhibit apoptosis and disrupt the nuclear membrane. In addition, both α- and ɣ-herpesviruses encode a thymidine kinase critical for viral replication as it phosphorylates nucleosides including thymidine. A third type of viral-specific kinase is homologous both in genome position and amino acid sequence, among all herpesviruses. This kinase is denoted the conserved herpesvirus-encoded protein kinase (CHPK). In KSHV, this is encoded by ORF36, and is often called vPK.

KSHV primary infection begins when the viral envelope glycoproteins K8.1 and gB first interact with extracellular heparan sulfate, which brings viral particles close to cell surface receptors. Several putative receptors such as the αvβ5, α3β1 and αvβ3 integrins facilitate KSHV entry into endothelial cells, however, they are not the sole receptors (8). The cysteine: glutamate transport protein xCT is involved in facilitating entry into adherent cells, whereas dendritic cell-specific intercellular adhesion molecule-grabbing nonintegrin (DC-SIGN) is implicated in the case of dendritic cells, macrophages and B cells. Once KSHV has attached to cell surface receptors, it is brought into the cell by endocytosis. Within the endosome, the lipid-rich viral envelop fuses with the lipid-rich endosome membrane, which releases the viral capsid and tegument into the cytosol. Thus, viral proteins that comprise the tegument enter the host cytoplasm early during infection and contribute to how the viral lifecycle proceeds. Upon infection, KSHV

can either enter the latent phase or the lytic phase of its lifecycle. Latency is associated with minimal protein expression, while lytic replication generates progeny virions that can infect naïve cells.

Life-long latency is a defining characteristic of all herpesviruses, KSHV latency is characterized by replication of the viral episome by the cellular replication machinery and minimal viral protein expression in order to evade host immune detection. Lytic reactivation periodically occurs, initiated by diverse stimuli including secondary viral infections (9), pro-inflammatory cytokines (10) and stressors such as reactive oxygen species (11).

Herpesvirus lytic gene expression is temporally classified into three distinct classes: immediate early (IE), early (E) and late (L). Lytic replication is initiated by a single viral protein called replication and transcription activator (RTA/ORF50); RTA is the first transcript detected in lytic cells. RTA binds to RTA-responsive elements in viral promoters of IE genes, leading to their transcription and consequent expression. Thus, RTA activation is a linchpin for lytic replication.

The RTA-responsive IE proteins are actively transcribed despite the presence of the protein synthesis inhibitor cycloheximide. The currently known IE proteins, RTA itself, ORF45 and K8 all serve as transactivators of E proteins. As described in the introductory chapter, ORF45 activates PI3K/AKT/mTOR signaling.

E genes are the next class of viral genes transcribed during lytic replication. By definition, E genes are sensitive to cycloheximide and are expressed independent of viral DNA synthesis. The main function of E gene products is to facilitate viral DNA replication. Thymidine kinase, DNA polymerase, and ribonucleotide reductase are examples of E genes. Once critical levels of E genes build up, viral DNA replication commences in the nucleus, at the two origin replication sites (*ori-lyt*) by the rolling circle mechanism.

L gene transcription begins once viral replication commences. Most L gene products are structural proteins that assemble to form the capsid and the envelope, whereas some are incorporated into the tegument. Once stoichiometric amounts of various L proteins have accumulated, capsid assembly of progeny virions begins in the nucleus. Newly assembled capsids exit the nucleus, acquire a protein-rich tegument, and are then cocooned by a glycoprotein-studded, lipid-rich envelope. These mature progeny virions exit the host cell by lysing, and are free to infect new cells.

Previous studies indicate that vPK is incorporated into the KSHV virion (6). Therefore, upon tegument release, vPK enters the cytoplasm and can phosphorylate both viral and cellular proteins relatively early in the viral lifecycle. Furthermore, vPK is classified as a late gene, since it is expressed concurrent with viral replication. Ectopic expression of vPK in uninfected cells results in phosphorylation of an important transcription factor c-Jun N-terminal kinase (JNK) and the Mitogen-activated kinases MKK4 and MKK7 (12). Ablating vPK's kinase activity by mutating the kinase catalytic site prevented JNK activation,

suggesting that vPK directly phosphorylates JNK. Binding assays revealed that vPK, JNK, MKK4 and MKK7 form an intracellular complex. Reactivated PEL cells were found to contain phosphorylated JNK, and inhibiting JNK activation reduced expression of viral late (but not early) genes. This was the first indication that vPK may regulate the KSHV lifecycle by manipulating viral or cellular transcription.

Subsequently, Izumiya and colleagues reported the physical association of vPK with K-bZIP, a viral protein which binds the viral origin of replication (*Ori-Lyt*) (13). VPK-mediated phosphorylation of K-bzip reduced its ability to repress viral transcription. Furthermore, the ORF34-37 gene cluster, in which vPK (ORF36) is contained, is activated by hypoxia due to a functional hypoxia-responsive element in the ORF34 promoter (14). Both pleural effusions and Kaposi's sarcoma are often hypoxic, due to the high cell density and tumor volume, which reduce the local oxygen supply. Hypoxia presents a barrier to viral propagation, because it down-regulates protein synthesis in an mTOR-regulated, 4EBP1-dependent manner (15). Therefore, it is possible to presume that a viral protein expressed during sub-optimal conditions like hypoxia, may actually serve to alleviate the effects of hypoxia on the host cell. Therefore, we decided to investigate whether vPK, already known to post-translationally modify a host of cellular proteins (16), may alleviate PI3K/AKT/mTOR inhibition.

METHODS

Cell Culture

Human embryonic kidney-293 (HEK293) cells were cultured in DMEM supplemented with 10% heat-inactivated fetal bovine serum, 100 IU/ml Penicillin G, 100 μg/ml Streptomycin, and 2 mm L-glutamate. Immortalized rhesus macaque skin fibroblasts (i.e., RhF) with puromycin resistance were described previously (17). Immortalized human umbilical vein endothelial (huvecs) were cultured in endothelial cell growth medium supplemented with 10% heat-inactivated fetal bovine serum, as previously described (18). All cells were cultured at 37°C in 5% CO_2.

Inhibitors

Rapamycin, LY294002 and Torin were purchased from LC Biosciences, Calbiochem and Cayman Chemical, respectively.

MTS cell proliferation assay

To observe alterations in growth and proliferation, 1 X 10^4 HEK293 cells were treated with the therapeutic compounds at the indicated doses or with appropriate vehicle as a negative control. Cells were followed for 72 hours, and cell viability was determined by trypan blue exclusion performed in quadruplicate. Actively metabolic cells were quantified every 24 hours using the Cell Titer 96® Aqueous One Solution Cell Proliferation Assay (Promega) according to the

manufacturer's instructions. Absorbance was measured using Fluostar OPTIMA (BMG Labtech).

Western blots

Cells were treated with various compounds as indicated. After washing harvested cells with ice-cold PBS, cell lysates were prepared in a buffer containing 150 mm nacl, 50 mm Tris-HCl (ph 8), 0.1% NP40, 50 mm NaF, 30 mm β-glycerophosphate, 1 mm Na_3VO_4 and 1x Complete Protease Inhibitor cocktail (Roche). Equal amounts of proteins were electrophoresed on either 10 or 12% SDS-PAGE denaturing gels, followed by transfer onto a Hybond™-ECL nitrocellulose membrane (GE Healthcare). Membranes were blocked with 5% fat-free milk for 1 hour at room temperature, followed by overnight incubation at 4°C in the indicated primary antibodies directed against either phosphorylated or total protein. The following primary antibodies against phosphorylated proteins were used: AKT (Ser473), AKT (Thr308), mTOR (Ser2448), S6K (Thr421/Ser424), S6 ribosomal protein (Ser235/236) (Cell Signal). Tubulin (Cell Signal) was used as a loading control, and anti-vPK antibody was a kind gift of Dr. Yoshihiro Izumiya (UC Davis). After washing, the membrane was incubated with anti-rabbit igg conjugated to HRP. The results were visualized with the ECL Plus Western Blotting Detection System (GE Healthcare) according to the manufacturer's instructions.

Recombinant protein production and purification

Large scale cultures (ten T150 flasks) of *Spodoptera fugiperda* SF9 cells, maintained at 27°C in EX-CELL 420 medium (Invitrogen) were infected with baculoviruses encoding FLAG-tagged ORF36 for 48 hours. Expression of ORF36 was confirmed by immunoblotting. Cells were harvested with FLAG lysis buffer (50 mm Tris-hcl [ph 7.5], 500 mm nacl, 1 mm EDTA, 1% Triton X-100) supplemented with Complete© protease inhibitor cocktail. Cell lysate was cleared by centrifugation and FLAG-tagged ORF36 was immunoprecipitated using anti-FLAG antibody-conjugated agarose beads (Sigma), as per the manufacturer's instructions. Protein was eluted with 150 μg/ml of 3x FLAG peptide (Sigma) in TBS buffer. Purification was confirmed with immunoblotting. Silver staining of SDS-PAGE gels was carried out to determine protein concentration by comparison to a BSA standard.

In vitro kinase assay

Purified kinases were first adjusted to 100 ng/μl in kinase dilution buffer (50 mm Tris-HCl ph 7.5, 0.1 mm EGTA, 1 mg/ml BSA, 0.1% (v/v) 2-mercaptoethanol). 100 ng kinase was incubated with 2 μg of S6 peptide (Carboxy terminus -STSKSESSQK- amino terminus) in kinase reaction buffer (20 mm HEPES pH 7.5, 5 mM $Mncl_2$, 10 mM 2-mercaptoethanol) supplemented with 10 μCi [γ-^{32}P] ATP (Perkin-Elmer) at 37°C for 30 minutes, after which the entire reaction was spotted onto P81 phosphocellulose paper and plunged into 75 mm H_3PO_4 to terminate the reaction. Phosphocellulose papers were washed three times and allowed to dry at room temperature after the last wash, and placed in

scintillation vials. Counts were assayed using liquid scintillation counting (Perkin-Elmer).

Genome quantification and plaque assay

Genome quantification was performed by qPCR and comparison to known standards, as previously described (19); Rhesus monkey Tubulin gene was used as an endogenous housekeeping control. Plaque assays were performed by infecting confluent primary Rhesus fibroblasts with viral supernatants, as previously described (17).

RESULTS

KSHV vPK phosphorylates cellular proteins that regulate host protein synthesis

Eukaryotic expression vectors were transiently transfected into HEK293 cells for 48 hours, after which cells were harvested, and prepared lysates were subjected to immunoblotting. Probing membranes with phospho-specific antibodies indicated that vPK expression increased phosphorylation of S6 ribosomal protein (S235/236), eukaryotic initiation factor 4B (eIF4B) (S422) and 4E binding protein (4EBP1) (Th37/46), as shown in Figure 1. In data not shown, these increases were found to correlate with the amount of transfected DNA, thus attributing enhanced phosphorylation of these cellular targets with levels of vPK expression. Tubulin is shown as a loading control.

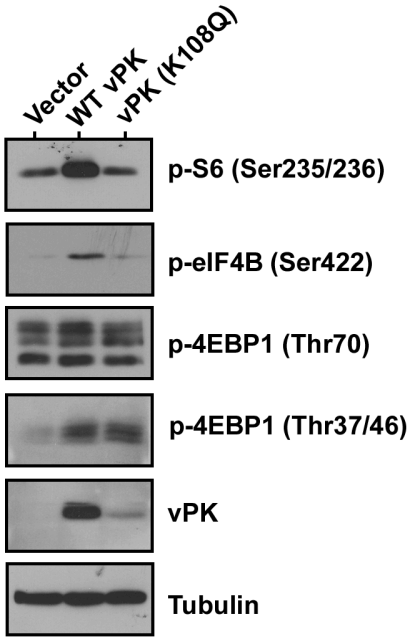

Figure 1: vPK activates proteins downstream of PI3K/AKT/mTOR signaling. Immunoblot analysis of vPK-transfected HEK293 cells demonstrates increases in phosphorylated S6, eIF4b and 4EBP1 proteins, correlating with vPK expression; these increases are absent in vector and mutant vPK K108Q (kinase dead)-expressing cells.

vPK expression confers resistance to PI3K/AKT/mTOR inhibitors

As described above and in methods, cells were transfected with vPK for 48 hours. Cells were cultured in reduced serum (2%) medium for a further three hours, after which cells were treated with 10 nm of either LY294002 (PI3K inhibitor), Rapamycin (mTORc1 inhibitor) or Torin1 (mTORc1 and 2 inhibitor), or the vehicle control (DMSO) for 30 minutes, and then harvested. Cell lysates were

subjected to immunoblot analysis. Analysis of the immunoblots with phospho-specific antibodies indicated sustained phosphorylation of PI3K/AKT/mTOR effector proteins, namely S6, eIF4E and 4EBP1, despite treatment with these inhibitors (Figure 2).

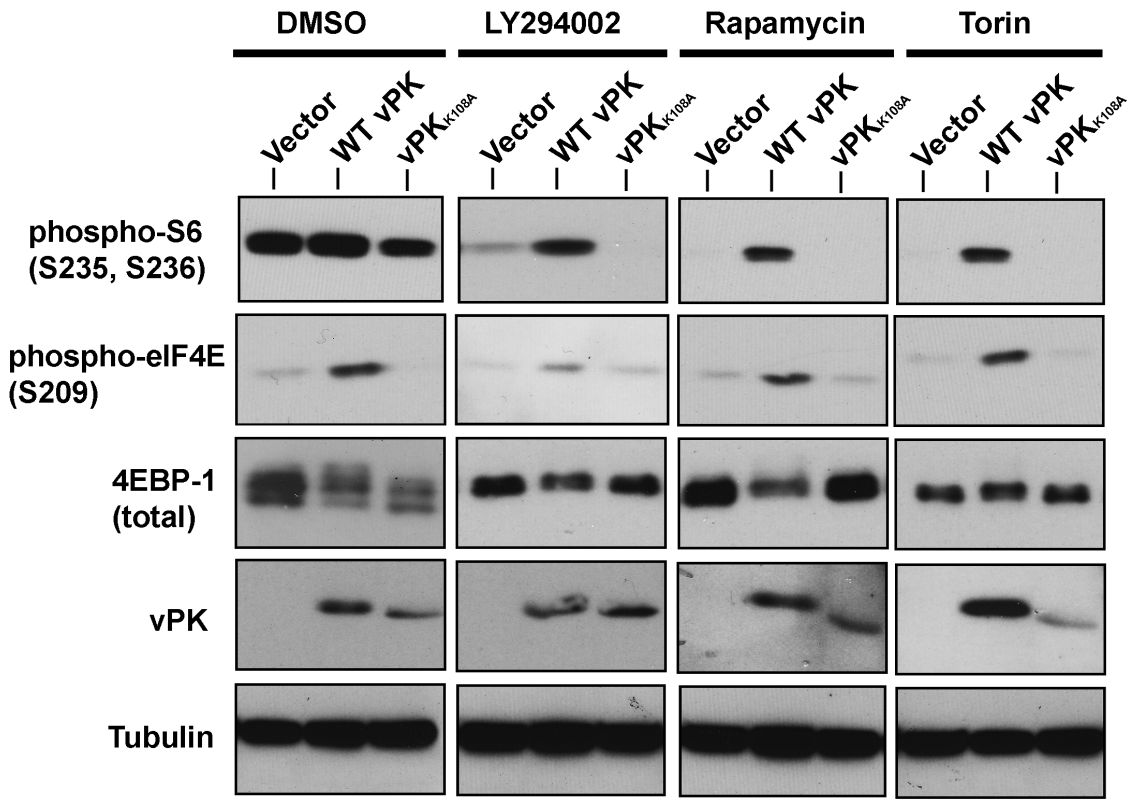

Figure 2: vPK imparts resistance to PI3K/AKT/mTOR inhibitors. Phosphorylation of S6, eIF4e and 4EBP1 is sustained in vPK-expressing HEK293 cells, in spite of treatment with LY294002, Rapamycin or Torin. This effect is absent in vector- and mutant vPK-expressing cells.

Treating cells stably expressing vPK with increasing doses of the mTOR inhibitors Torin1 and Rapamycin did not significantly inhibit cell proliferation as measured by MTS activity (Figure 3A and 3B, respectively), although this effect was lost at higher concentrations of both inhibitors (greater than 10 μM). The corresponding vector-expressing cells succumbed at all doses of the inhibitor.

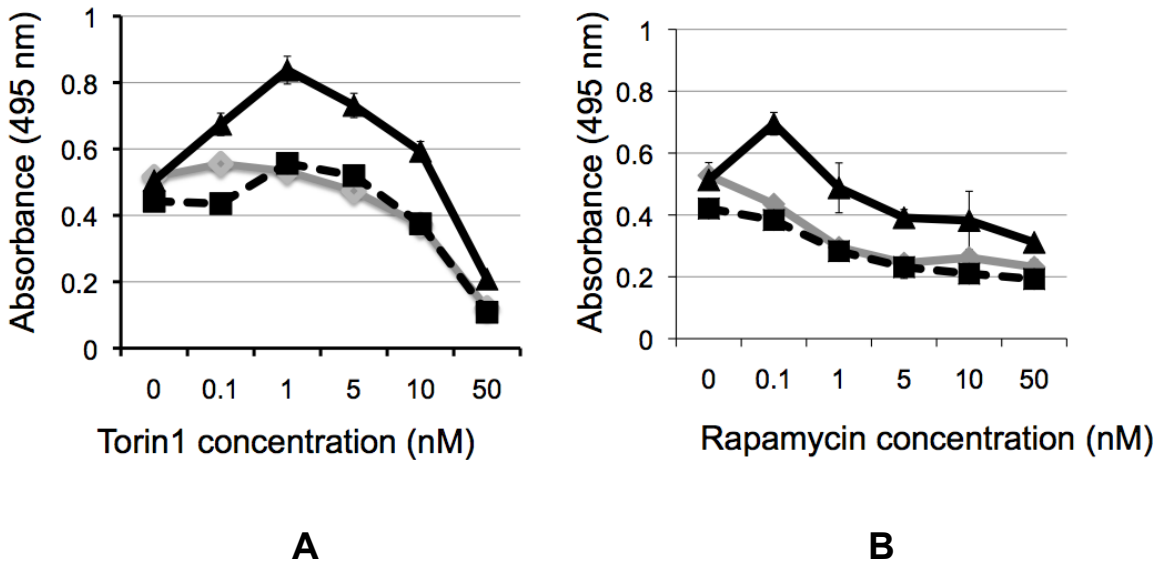

Figure 3: vPK protects cells from mTOR inhibition. HEK293 cells stably expressing vPK, mutant vPK or vector were treated with increasing doses of Torin1 (Panel A, left) or rapamycin (Panel B, right) for 72 hours, and cell viability was analyzed by MTS assay. VPK expression confers resistance to these inhibitors, whereas mutant- and vector-expressing cells succumb to these treatments.

ɣ-herpesvirus replication ensues in the presence of PI3K/AKT/mTOR inhibitors

To test whether resistance to PI3K/AKT/mTOR inhibitors occurs in the context of the KSHV viral lifecycle, we first infected htert-HUVEC with KSHV by spinoculation, as described previously (20). Following infection, cells were cultured at 37°C for one hour in reduced-serum (2%) medium containing 10 nm of Torin1, after which cells were harvested and lysates prepared and subjected to immunoblotting as described above. As previously reported, KSHV infection leads to phosphorylation of AKT at Ser473 (1) (Figure 4). p70S6K and it's substrate ribosomal S6 protein were also phosphorylated at sites denoting their activated status in KSHV-infected cells, as previously described. Surprisingly, phosphorylation of both of these targets was maintained despite treatment with Torin1, the inhibitor of mTOR which is the upstream kinase responsible for regulating both S6K and 4EBP1 phosphorylation; 4EBP1 was also inhibited (by phosphorylation) in KSHV-infected cells treated with either vehicle or Torin1, (data not shown*).* Torin1 inhibits both mTOR kinase activity, and therefore can countermand mTORc2 feedback activation of AKT by phosphorylation at S473. We see a corresponding loss of activated AKT in KSHV-infected, Torin1-treated htert HUVEC cells, thus confirming the on-target effect of the compound.

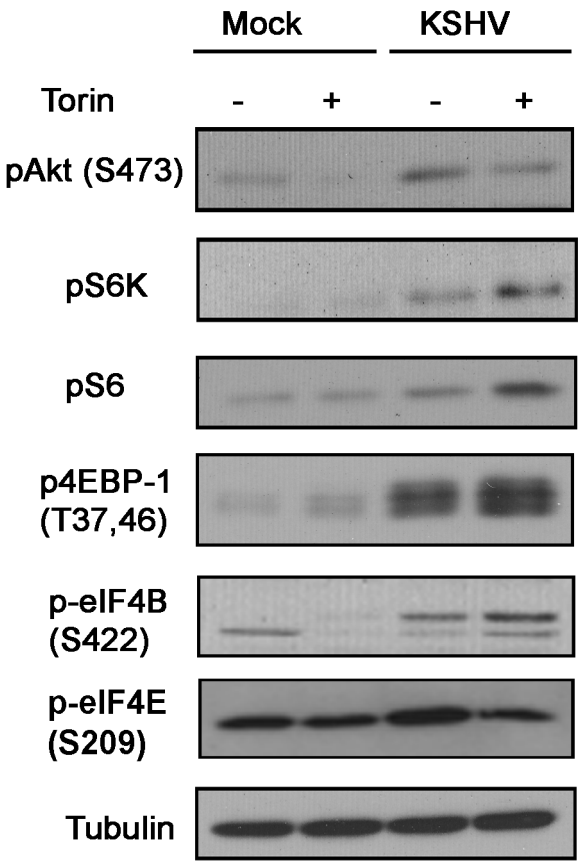

Figure 4: mTOR targets are activated in KSHV-infected hTERT-HUVEC. Phosphorylated S6K, S6 and 4EBP1 levels are sustained in spite of treatment with mTOR inhibitor Torin1, in infected cells.

Rhesus Rhadinovirus (RRV), the simian homolog of KSHV, infects and replicates to high titers within permissive rhesus fibroblasts, making this a useful model system to study the ɣ-herpesvirus lytic lifecycle. At a low multiplicity of infection (MOI of 0.1), RRV genome replication occurs in the presence of the mTOR inhibitor rapamycin (10 nm) as shown in Figure 5A, and to similar levels as vehicle-treated cells. Significantly, infectious virion production is also

impervious to rapamycin, as evidenced in equivalent plaque-forming units (Pfu/ml) of virus derived from both vehicle- and rapamycin-treated cells (Figure 5B).

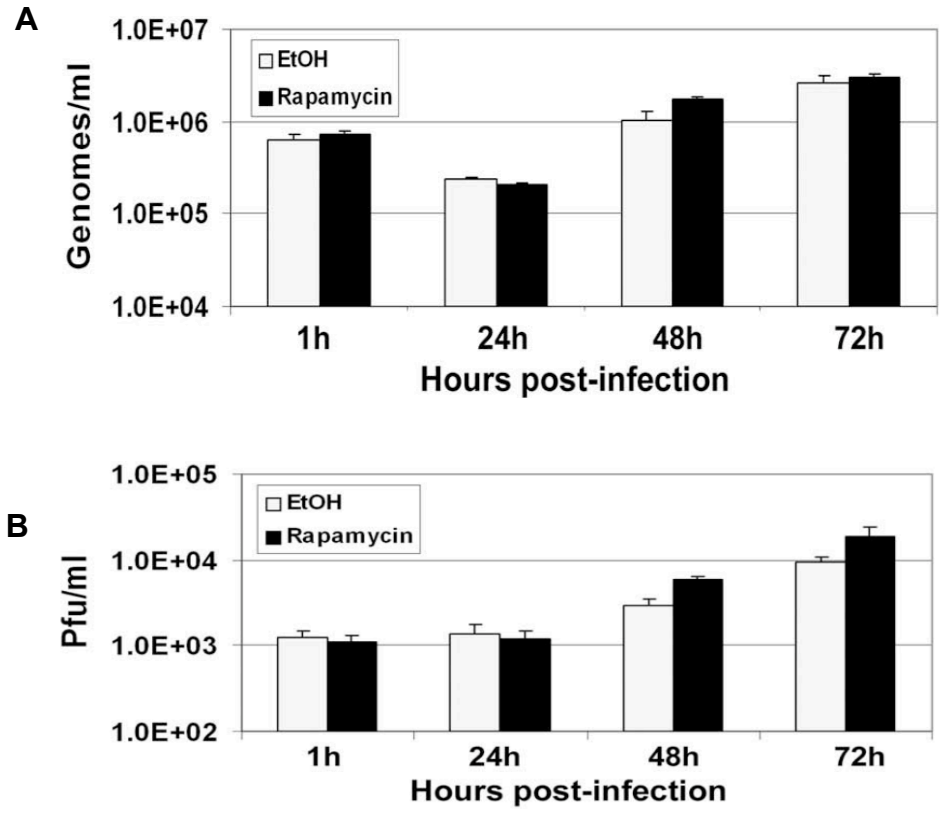

Figure 5: RRV lytic lifecycle is impervious to rapamycin treatment. RRV genome amplification (panel A, top) and infectious virion production (panel B, bottom) ensues in the presence of 0.5 um rapamycin, at levels similar to vehicle-treated infected RhF.

vPK exerts kinase activity downstream of PI3K/AKT/mTOR kinases

To determine the mechanism by which vPK-dependent activation of PI3K/AKT/mTOR downstream targets occurs, we tested whether vPK phosphotransferase activity extends to these effector proteins. 100 ng of vPK purified from SF9 insect cells was incubated with different synthetic peptides, and in an in vitro kinase reaction as described above. The unrelated CDK1 substrate EF1 α, which served as a negative control. Analysis of the background-subtracted counts indicated that vPK efficiently and specifically phosphorylates S6 peptide (Figure 5), at levels comparable to the upstream regulatory cellular p70 S6 Kinase.

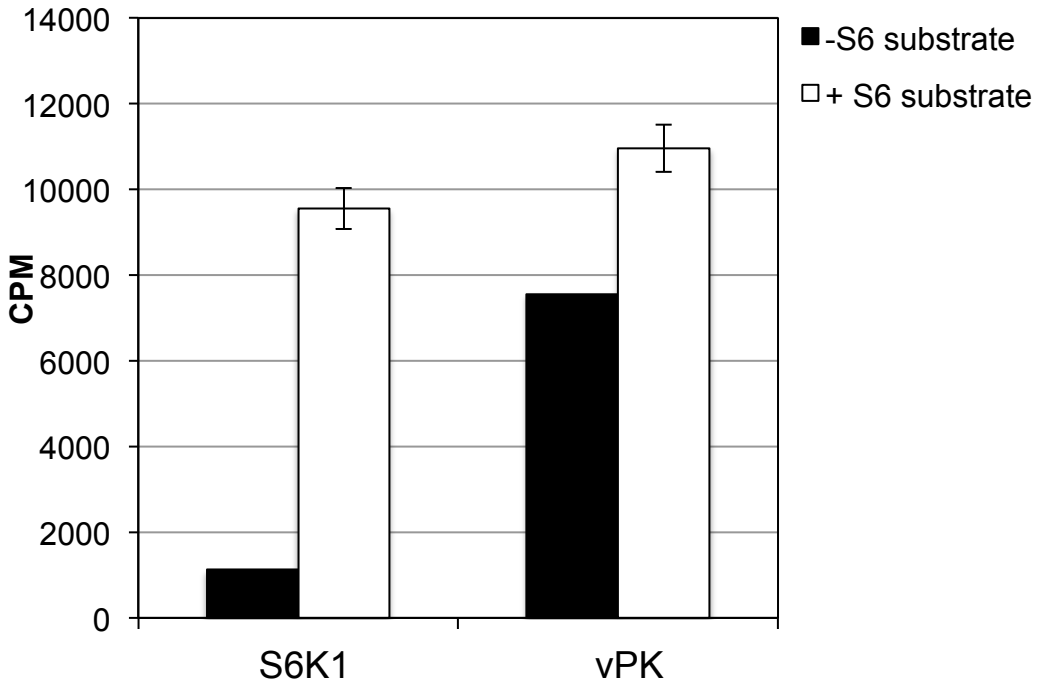

Figure 6: KSHV vPK phosphorylates a synthetic S6 peptide in an vitro kinase reaction.

DISCUSSION

As an obligate intracellular parasite, KSHV depends on the host for replication, propagation and dissemination. To ensure fulfillment of all the necessary requirements for successful replication, KSHV encodes a plethora of viral proteins, many of which are multi-functional and have diverse effects upon the host cell depending upon which compartment they are expressed in. These viral proteins alter the cellular signaling milieu by interacting with cellular adaptors (e.g. LANA), acting as scaffolds to bring cellular proteins together (e.g. ORF45), or by possessing enzymatic function allowing direct modification of host proteins (e.g. ORF64). An example of the latter is the viral protein kinase (vPK), which phosphorylates serine and threonine residues in specific proteins. Preliminary studies demonstrated that vPK activates JNK signaling, thereby putatively activating cellular and/or viral transcription programs. Significantly, although vPK is expressed late during the viral lifecycle, studies revealed that vPK is a tegument protein, therefore it may activate cell signaling during primary infection of naïve cells.

A recent report uncovered a plethora of vPK targets using a phosphoproteomics approach (16). Recombinant eukaryotic substrates were purified from yeast and spotted onto glass micro-slides, and subsequently incubated with purified vPK in an in vitro kinase reaction. An astonishing 178 cellular proteins were found to be putative vPK targets. Using a systems biology approach to analyze these results, vPK (and indeed, all other conserved herpesvirus kinases) was found to target proteins involved in the cellular

response to DNA damage, and the histone acetyltransferase TIP60, an upstream regulator of DNA damage response (DDR) was specifically found to be essential for efficient α-, β-, and γ-herpesvirus replication (16).

The objective of the current study was to determine whether vPK activates the cellular PI3K/AKT/mTOR signaling pathway. Using an overexpression approach, vPK was found to activate downstream effectors of PI3K/AKT/mTOR signaling, specifically the ribosomal S6 protein, the eukaryotic initiation factors 4E and 4B as well as the repressor 4E binding protein.

Phosphorylation of these effectors was sufficient to overcome upstream inhibition by compounds such as the PI3K inhibitor LY294002, the mTORc1 inhibitor rapamycin and the mTOR kinase inhibitor Torin1. Moreover, vPK expression in cells treated with these inhibitors conferred a survival advantage over an extended period of 72 hours, whereas vector-expressing cells succumbed to the growth-inhibitory effects of these compounds.

Since vPK is a tegument protein, we tested whether resistance to mTOR inhibitors occurs early during KSHV infection. Indeed, we found phosphorylation of S6, 4EBP1 and eIF4e was sustained in Torin1-treated hTERT-HUVECs following infection. Additionally, because vPK is a late lytic protein, it is possible that resistance to PI3K/AKT/mTOR inhibitors may also occur late in the lytic lifecycle. Therefore, we measured RRV lytic replication 72 hours following infection in the presence of PI3K/AKT/mTOR inhibitors. RRV genome amplification and progeny virion production was found to be impervious to

rapamycin. Two major caveats prevent us from concluding that resistance is imparted by vPK expression: the lack of a vPK-deleted recombinant KSHV (or RRV) virus, as well as the difficulty in detecting endogenous vPK protein following infection by immunoblot, despite the existence of a vPK-specific antibody.

To arrive at a mechanism by which resistance to upstream kinase inhibitors was attained, we performed an in vitro kinase assay using recombinant vPK and synthetic S6 peptide as the substrate. We found that vPK phosphorylates S6 peptide at the same residues phosphorylated by cellular S6K, which corresponds with activation of protein translation (7). These data suggest that vPK can bypass any inhibitory signaling upstream of S6, and directly activate protein translation by phosphorylating S6 ribosomal protein. This is significant considering that PI3K/AKT/mTOR-hyperactivation can improperly activate S6, and this is a common occurrence in neoplasms. Moreover, KSHV is an oncogenic herpesvirus, so determining whether sporadic expression of vPK, a lytic protein, contributes to KSHV-associated tumorigenesis is a future goal.

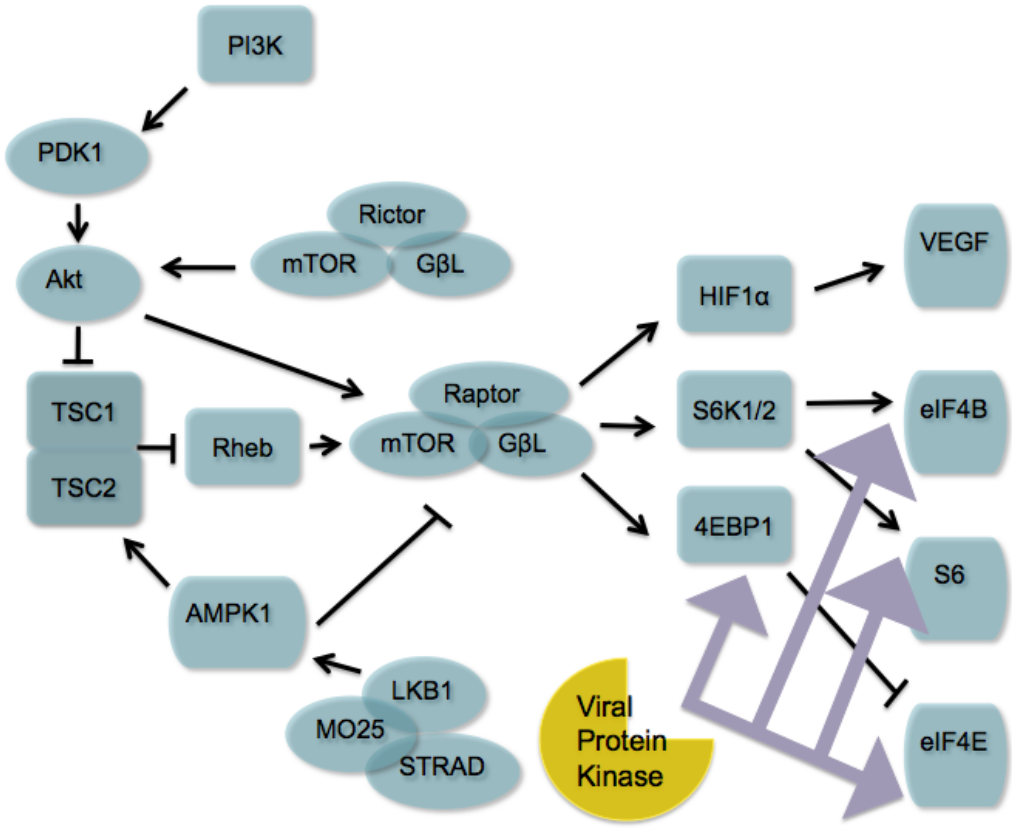

Figure 7: Proposed model for vPK's function in the host cell. By acting downstream of PI3K, AKT and mTOR, vPK imparts resistance to inhibitors to these kinases by directly phosphorylating their effector proteins.

REFERENCES

1. **Moore PS, Boshoff C, Weiss RA, Chang Y.** 1996. Molecular mimicry of human cytokine and cytokine response pathway genes by KSHV. Science **274:**1739-1744.

2. **Swanton C, Mann DJ, Fleckenstein B, Neipel F, Peters G, Jones N.** 1997. Herpes viral cyclin/Cdk6 complexes evade inhibition by CDK inhibitor proteins. Nature **390:**184-187.

3. **Sun Q, Matta H, Chaudhary PM.** 2003. The human herpes virus 8-encoded viral FLICE inhibitory protein protects against growth factor withdrawal-induced apoptosis via NF-kappa B activation. Blood **101:**1956-1961.

4. **Lagunoff M, Majeti R, Weiss A, Ganem D.** 1999. Deregulated signal transduction by the K1 gene product of Kaposi's sarcoma-associated herpesvirus. Proc Natl Acad Sci U S A **96:**5704-5709.

5. **Gonzalez CM, Wang L, Damania B.** 2009. Kaposi's sarcoma-associated herpesvirus encodes a viral deubiquitinase. J Virol **83:**10224-10233.

6. **Park J, Lee D, Seo T, Chung J, Choe J.** 2000. Kaposi's sarcoma-associated herpesvirus (human herpesvirus-8) open reading frame 36 protein is a serine protein kinase. The Journal of general virology **81:**1067-1071.

7. **Manning G, Whyte DB, Martinez R, Hunter T, Sudarsanam S.** 2002. The protein kinase complement of the human genome. Science **298:**1912-1934.

8. **Chandran B.** 2010. Early events in Kaposi's sarcoma-associated herpesvirus infection of target cells. J Virol **84:**2188-2199.

9. **Gregory SM, West JA, Dillon PJ, Hilscher C, Dittmer DP, Damania B.** 2009. Toll-like receptor signaling controls reactivation of KSHV from latency. Proc Natl Acad Sci U S A **106:**11725-11730.

10. **Chang J, Renne R, Dittmer D, Ganem D.** 2000. Inflammatory cytokines and the reactivation of Kaposi's sarcoma-associated herpesvirus lytic replication. Virology **266:**17-25.

11. **Li X, Feng J, Sun R.** 2011. Oxidative stress induces reactivation of Kaposi's sarcoma-associated herpesvirus and death of primary effusion lymphoma cells. J Virol **85:**715-724.

12. **Hamza MS, Reyes RA, Izumiya Y, Wisdom R, Kung HJ, Luciw PA.** 2004. ORF36 protein kinase of Kaposi's sarcoma herpesvirus activates the c-Jun N-terminal kinase signaling pathway. J Biol Chem **279:**38325-38330.

13. **Izumiya Y, Izumiya C, Van Geelen A, Wang DH, Lam KS, Luciw PA, Kung HJ.** 2007. Kaposi's sarcoma-associated herpesvirus-encoded protein kinase and its interaction with K-bZIP. J Virol **81:**1072-1082.

14. **Haque M, Wang V, Davis DA, Zheng ZM, Yarchoan R.** 2006. Genetic organization and hypoxic activation of the Kaposi's sarcoma-associated herpesvirus ORF34-37 gene cluster. J Virol **80:**7037-7051.

15. **Connolly E, Braunstein S, Formenti S, Schneider RJ.** 2006. Hypoxia inhibits protein synthesis through a 4E-BP1 and elongation factor 2 kinase pathway controlled by mTOR and uncoupled in breast cancer cells. Mol Cell Biol **26:**3955-3965.

16. **Li R, Zhu J, Xie Z, Liao G, Liu J, Chen MR, Hu S, Woodard C, Lin J, Taverna SD, Desai P, Ambinder RF, Hayward GS, Qian J, Zhu H, Hayward SD.** 2011. Conserved herpesvirus kinases target the DNA damage response pathway and TIP60 histone acetyltransferase to promote virus replication. Cell host & microbe **10:**390-400.

17. **DeWire SM, Damania B.** 2005. The latency-associated nuclear antigen of rhesus monkey rhadinovirus inhibits viral replication through repression of Orf50/Rta transcriptional activation. J Virol **79:**3127-3138.

18. **Wang L, Wakisaka N, Tomlinson CC, DeWire SM, Krall S, Pagano JS, Damania B.** 2004. The Kaposi's sarcoma-associated herpesvirus (KSHV/HHV-8) K1 protein induces expression of angiogenic and invasion factors. Cancer Res **64:**2774-2781.

19. **Wen KW, Dittmer DP, Damania B.** 2009. Disruption of LANA in rhesus rhadinovirus generates a highly lytic recombinant virus. J Virol **83:**9786-9802.

20. **West J, Damania B.** 2008. Upregulation of the TLR3 pathway by Kaposi sarcoma associated herpesvirus during primary infection. J Virol **82:**5440-5449.

CHAPTER 5: SUMMARY, CONCLUSIONS AND FUTURE DIRECTIONS

GENERAL SUMMARY

Investigating the interplay between the oncogenic herpesvirus KSHV and host cell PI3K/AKT/mTOR signaling is the broad goal of my dissertation research, performed under the guidance of Dr. Blossom Damania. Specifically, I studied the extent to which KSHV manipulates host cell signaling, metabolism and protein synthesis to ensure viral persistence, and the resulting consequences for the host. My dissertation research has confirmed the rationale of using PI3K/AKT/mTOR-targeted inhibitors for KSHV-associated primary effusion lymphoma (PEL). My work has also generated hypotheses and opened up diverse research into the nascent field of KSHV-driven metabolic reprogramming. Further, the discovery of a novel substrate for the viral protein kinase (vPK) poses the question of its functional relevance for the viral lifecycle. Further investigation into this biology may uncover fascinating insights into the ability of KSHV to usurp and manipulate host cell processes.

Chapter One provides a broad background of the KSHV lifecycle, and literature reviews describing how four viral proteins alter the cellular PI3K/AKT/mTOR signaling pathway, and the implications for oncogenesis. In Chapter Two, I confirmed that KSHV-infected primary effusion lymphoma (PEL)

cells are addicted to PI3K/AKT/mTOR signaling, and, using a preclinical mouse model of PEL, found that exploiting this dependence is an efficacious therapeutic strategy. In Chapter Three, with the help of metabolomics, I discovered extensively altered cellular metabolism in PEL, specifically upregulated glycolysis and fatty acid synthesis. Using classical biochemical flux analyses, I confirmed this metabolic reprogramming in PEL and other B-NHL, was PI3K/AKT-dependent, and identified metabolic pathways that various B-NHL are reliant upon. I further found that this reliance results from abnormal activation of the metabolic oncogene FASN, whose inhibition selectively kills B-NHL while sparing normal cells; thus, I have discovered a new molecular target for B-NHL therapeutics. In Chapter Four, I discovered that the KSHV viral protein kinase activates PI3K/AKT/mTOR signaling, and the functional implications of this protein's expression in the context of both the latent and lytic stages of the KSHV life cycle.

Although all three chapters comprise three distinct projects undertaken during my graduate career, at their confluence is a common theme: that viruses, as obligate intracellular parasites, manipulate the host cell in diverse ways. KSHV encodes several proteins that mimic or hijack the function of eukaryotic proteins to acutely alter the cellular signaling milieu and propagate the virus. My dissertation places the PI3K/AKT/mTOR pathway at the nexus of viral latency and lytic replication. KSHV viral proteins directly and indirectly activate PI3K/AKT/mTOR signaling in both lytic and latent stages of the lifecycle, with the unintentional consequence of cancer in the host, resulting from pathway

hyperactivation. This chapter synthesizes these independent projects and proposes future directions, in order to prepare the groundwork for further preclinical research towards safe and effective therapeutics for KSHV-associated malignancies, and other B-NHL in general.

KSHV-associated malignancies are characterized by hyperactive signaling.

Kaposi's sarcoma-associated herpesvirus is an oncogenic herpesvirus associated with three neoplasms: Kaposi sarcoma, primary effusion lymphoma and multicentric Castleman's disease. Most human cancers arise from complex interplay between environmental factors, genetic predisposition and somatic mutations, obscuring the single driver of the neoplasm (*1*). In contrast, virus-associated cancers present a model system to study carcinogenesis, as unlike other human cancers, viral infection primarily drives tumor development, altough cellular co-factors including host immunosuppression are also required. Viral oncogenic proteins contribute to the development of neoplasms and facilitate their progression, by manipulating cellular proteins to deregulate signaling pathways, thereby transforming the host cell.

KSHV is an enveloped, double-stranded DNA virus with a protein-rich tegument. KSHV infection itself is relatively innocuous, however may manifest as KSHV Inflammatory cytokine syndrome (KICS) in some instances (*2*). KSHV persists for the lifetime of the host by hiding from the immune system in a latent state, with minimal expression of a limited subset of viral proteins and microRNAs transcribed from the latency locus. The host replication machinery is

responsible for duplicating the viral genome, which exists as an episome tethered to host chromosomes via the viral protein LANA. Latency is a beneficial for KSHV, since the limited repertoire of expressed viral proteins generate fewer epitopes, thereby hiding KSHV from the host's immune system. Periodic bouts of lytic replication generate progeny virions that can infect naïve cells, thus disseminating the virus. Lytic replication places the host cell under stressful conditions, due to the increased requirements for nutrients, ATP, nucleotide precursors, lipids, etc.

Hyperactive PI3K/AKT/mTOR signaling is a common attribute of diverse human cancers. This pathway plays a critical role in cell proliferation and survival, as discussed in Chapter One. Pathway hyperactivation can result from deletion of the negative regulator PTEN and somatic mutations in the PI3K catalytic subunit. PI3K/AKT/mTOR signaling has pleiotropic effects, because of the wide array of effectors activated by PI3K, AKT or mTOR (*3*). For example, activation of S6K, the mTOR target, activates protein translation. Another example is inhibition of apoptosis, mediated by AKT-dependent inhibition of the FOXO family of pro-apoptotic transcription factors. Therefore, the functional output of PI3K/AKT/mTOR signaling depends on:

1. The kinase which is activated
2. The effectors of that specific kinase.

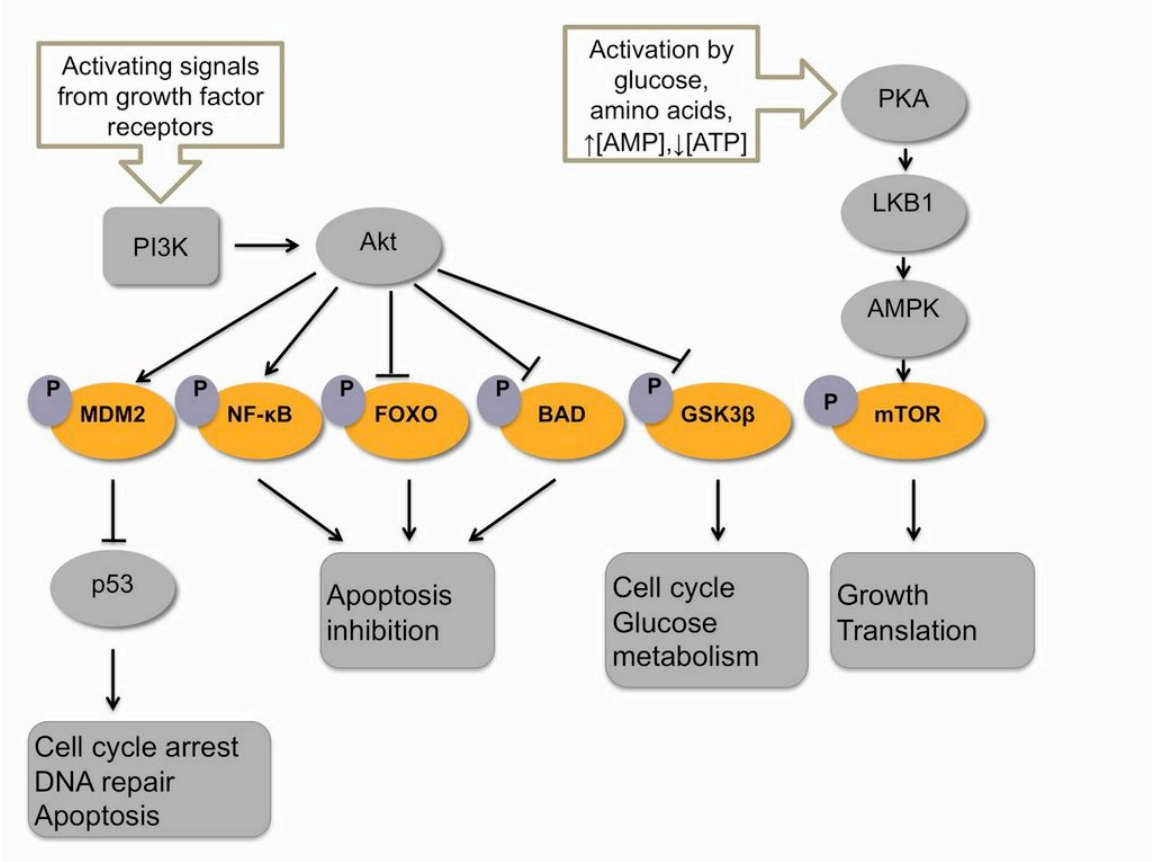

Figure 1: Schematic of various effectors of the PI3K/AKT/mTOR pathway.

Hyperactivated signaling results in sustained activation of proteins involved in protein translation, metabolism, secretion of angiogenic growth factors and cytokines, motility and adhesion, etc. Four KSHV-encoded proteins activate PI3K/AKT/mTOR signaling: K1, vIL-6, vGPCR and ORF45 (*4*). Low levels of both K1 and vIL-6 are detected in latent cells, with upregulated levels

once lytic replication commences (*5*). On the other hand, ORF 45 and vGPCR are expressed only during lytic replication.

DUAL INHIBITION OF PI3K AND mTOR INHIBITS AUTOCRINE AND PARACRINE PROLIFERATIVE LOOPS IN PI3K/AKT/mTOR-ADDICTED LYMPHOMAS

Stallone et al described the regression of iatrogenic Kaposi's sarcoma in a renal transplant recipient, once the immunosuppressive agent was switched from cyclosporine to rapamycin (*6*). Following this discovery, Dittmer and colleagues demonstrated activation of PI3K/AKT/mTOR kinases and their effector proteins in primary effusion lymphoma (PEL) (*7*). They showed that the allosteric mTOR inhibitor rapamycin inhibits PEL proliferation and reduces activation of mTOR targets such as S6K. When rapamycin was administered to immunocompromised mice bearing subcutaneous PEL tumors (xenografts), tumor burden was acutely reduced in rapamycin-treated animals, compared to those receiving vehicle

We hypothesized that single-agent inhibitors incompletely block the PI3K/AKT/mTOR pathway in PEL; as such, dual pathway inhibition would overcome the inadequacy of single-agent inhibition of PI3K/AKT/mTOR pathway. The hypothesis and pursuant studies directly benefited from the availability of a new compound, NVP-BEZ235 from Novartis. This drug blocks the kinase activities of both PI3K and mTOR.

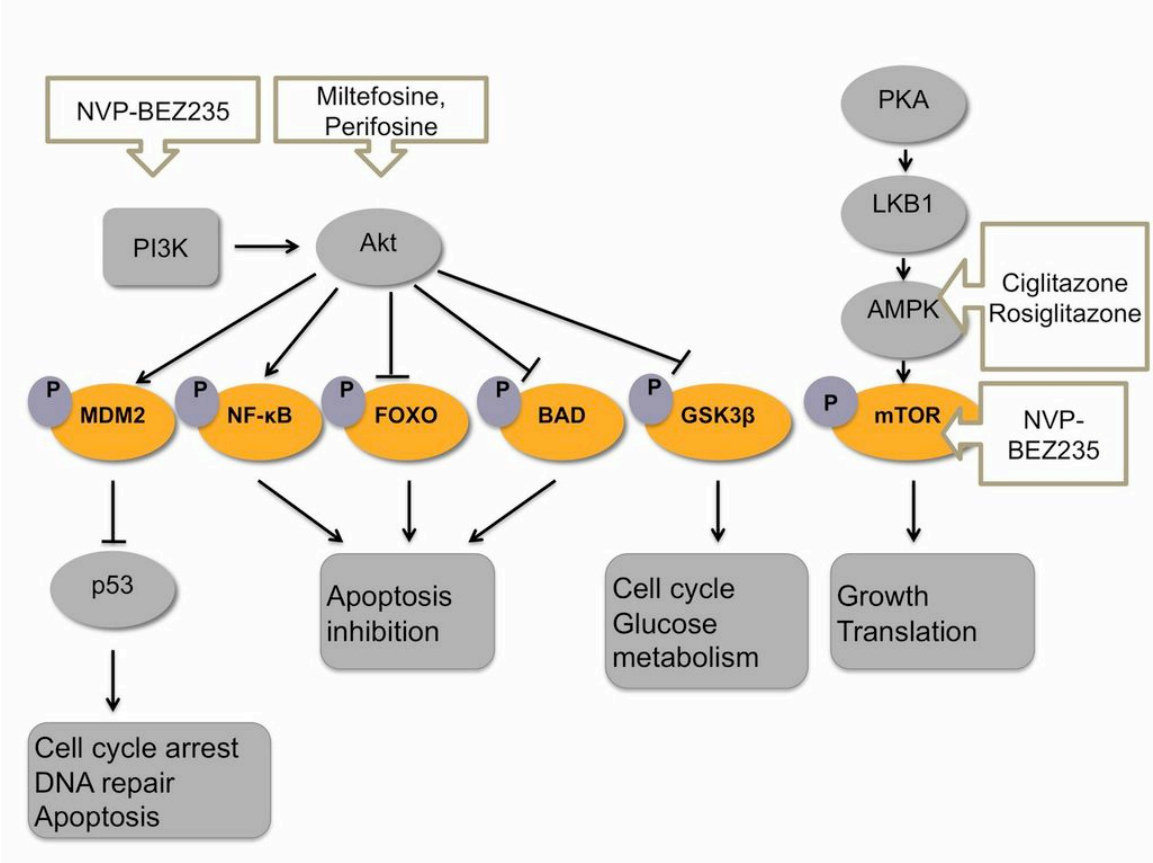

Figure 2: Various compounds inhibit PI3K/AKT/mTOR signaling either at one or two nodes, as shown. mTOR is indirectly inhibited by activating AMPK using glitazones. AKT is directly inhibited by Miltefosine and Perifosine, NVP-BEZ235 inhibits the kinase activity of both PI3K and mTOR kinases.

Thus, we were able to directly examine the impact of dual inhibition, as compared to single-agent inhibitors of either AKT or mTOR. This relatively straightforward first project of my graduate training promised immediate preclinical impact, should the dual-inhibitor prove a valuable agent for treating

PEL. Moreover, these studies would potentially establish the relative contribution of each branch of the PI3K/AKT/mTOR pathway in contributing to the hyperproliferative cancer phenotype displayed by PEL, permitting greater basic understanding of the oncogenic progression in KSHV-associated malignancies.

The results of this study, published in *Blood* (*8*), showed that inhibiting different arms of the PI3K/AKT/mTOR pathway has differing outcomes for PEL cell survival, with dual inhibition being a better strategy compared to single inhibitors. A combinatorial approach whereby both the protein synthesis and the apoptosis-inhibition arms are targeted greatly diminishes PEL proliferation both in cell culture and in an animal model. Based on the results of this study, one may speculate that combining PI3K/AKT/mTOR inhibitors with compounds targeting other upregulated pathways in PEL such as MAPK or NF-κB may further augment their efficacy, with the caveat that NF-κB inhibition seems to reactivate KSHV from latency (*17*). However, dual PI3K/AKT/mTOR inhibition may prevent lytic replication in this instance in a two-fold manner: firstly, by blocking the expression of viral proteins such as vPK (see Chapter Four) that may bestow resistance to PI3K/AKT/mTOR inhibitors; and secondly, by inhibiting signaling resulting from viral proteins that are currently present in the cell at stable levels.

The potency of dual PI3K/AKT/mTOR inhibition extends to non-viral B-NHL, e.g. Follicular lymphoma, as evident by work of my colleague Prasanna Bhende (*9*). Collectively, these data reinforce the growing consensus in the field of cancer biology that monotherapy, while effective in the short-term, is not as effective as dual therapy. Monotherapy may fail due to build-up of resistance to

the inhibitor, or activation of compensatory signaling (*10*). Dual inhibitors apply pressure at two different nodes, thus preventing compensatory feedback activation, leading to a potentially more beneficial therapeutic outcome. A future direction of this study would be to determine whether PEL develop resistance to dual inhibitors, and if so, the mechanism by which this occurs. If viral proteins are implicated in development of resistance, it will reveal new functions of these viral proteins.

DYSREGULATION OF FATTY ACID SYNTHESIS AND GLYCOLYSIS IN NON-HODGKIN LYMPHOMA

The PI3K/AKT/mTOR signaling pathway regulates many aspects of cellular metabolism such as the expression of glycolytic genes, translocation of glucose transporter, and both synthesis and oxidation of lipids and fatty acids (*11*). Cellular metabolism is the study of how cells obtain nutrients for fueling growth and cell division, and maintaining homeostasis, all of which are crucial for the survival of KSHV-infected cells.

A flurry of recent publications has revitalized interest in cellular metabolism, with a particular focus on studying the extent and mechanism of metabolic reprogramming of cancer cells. These publications confirm Otto Warburg's seminal observations that tumor cells perform aerobic glycolysis (*12*). The current understanding of tumor metabolism is that increased glycolysis is necessary for generating carbon-based precursors for anabolic pathways (*13*). Relatively little was known about metabolic reprogramming in lymphomas, and still less about tumors driven by oncogenic viruses. This led us to investigate

whether primary effusion lymphoma (PEL), a B cell malignancy characterized by latent KSHV, bore any metabolic alterations. We hypothesized that PEL would significantly differ in their metabolic program compared to normal, uninfected B cells. The goal of the study was to identify the extent of metabolic reprogramming in PEL, a representative B-NHL. These data could aid in the identification of novel molecular targets for therapy, and biomarkers for early diagnosis.

We used a metabolomics approach to profile metabolites in PEL cells. In order to uncover differences from normalcy, we compared both intra- and extra-cellular metabolites of PEL to those of primary B cells isolated from the blood of anonymous, healthy donors. The reasons for this comparison were twofold: based on the relative distribution of metabolites, we could determine which metabolic pathway was dysregulated in PEL, and investigate whether enzymes mediating the dysregulation may serve as molecular targets for chemotherapy. Secondly, identifying metabolites specifically generated in PEL but not in normal cells may serve as biomarkers for early detection of disease.

Global metabolite profiles revealed significantly altered metabolism in PEL, compared to primary B cells. We found that glycolytic intermediates were over-represented in PEL, as were intermediates of fatty acid synthesis. While profiling global metabolites is strength of a metabolomics approach, it only offers a static representation of the metabolome, rather than the rate at which a specific biochemical reaction occurs. Therefore, we employed classical biochemical flux determination assays, using radiolabeled precursors. To broaden the scope of our experiments, we also included cell lines representative of other B-NHL in our

experiments. These included Burkitt lymphoma, follicular lymphoma, and two EBV-transformed lymphoblastoid cell lines (LCLs) that we generated.

Biochemical flux analysis revealed that, like most human cancers, all B-NHL have an exuberant glycolytic flux, compared to primary B cells. PEL in particular, are addicted to glucose, and PEL survival correlated with glucose concentration of the growth medium. Further, inhibiting glycolysis was toxic to all B-NHL. Metabolomics also revealed other extensive biochemical pathway alterations in PEL, whose further study will surely be productive and illuminating.

Fatty acid oxidation (FAO) rates were not significantly different between B-NHL lines and primary B cells. This was a puzzling finding, given that FAO is capable of efficiently generating vast amounts of ATP that can fuel the energy demands of rapidly growing cancer cells. Despite approximately equivalent FAO rates, PEL were less efficient than primary B cells at fully oxidizing fatty acids; this may indicate an underlying defect in FAO, and merits future study. Interestingly, we found that FAO intermediates in primary B cells have a profile indicating preferential oxidation of amino acids rather than fatty acids; it would be interesting to investigate whether this preference bears functional significance.

When fatty acid biosynthesis was measured, we found that this pathway is highly active in PEL. Fatty acid synthesis (FAS) is an energy-demanding process, with the additional cost of diverting carbon precursors into synthesis of fatty acids, rather than other more physiologically useful biomolecules. All B-NHL had active FAS, with intracellular accumulation of hydrophobic lipid droplets visualized by

microscopy. Fatty acid synthase (FASN) synthesizes fatty acids and is expressed only in the liver. All peripheral cells obtain requisite fatty acids from circulating blood, which contains diet-derived fatty acids and lipids. However, some cancer subtypes aberrantly express FASN, therefore FASN has been proposed to be a metabolic oncogene (*14*). We discovered that FASN is over-expressed in PEL, compared to primary B cells, which express very little FASN. This means that metabolic reprogramming in PEL begins at the level of aberrant protein expression. It is possible that viral latent proteins may induce FASN expression, since FASN is expressed at lower levels (and therefore FAS rates are correspondingly lower) in a few of the B-NHL we analyzed. Our discovery of an enzyme whose expression is restricted to malignant cells indicates that FASN may be a molecular target for therapies to treat PEL and possibly, other B-NHL (*15*).

We tested whether PEL are sensitive to FASN inhibitors. C75 is an irreversible inhibitor of FASN, and is a known anorexigenic compound, causing acute weight loss and inhibiting feeding behaviors in obese mice (*16*). We found that PEL were acutely sensitive to C75, with reduced FAS rates resulting from reduced FASN biosynthetic activity. C75 induced apoptosis in PEL, underlining the importance of FAS for PEL survival. Other B-NHL lines were also susceptible to C75 treatment, although slightly less than PEL. This may be due to comparatively lower FASN expression in other B-NHL.

C75 treatment decreased the expression of FASN protein, indicating that the compound not only blocks FASN enzymatic function, but may also regulate

FASN expression, by an as-yet undetermined mechanism. Combining C75 treatment with LY294002, a PI3K inhibitor, decreased the total concentration of each compound required to induce apoptosis. These data hint at the possible use of FAS inhibitors as sensitizing agents for PI3K/AKT/mTOR pathway-targeted therapeutics, such as rapamycin and NVP-BEZ235.

PEL preferentially synthesize abundant amounts of building blocks for daughter cells from glucose, compared to primary B cells. Thus, the reason, teleological in part, is that PEL upregulate glycolysis in order to generate FAS precursors, which in turn, are incorporated into cell membranes of daughter cells. It is possible that a KSHV viral latent protein imparts this phenotype, since it would guarantee propagation of the viral episome into new cells. Therefore, investigating the mechanism by which FAS is activated by KSHV bears further investigation.

In addition to observing upregulated glycolysis and FAS in PEL, we discovered an inextricable link between these two biochemical pathways. We found that inhibiting glycolysis abated FAS rates, suggesting that glycolysis intermediates are essential for feeding FAS. Conversely, FAS inhibition diminished glycolytic flux, possibly because reduction in FASN biosynthetic activity may itself reduce the demand for glycolysis-derived intermediates.

Collectively, these data revealed extensive metabolic reprogramming in KSHV-infected PEL cells, compared to uninfected, normal primary B cells. We first discovered which metabolic pathways are altered in PEL, compared to

primary B cells. We validated the metabolomics analyses with biochemical flux measurements, and discovered that upregulated FAS is driven by abnormal expression of FASN. Based on the sensitivity of PEL to FASN inhibitors, and their ability to sensitize PEL to other chemotherapeutic compounds, we propose FASN to be a target for molecular therapeutics for PEL, and moreover, for other B-NHL. These findings were reported in *Proceedings of the National Academy of Science* (*15*).

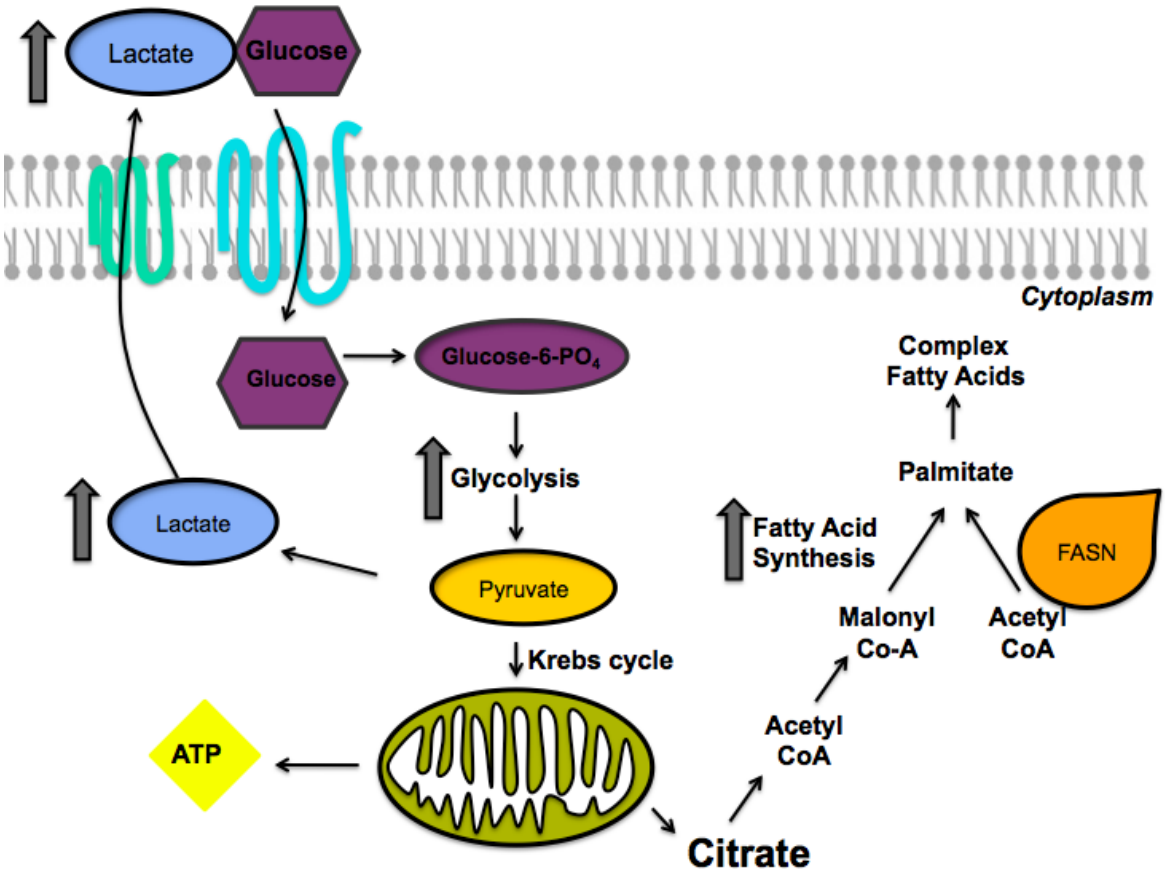

Figure 3: Overview of metabolic reprogramming in cancer cells

KSHV VIRAL PROTEIN KINASE ACTIVATES PI3K/AKT/mTOR TARGETS

Chapters Two and Three of my dissertation investigated the consequences of PI3K/AKT/mTOR activation in the latently infected host cell. Chapter Four of this dissertation uncovers how a viral protein, the KSHV viral protein kinase (vPK) activates PI3K/AKT/mTOR signaling. We found that vPK activates cellular factors involved in protein synthesis, such as the ribosomal protein S6. Using an in vitro approach, we found that S6 is a specific target of vPK's phosphotransferase activity. Our most immediate course of action is to identify other cellular substrates of vPK and their relative contributions to cellular transformation. Whether vPK expression directly alters protein synthesis, and whether viral or cellular proteins are preferentially synthesized remains to be investigated, and is a future direction of this study.

Further, we found that vPK imparts resistance to PI3K/AKT/mTOR-targeted compounds such as LY294002, rapamycin and Torin1. Because S6 is activated during primary KSHV infection, even in the presence of the mTOR inhibitor Torin1, it is possible that a tegument-containing viral protein released during primary infection imparts this resistance. Moreover, genome replication and infectious virion production of RRV, a KSHV homolog, ensues despite the presence of PI3K/AKT/mTOR inhibitors. This suggests that γ-herpesvirus replication is relatively insensitive to PI3K/AKT/mTOR inhibitors. vPK is expressed during de novo and lytic replication, therefore it is tempting to speculate that vPK may confer resistance to these inhibitors. It may also explain why some instances of KS are refractory to rapamycin treatment. Therefore, it is

imperative to further investigate how vPK counteracts pathway inhibitors, to preempt adverse events in patients receiving molecular targeted therapies for KS or PEL. Further, if vPK is indeed directly responsible for imparting resistance, it may be important to find a way to inhibit vPK's kinase activity. A manuscript describing these data is currently in preparation.

Collectively, our data suggest that while latent KSHV infection is susceptible to PI3K and mTOR inhibitors, lytic replication may be impervious to them, due to vPK's ability to activate components downstream of mTOR.

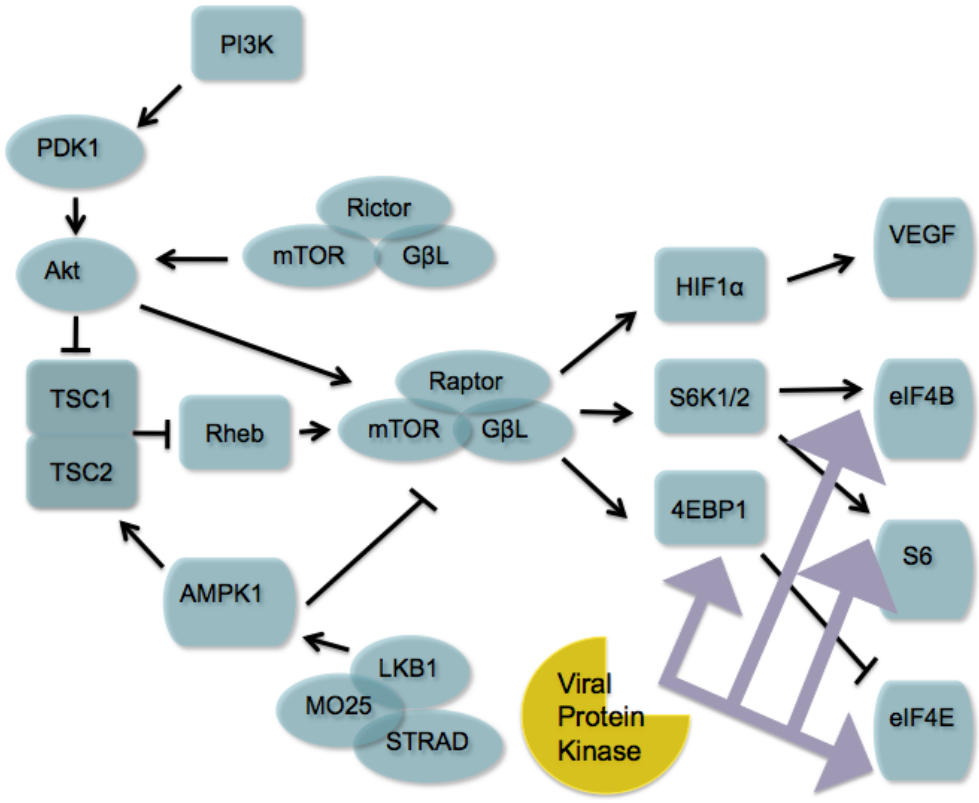

Figure 4: Proposed model of how vPK activates downstream effectors of PI3K/AKT/mTOR signaling, thus granting resistance to pathway inhibitors

REFERENCES

1. **Hanahan D, Weinberg RA.** 2011. Hallmarks of cancer: the next generation. Cell **144:**646-674.

2. **Polizzotto MN, Uldrick TS, Hu D, Yarchoan R.** 2012. Clinical Manifestations of Kaposi Sarcoma Herpesvirus Lytic Activation: Multicentric Castleman Disease (KSHV-MCD) and the KSHV Inflammatory Cytokine Syndrome. Front Microbiol **3:**73.

3. **Manning BD, Cantley LC.** 2007. AKT/PKB signaling: navigating downstream. Cell **129:**1261-1274.

4. **Bhatt AP, Damania B.** 2012. AKTivation of PI3K/AKT/mTOR signaling pathway by KSHV. Front Immunol **3:**401.

5. **Chandriani S, Ganem D.** 2010. Array-based transcript profiling and limiting-dilution reverse transcription-PCR analysis identify additional latent genes in Kaposi's sarcoma-associated herpesvirus. J Virol **84:**5565-5573.

6. **Stallone G, Schena A, Infante B, Di Paolo S, Loverre A, Maggio G, Ranieri E, Gesualdo L, Schena FP, Grandaliano G.** 2005. Sirolimus for Kaposi's sarcoma in renal-transplant recipients. N Engl J Med **352:**1317-1323.

7. **Sin SH, Roy D, Wang L, Staudt MR, Fakhari FD, Patel DD, Henry D, Harrington WJ, Jr., Damania BA, Dittmer DP.** 2007. Rapamycin is efficacious against primary effusion lymphoma (PEL) cell lines in vivo by inhibiting autocrine signaling. Blood **109:**2165-2173.

8. **Bhatt AP, Bhende PM, Sin SH, Roy D, Dittmer DP, Damania B.** 2010. Dual inhibition of PI3K and mTOR inhibits autocrine and paracrine proliferative loops in PI3K/Akt/mTOR-addicted lymphomas. Blood **115:**4455-4463.

9. **Bhende PM, Park SI, Lim MS, Dittmer DP, Damania B.** 2010. The dual PI3K/mTOR inhibitor, NVP-BEZ235, is efficacious against follicular lymphoma. Leukemia **24:**1781-1784.

10. **Das Thakur M, Salangsang F, Landman AS, Sellers WR, Pryer NK, Levesque MP, Dummer R, McMahon M, Stuart DD.** 2013. Modelling vemurafenib resistance in melanoma reveals a strategy to forestall drug resistance. Nature **494:**251-255.

11. **Duvel K, Yecies JL, Menon S, Raman P, Lipovsky AI, Souza AL, Triantafellow E, Ma Q, Gorski R, Cleaver S, Vander Heiden MG, MacKeigan JP, Finan PM, Clish CB, Murphy LO, Manning BD.** 2010. Activation of a metabolic gene regulatory network downstream of mTOR complex 1. Mol Cell **39:**171-183.

12. **Warburg O.** 1956. On respiratory impairment in cancer cells. Science **124:**269-270.

13. **DeBerardinis RJ, Lum JJ, Hatzivassiliou G, Thompson CB.** 2008. The biology of cancer: metabolic reprogramming fuels cell growth and proliferation. Cell Metab **7:**11-20.

14. **Flavin R, Peluso S, Nguyen PL, Loda M.** 2010. Fatty acid synthase as a potential therapeutic target in cancer. Future Oncol **6:**551-562.

15. **Bhatt AP, Jacobs SR, Freemerman AJ, Makowski L, Rathmell JC, Dittmer DP, Damania B.** 2012. Dysregulation of fatty acid synthesis and glycolysis in non-Hodgkin lymphoma. Proc Natl Acad Sci U S A.

16. **Thupari JN, Landree LE, Ronnett GV, Kuhajda FP.** 2002. C75 increases peripheral energy utilization and fatty acid oxidation in diet-induced obesity. Proc Natl Acad Sci U S A **99:**9498-9502.